EXPERIMENTAL INVESTIGATION ON MECHANICAL PROPERTIES OF ALUMINUM METAL MATRIX COMPOSITE AND OPTIMIZATION OF TRIBOLOGICAL PROPERTIES USING TAGUCHI METHOD

A thesis submitted to the

UPES

For the Award of

Doctor of Philosophy

in

Mechanical Engineering

BY

RAMESH M

March 2025

Supervisor

Dr. Deepak Kumar

Co-Supervisor

Dr. Ajay Kumar

Department of Mechanical Engineering
School of Engineering
UPES
Dehradun - 248007: Uttarakhand INDIA

EXPERIMENTAL INVESTIGATION ON MECHANICAL PROPERTIES OF ALUMINUM METAL MATRIX COMPOSITE AND OPTIMIZATION OF TRIBOLOGICAL PROPERTIES USING TAGUCHI METHOD

A thesis submitted to the

UPES

For the Award of

Doctor of Philosophy

in

Mechanical Engineering

BY

RAMESH M

(SAP ID- 500072286)

March 2025

Supervisor

Dr. Deepak Kumar

Sr. Associate Professor

Department of Mechanical Engineering, UPES

Co-Supervisor

Dr. Ajay Kumar
Professor
Department of Mechanical Engineering, UPES

Department of Mechanical Engineering
School of Engineering
UPES
Dehradun - 248007: Uttarakhand INDIA

DECLARATION

I hereby affirm that the thesis titled "**Experimental Investigation on Mechanical Properties of Aluminum Metal Matrix Composite and Optimization of Tribological Properties Using Taguchi Method**" has been written by me under the guidance of Dr. Deepak Kumar, Professor and Dean R & D, Dev Bhoomi Uttarakhand University, Dehradun and Dr. Ajay Kumar, Professor, Department of Mechanical Engineering, UPES, Dehradun. No part of this thesis has formed the basis for the award of any degree or fellowship previously.

Ramesh M

Department of Mechanical Engineering

School of Engineering, UPES

Dehradun-248007

Uttarakhand, India.

DATE: 05-04-2024

UPES
UNIVERSITY OF TOMORROW

Great Place To Work. Certified FEB 2024-FEB 2025 INDIA

CERTIFICATE

We certify that **Ramesh M** has prepared his thesis entitled "**Experimental Investigation on Mechanical Properties of Aluminium Metal Matrix Composite and Optimization of Tribological Properties Using Taguchi Method**", for the award of PhD degree in the UPES, under our guidance.

Supervisor
Dr. Deepak Kumar
Professor and Dean, R & D
Dev Bhoomi Uttarakhand University, Dehradun
Ex-Senior Associate Professor, UPES

Co supervisor
Dr. Ajay Kumar
Professor
Department of Mechanical Engineering, UPES, Dehradun

ABSTRACT

Graphene-reinforced aluminum metal matrix composites (AMMCs) have greater focus towards research due to their enhanced properties and extensive uses. This study presents a comprehensive investigation into the mechanical, hardness, compression, fatigue, wear, corrosion behavior, and microstructural characteristics of graphene-reinforced AMMCs, through an emphasis on the consequences of heat treatment. The fabrication of composites involved the incorporation of varying weight percentages of graphene (ranging from 5% to 15%) into an aluminum matrix using liquid metallurgy techniques. Subsequently, heat treatment or ageing process is employed to assess the mechanical properties like wear, fatigue corrosion and also microstructure of the composites.

Mechanical characterization tests, including tensile, hardness, and compression tests, were performed to evaluate the efficiency of graphite reinforcement on the mechanical properties of composites. The results indicated a remarkable enhancement in the properties like tensile property, compression property and hardness upon adding graphene. The maximum content of 15% graphene reinforcement exhibited the most pronounced enhancement in these properties. Fatigue behavior analysis was carried out using cyclic loading tests to assess the composite's fatigue resistance. The incorporation of graphene reinforcement effectively mitigated the propagation of crack and enhanced the fatigue property of the composites, demonstrating their improved durability and resistance to cyclic loading. Wear investigations were carried out through sliding wear tests to simulate real-world operating conditions. The graphene-reinforced AMMCs displayed enhanced wear resistance, attributed to the improved hardness and reduced friction coefficient imparted by graphene reinforcement.

Corrosion studies were conducted on the composites under aggressive environments. The gravimetric method is used for conducting corrosion test. The results demonstrated improved corrosion resistance in the graphene-reinforced AMMCs, which resulted in the development of a graphene layer which protects the surface of composite. Furthermore, microstructural analysis technique such as Scanning Electron Microscope (SEM) was used to examine the micro structure properties of the composites. Uniform distribution of graphene within the aluminums matrix was revealed after microstructural analysis indicating good bonding sandwiched amongst the matrix metal and reinforcement.

In summary, this study enlightens on complete understanding of the mechanical properties, hardness, compression, fatigue, wear, corrosion behavior, and microstructure of graphene-reinforced AMMCs with heat treatment. The results demonstrate that graphene reinforcement enhances the various properties like wear resistivity, corrosion resistance and fatigue property of the composites. A uniform dispersal of graphite reinforces inside the aluminum matrix was revealed after microstructural analysis indicating good bonding sandwiched amongst the matrix metal and reinforcement. These findings explored the advancement of graphite-reinforced AMMCs and their prospective for various industrial applications where improved mechanical performance and durability are required.

ACKNOWLEDGMENT

I heartily express my gratefulness to my supervisors Dr. Deepak Kumar and Dr. Ajay Kumar, for their continuous encouragement, motivation and support in completing my thesis work. I am very much grateful to them for exploring this emerging research area and for their guidance, which made me to contribute towards the research during the entire tenure of my research.

Along with my Supervisors, I want to extend my deep gratitude to Dr. Sunil Rai (Chancellor), Dr. Ram Sharma (Vice-Chancellor and Dean, SoE), University of Petroleum & Energy Studies for their precious support for my research work.

I also extend my gratefulness to Dr. Devesh Kumar Avasthi (Dean R &D), Dr. Pankaj Kumar Thakur (Associate Dean, R&D), Dr. Adesh Kumar (Associate Dean, R&D), Dr. Ashish Karn (Head of Mechanical Cluster), Dr. Ramesh Kumar Donga, Dr. Jitendra Yadav, Dr. Rajiv Kumar Gupta, University of Petroleum and Energy Studies, for their kind support during my research.

I further extend my special regards to my dearest friends Dr. Prem Kumar G, Dr. Sumana B G, Dr. Ranganath S, Dr. Santhosh Kumar, Dr. C M. Ravi Kumar, Mr. Manjunath E, Mr. Nagaraj G S, Revanna Siddu, and Mrs. Akhila. E who supported morally and stood with me during entire research work.

I would like to acknowledge Dr. Krishna, Head, Mechanical Engineering, R V College of Engineering, Bangalore, for his support in providing the facilities at R&D Department, Advanced Metallurgical Laboratory (AML), Peenya, Bangalore, Raghavendra Spectro Metallurgical Laboratory, Bangalore where I have carried out part of my research work.

DEDICATION

I would like to dedicate my research work to my parents, wife Mrs. Shilpa Kumari H, Son Mr. Vaibhav R and Daughter Miss Ridhi R, without their moral support, it would have been difficult for me to complete my PhD during the pandemic situation.

TABLE OF CONTENTS

LIST OF TABLES

LIST OF FIGURES

ABBREVATIONS

Al	Aluminum
Al/Gr MMC	Aluminum Graphite Metal Matrix Composites
AMMC	Aluminum Metal Matrix Composites
ASTM	American society for Testing and Materials
CTE	Coefficient of Thermal Expansion
DOE	Design Of Experiments
GRA	Gray Rational Analysis
HCl	Hydrochloric acid
MPa	Mega Pascal
NaCl	Nitrogen Chloride
OEM	Optical Electron Microscope
% wt.	Percentage Weight
SEM	Scanning Electron Microscope
SiC	Silicon carbide
TEM	Transmission Electron Microscope
UCS	Ultimate Compression Strength
UTS	Ultimate Tensile Strength
XRD	X Ray Diffraction

CHAPTER 1

INTRODUCTION

1. BACKGROUND STUDIES

Castings of aluminum alloy are preferred for many applications in transportation sectors outstanding to the ratio of weight to strength coupled with excellent abrasive resistance and corrosion resistance. It is gaining its interest to consider that up to 90% of casted aluminum components made with aluminum alloys which makes them extremely important in aluminum casting industries. Particularly, automobile structural components like housings, frames, wheels and brackets which are developed with cast aluminum alloys [1]. In particular, these alloys now a days replacing the components made up of cast iron like cylinder liners because of its enhanced physical characteristics with excellent wear resistance. Al 7007 is a cast alloy having composition like 5.9 - 7.5% zinc, 0.40 - 0.70% magnesium, 0.045 - 0.075% beryllium, 0.14% iron and 0.12% copper [2]. A microstructure study revealed α-Al phase, primary Si and $CuAl_2$ or Cu-Al-Si-Mg phase which are rich in Cu, Fe based brittle crystals and Al-Si eutectic [3]. Here, the incorporation of each element has its own importance indicating improvement in fluidity due to addition of silicon, Magnesium is added to enhance its hardiness during precipitation, Nickel is incorporated to improve tensile strength, copper is added to increase the resistance during peak temperature and manganese is incorporated to transform Ferric intermetallic. Beryllium is incorporated to modify the properties and to transform insoluble Al-Mg-Fe-Si phase to nodular phase & hence to alter the chemistry of insoluble phase which eliminate magnesium confirming its accessibility for hardness during precipitation. Meanwhile the alloy is heat treatable and its properties like strength, corrosion resistance and fatigue have improved substantially after T6 tempered heat treatment. During this process, molten metal is made to treat with grain refining alloys like Al-Ti-C, Al-3Ti-B, Al-5Ti-B [4]. Alterations during molten stage during heat treatment modifies the silicon morphology from its coarse acicular to fibrous form, because of which, it enriches the properties of

Composites. Certain other methods are employed to enrich the wear resistance and strength of Al 6061 by incorporating hard reinforcements like ceramics. Further, focus is made to incorporate with other reinforcements like graphite fibers, TiB_2& Al_2O_3 to modify elastic modulus, thermal and electrical properties. Because of its exterior mechanical and tribological properties, Al 6061 is considered as metal matrix to fabricate composites in this present research work.

Modern industries require advanced materials with unconventional combinations of materials such as alloys, ceramics and polymers to provide exceptional properties. Due to their attractive properties, they find many applications in aerospace, underwater and ground vehicles. Metal matrix composites (MMCs) got better scope for researchers because of its specific properties. Generally, MMCs in combination with ductile matrix and brittle reinforcement's exhibits excellent properties. Incorporation of reinforcements with aluminum metal matrix modifies microstructure, mechanical, wear, corrosion and other properties.

1.1 FABRICATION METHODS OF MMCS

The MMCs are fabricated by two techniques such as solid state and liquid state techniques. In solid state techniques like powder metallurgy, diffusion bonding, etc. there is very little time available to fabricate composites and it is difficult to produce complex shapes. But in liquid route technique, since the alloy found to be liquid state, it can be able to attain any shape owing to its fluidity, which helps in producing any complex shapes of the components during stir casting, squeeze casting, etc., methods. In both the methods, the reinforcement should be chemically treated or coated which helps to improve the wettability of reinforcement and avoid unnecessary reaction amongst reinforcements and metal matrix.

1.1.1 **SOLID STATE FABRICATION**

Diffusion bonding is one of the innovative methods for fabricating MMC sheets. The reinforcement is spread on metal / alloy sheets in a predetermined direction in the form of layers. Then uniform pressure is applied on these layers using hydraulic or mechanical press directly as shown in Fig.1.1. The specialty of this method is, it can produce functionally graded materials. Although it produces good quality of casting, but is too expensive [4].

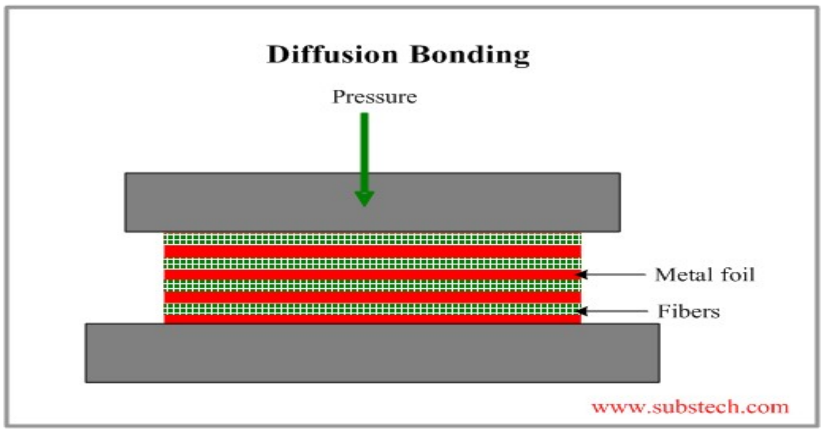

Fig. 1.1 Diffusion Bonding for fabricating MMCs sheet Materials

Powder-metallurgy is also most popular method to develop particle reinforced composites. In this process, both metallic and reinforcement particles were mixed and poured into the die which is of pre-determined shape. The mixture of powder is compacted using cold pressing by means of hydraulic press. This compact mixture is now heated up to its recrystallization temperature which is below its melting point of metal matrix during sintering process as shown in Figure. 1.2. Powder metallurgy method can produce 80 - 90% of theoretical density. Matrix metals Such as Al, Ti, Co, etc. are blended with SiC, alumina graphite, etc. being used as reinforcement using a suitable method for producing small and complex shape composites [5].

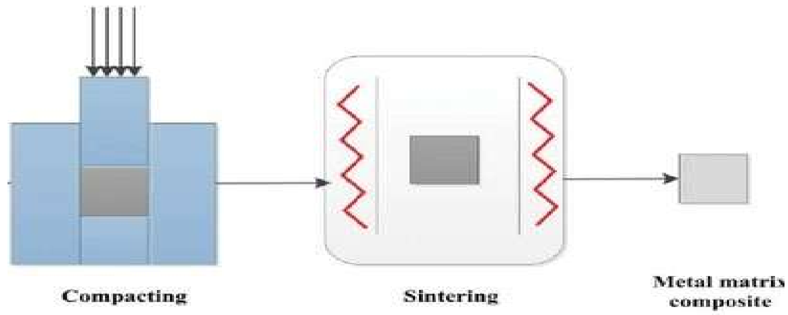

Fig. 1.2 Diffusion Bonding for fabricating MMCs sheet materials

1.1.2 LIQUID STATE FABRICATION

Infiltration casting technique produces various composites under vacuum pull or pressure and push the molten metal into the reinforcement. It enhances the surface properties and wettability of the reinforcements to develop sound castings. Alloys such as Al, Mg, and Zn etc. whose melting point is lower can be fabricated with infiltration casting techniques. The reinforcement generally used in the form of fibers are most suitable due to capillary action which leads to improved wettability. The degree of casting depend upon the surface tension of molten metal & degree of wetting condition of the reinforcement [6]. The popular method of gas pressure metal infiltration to develop composites is shown in Fig 1.3.

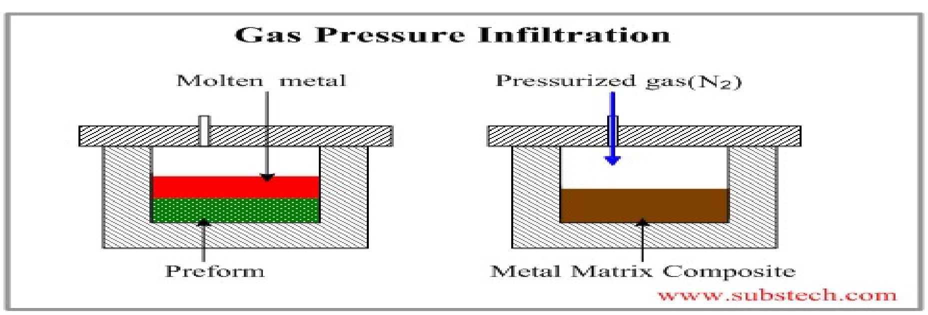

Fig. 1.3 Gas pressure metal infiltration method of composite preparation

Squeeze Casting is the popular hybrid technique to produce composite structures. In this method, both pressure and gravity are used to squeeze the molten metal into the fiber. The pressure and gravity get drastically reduce the shrinkage & thus eliminating the casting defects. In this technique, all types of metal and reinforcements can be used for making sound casting. Any complex shape can be produced easily and comfortably. Similar to infiltration, it is also used for fiber reinforced composites, but it can be extended even with particles and whiskers [7]. The set up used for squeeze casting process is shown in Fig 1.4.

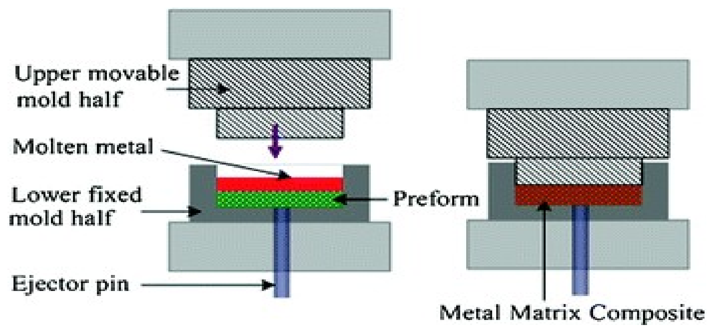

Fig. 1.4 Squeeze casting for composite preparation

Compo casting is considered as cost effective process for casting composite reinforced with particulates or whisker whose detailed procedure is shown in Fig.1.5.

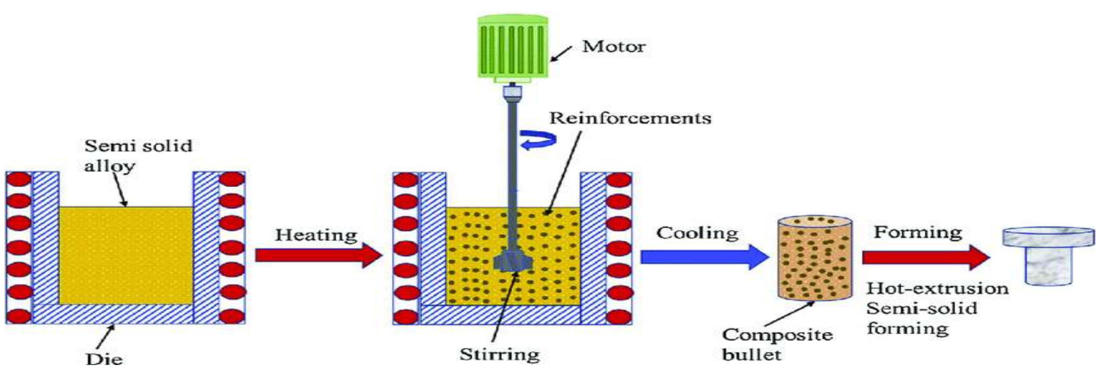

Fig. 1.5 Compo casting method for composite preparation

It leads to fracture of particles during stirring process where in, the high speed blades fracture the reinforcements during mixing of both matrices and reinforcement in molten slurry. It is slightly distinct from that of ordinary casting technique during which, the solidification is followed by re melting. The high % volume of reinforcement composites can be produced with excellent mechanical properties [8].

Spray Co-deposition is one of the best method to produce particulate reinforced composites. The molten liquid metal is sprayed on to surface of the metal matrix as a first layer followed immediately by spraying the reinforcement on the surface as shown in Fig. 1.6. This process continues until required thickness is obtained. The matrix and reinforcement are piled up and the specimens got ready after cooling and with subsequent stages of operations. The billets, rings and plates can be casted for the particulate reinforced MMCs with liquid metal and solid reinforcement. Sprayed preforms have characteristically equiaxed grains of 15-50 μm diameter at all preform locations and low- levels of micro-segregation and macro-segregation [9].

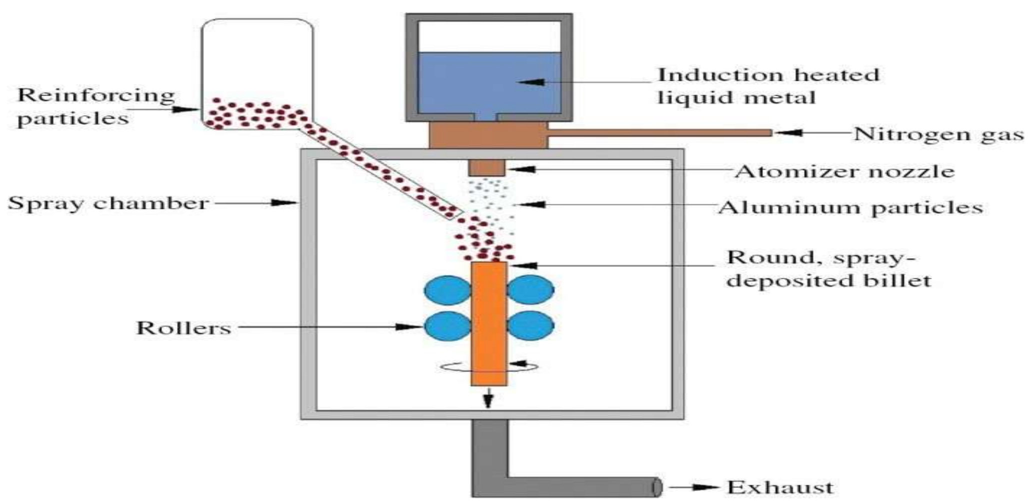

Fig. 1.6 Compo casting for composite preparation

1.1.3 INSITU FABRICATION TECHNIQUE

This technique provides unidirectional solidification of matrix alloy, which leads to a multiphase / heterogeneous / composites microstructure that clearly distinguishes the distribution in the matrix alloy. The process of insitu fabrication of MMCs as shown in Fig. 1.7. The uniqueness of this process is, during particle distribution and dispersion into the matrix alloy, the precipitation occurs during solidification. The crucibles filled with ingots moves downwards during the melting of alloy and the solidification occurs simultaneously. This insitu fabrication casting technique gives higher strength, low creep and thermal stability of the composites [10].

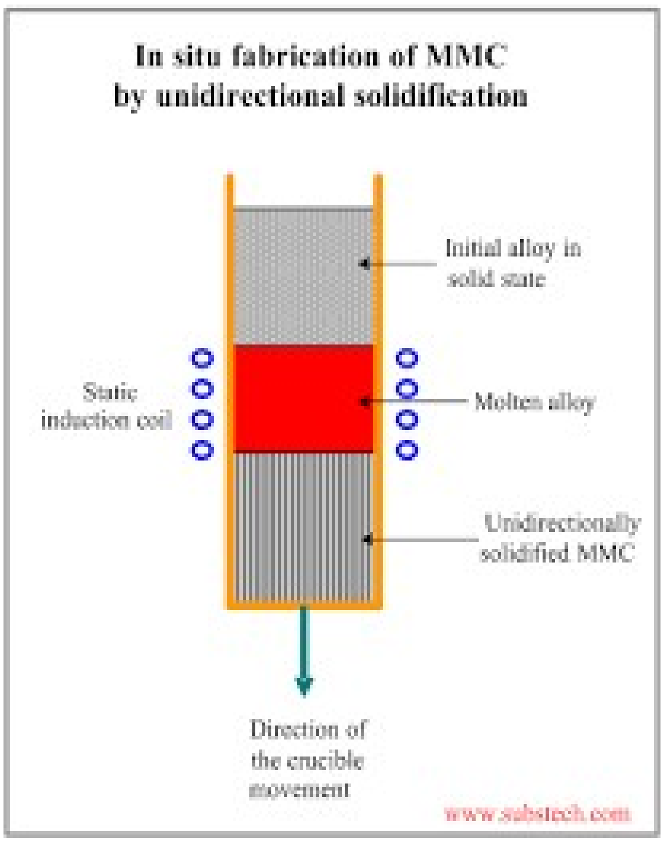

Fig. 1.7 Insitu Fabrication method for composite preparation

1.2 FORMING PROCESS OF MMCS

The forming process provides pre-defined shape without removal of material using compression, tension, shear and combined stresses in order to malleably deform the materials. Few methods of fabrication process of MMCs are given below.

Forging [12-13] is one of the greatest extensively used technique of forming processes to develop finished product by means of applied compressive forces using hand hammers, power hammers, hydraulic systems etc. Higher temperature forging i.e., hot forging is one of the cost effective fabrication technique for developing composites as shown in Figure 1.8.

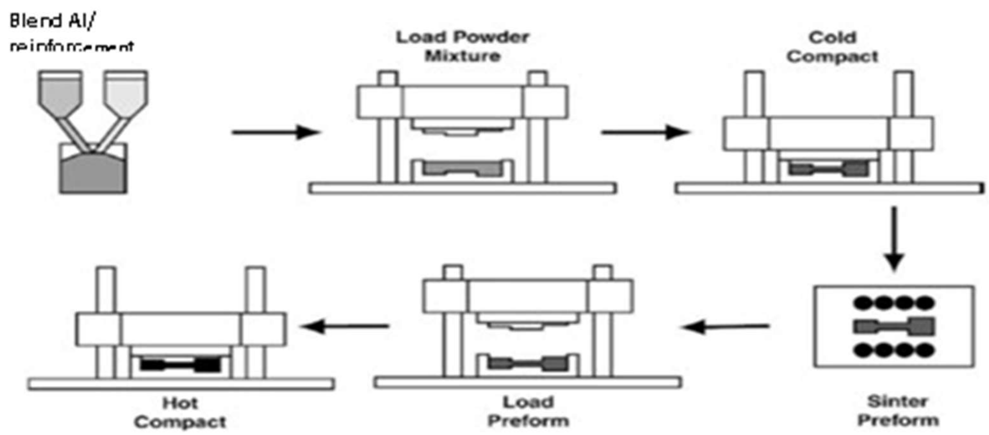

Fig. 1.8 Forging method for composite preparation [11]

The forging operations are categorized into cold and hot forging for shaping composites with enhancement in hardness, work hardening, good surface quality with high accuracy. It also improves the mechanical and fatigue properties.

Rolling [14] process for MMCs is most popular industrial metal forming processes in which compressive forces are utilized for compacting the specimens, which leads to reduce the geometry of the materials. In this process, materials get

Squeezed in between too hard and hot rollers as a result, the thickness of the materials drastically reduces as shown in Fig. 1.9.

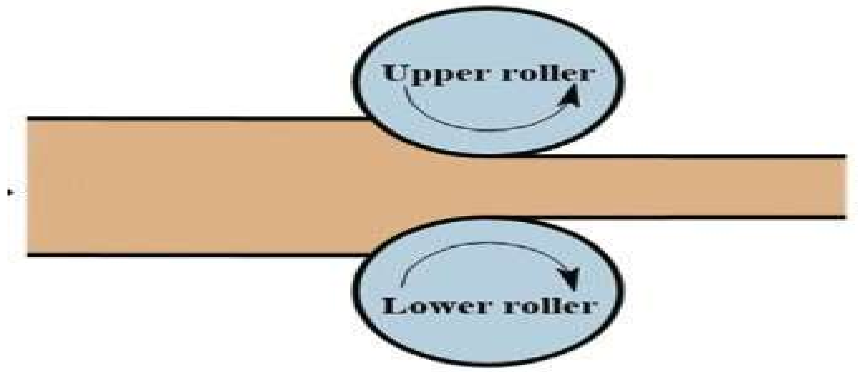

Fig. 1.9 Rolling method for composite preparation

Generally, all rolling processes require high temperature, due to which industries need a very large deformation. Another advantage is higher deformation metal forming is the products obtained are of generally free from residual stress. The important features of rolling is that fast forming operation and high output product and free from any type of damage.

Extrusion process [15-16] involves forcing the MMCs through a small opening or narrow aperture opening in order to reduce the geometry of samples such as reducing the diameter and increasing the length of the specimens by means of with or without temperature as shown in Fig.1.10. Complicated aluminum metal matrix composite sections are forward extruded for various applications.

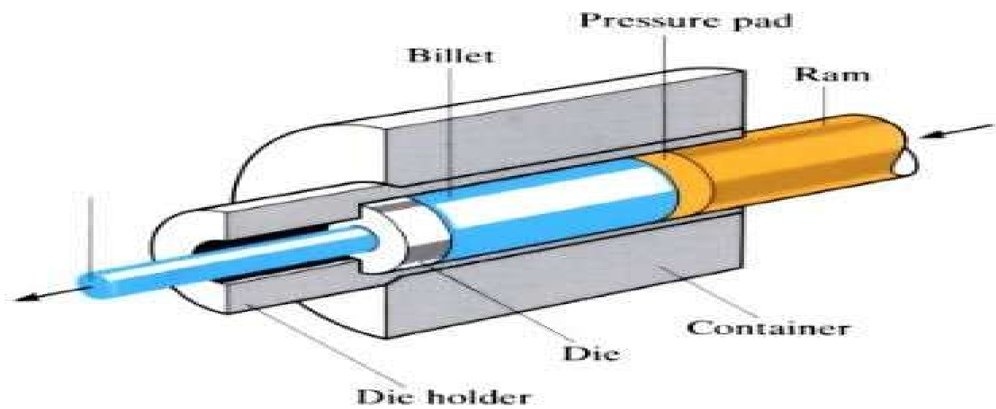

Fig. 1.10 Extrusion process method for composite preparation

1.3 PROPERTIES OF MMC'S

MMCs offer a significant contribution for designing structures with excellent mechanical and physical properties in comparison with conventional metal alloys. There is a huge selection of alloys and reinforcement allows to develop the MMCs with lower density, thermal coefficient of expansion, good mechanical strength. Addition of strong reinforcement into the alloys exhibited superior mechanical properties like high specific strength, tensile property, creep and fatigue property, simultaneously decreased the fracture toughness and ductility property of composites, which limits its usage in industries [17].

The nature of reinforcement and % volume of reinforcement incorporated have affected its young's modulus of the composites developed. For example, elastic modulus which is reported in literature review, found to be improved with addition of reinforcement. Even, the heat treatment or ageing also increases the young's modulus slightly. Many factors like type & size of the reinforcements added , % volume of reinforcement, secondary operation processes influence both tensile strength and yield strength of the MMCs and influences its elasticity nature of the material behavior. The peak aged specimens exhibited higher hardness, mechanical strength, greater amount of elastic strain, etc. Due to secondary

Processes, the residual stresses found to be developed in the structure which results in reduction in ductility. The residual stresses are developed in the structure because of the variances in coefficient of thermal expansion among the metal matrix alloy & reinforcement [18].

The study of friction and wear of the surfaces of two components during their relative motion is popularly known as tribology which is an interdisciplinary area. Thus when the surface of pure aluminum and its alloys slides or comes in contact with the hard surface like steel or iron, then, there is a progressive loss of material is found in aluminum. The process of adherence of material in the form of layer by layer which is removed from the surface of aluminum onto the surface of iron/steel followed by the formation of an interface with shear strength. The adherence of layer of aluminum to the surface of steel substrate occurs when there is increase in relative motion of these two counterparts [19]. When there is an increase in sliding action, shear debris is developed because of the ploughing action caused by hard sharpness of metal surface. Sometimes, due to improper lubrication, aluminum alloys found to be more susceptible to get seized. Moreover, it is essential to understand that both friction and wear are system dependent properties rather than intrinsic properties of material. Hence, it is essential to realize the responses of materials and alter their properties to acquire required resistance property in reducing friction and wear. Hence, by altering its composition during the stage of processing itself, the properties of the component can be altered as per the requirement for a specific application. Orchard equation under dry sliding wear condition can be used to develop simple correlation between hardness and wear resistance. Even then, the recorded experiential data cannot be related with that of generalization of wear behavior because of the wide range of discrepancy found in operating conditions. Many researchers were of opinion that the incorporation of ceramic reinforcements which demonstrated remarkable enrichment in wear resistivity of MMC's [20]. But then, to achieve enhanced wear resistivity, the boundary amongst the reinforcement and the matrix metal need to be strong enough so that the deboning of reinforcements occur during wear test. The detailed literature survey clearly favors that the silicon carbide particles provide enhanced better wear resistivity property compared to other reinforcements. Hence, it is very much interesting to explore the tribological properties of Al composites reinforced with dual size SiC [21].

After conducting enormous literature survey, it is found that various mechanical properties and tribology properties of Al composites reinforced with dual size graphite particle were not explored and to bridge this gap, a research work is conducted. As mentioned, the matrix material chosen is Al 6061 which is strong candidate material for automotive applications and graphite particles of different sizes is chosen as reinforcement material. The dual particle size aluminum composites having different weight ratios of large and fine graphite particles is fabricated with stir casting technique. In addition to this, the consequence of T6 heat treatment on aluminum composites on various properties is studied. The microstructure is studied using both optical electron microscope and scanning electron microscope to analyze the uniform dispersion of graphite particles and interfacial bonding amongst aluminum matrix alloy & graphite particles [22]. The precipitates and dislocations are studied using high resolution transmission electron microscope (TEM). Mechanical properties like yield strength, tensile strength and elongation were deliberated by conducting tensile test according to ASTM standards. Dynamic property like free vibration behavior was obtained by conducting finite element analysis. Finally, tribological behavior in terms of wear as a function of varying load was obtained by performing wear test under dry sliding as per ASTM standard. The wear debris from the worn out surface were analyzed using scanning electron microscope to arrive at possible mechanism of composites during wear process [23].

A polarization resistance also demonstrate a vigorous role in the area of applied metallic corrosion under corrosive environment. In this context, the kinetics of corrosion on active metals is more relevant than that of the passive metals during aggressive environment [24]. Because of pitting action, the protective passivation film breaks down, resulting in corrosion on metal surface. In other hand, Shi et al. [25] Have deliberated the impact of extrusion on the of magnesium alloy's properties during corrosion, because of its grain size of the refinement, the rate of corrosion was noted to be lower. The enhancement of corrosion resistance in aluminum alloys due to extrusion and due to effective refinement of secondary phase [26] who disclosed that the extrusion significantly enhances the corrosion resistive property of aluminum alloy [27]. But there is no enough investigation on the consequence of an extrusion process on the behavior of aluminum composites during corrosion process at present. Hence, it is really needed to explore the consequence of extrusion on the corrosion resistivity of aluminum composites for structural applications.

1.4 APPLICATIONS

MMCs find many potential applications like mechanical, packages for electronic components, thermal insulations, housings for mechanisms and bushings as show in Fig. 1.11.

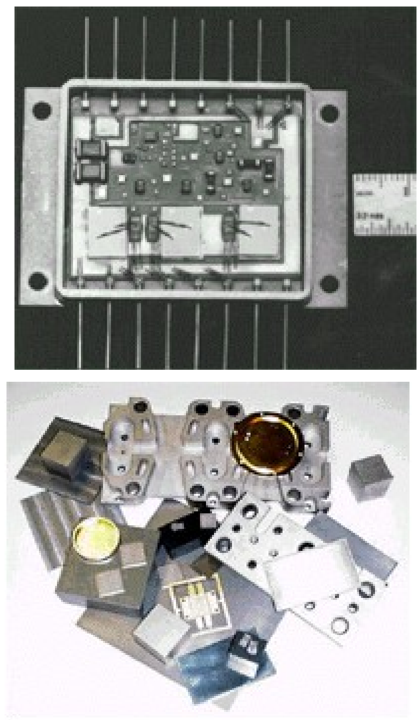

Fig. 1.11 Al MMCs for electronic packaging applications

MMCs are of combination of tailorable thermal coefficient of expansion and high thermal conductance with low density which found their usage in electronic and thermal packing materials. Many aluminum composites are been qualified during Space applications. The MMCs with significant high specific strength those produced from mother alloys, which leads to cost saving during any net shape manufacturing processes. Many MMCs are used in space thermal management for geosynchronous earth orbit communication satellites due to higher conductivity during thermal expansion than that of the matrix alloys. The MMCs flourish for space applications because of their specific strength and thermal

Conductivity. Major application of AMMC is found in Hubble space telescopic antenna having high gain boom of the length 3.6 m prepared with a sheet of bonded diffusion of P-100 graphite fiber reinforced Al MMCs [28].

Al MMCs incorporated with graphite particulates which are used for Hubble space craft structure as shown in Fig. 1.12 due to their stiffness, thermal stability & low thermal coefficient of expansion to monitor the position of antenna in the course of space maneuvers which have a good electrical resistance, which provide the wave guide function enabling electro-magnetic signal between the spacecraft and antenna dish on the earth [29].

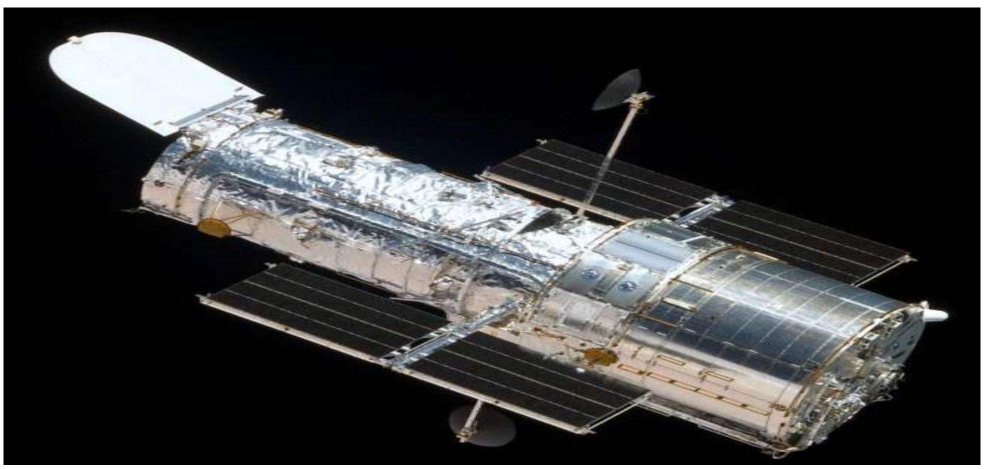

1.12 Hubble Space Telescope

All MMCs are used in automobile sectors, aviation industries and domestic industries. Light weight Al MMCs already fabricated components like piston rods, piston rings, valve trains, piston and gudgeon pins, cylinder-head, crankshaft-bearing etc.[30]. Ti MMCs are already used in aircraft propulsion components because of higher thermal conductivity and temperature stability, lower CTE and high specific strength. Al-Gr MMCs mostly find application in power electronics and electronic devices. Presently MMCs are also used for bicycle frames but are more costly.

1.5 ORGANIZATION OF THE THESIS

The following chapters insights the objectives, framework and context of the present research.

CHAPTER 1 INTRODUCTION: gives a brief information about problems in primary process (stir casting), other composite preparation process, secondary forming process, applications, properties, research gap, objectives and organization of report.

CHAPTER 2 LITERTURE REVIEW: presents detailed theory on MMC such as types, advantages, applications and gives theory on extrusion process.

CHAPTER 3 OBJECTIVES AND METHODOLOGY: outlines the methodology adopted to attain objectives framed out for the current research work.

CHAPTER 4 EXPERIMENTAL STUDIES: demonstrates the methodology and its performance to proceed with the Al MMCs using liquid metallurgical casting and the characterization of the Aluminum composites were performed by determining wt. %, reinforcement distribution for mechanical, fatigue and wear properties.

CHAPTER 5 RESULTS AND DISCUSSION: deals with of exploration of several mechanical properties viz compression strength, tensile strength, ductility, hardness and tribological properties of aluminum and its alloys with parameters like variable speeds, loads and distances and fatigue behavior studies.

CHAPTER 6 CONCUSION: reveals the detailed conclusions and the prospective scope for future research work.

CHAPTER 7 FUTURE SCOPE based on the current research work, future scope is suggested further who pursue research in this area.

CHAPTER 2

LITERATURE REVIEW

Exhaustive review of the previously published literatures pertaining to the current work is explored in this chapter which begins with prior work on ALMMC's. Further, a review of previously conducted studies on tribological properties of ALMMC's is demonstrated. To end with, an assessment on composites reinforced with dual particles is presented based on prior literatures.

2.1 ALUMINUM ALLOY

Aluminum is the second important plentiful material available in universe. Having high abundance and exceptional mechanical properties like low weight, low density and high strength is one of the abundantly used material after steel for structural applications with its density of one-third of steel. Depending on the need and application, there are several series and grades of aluminum alloy like 1xxx series up to 8xxx series. Al6xxx series with magnesium as the principal alloying element is sued for high stresses structural applications as they exhibit high specific strength in comparison to other aluminum series.

AA6061 is one of the most widely used aluminum during various structural applications likes hafts, engine castings, turbine casting inline skating frames, rifles for military, hang glider airframes, components of bicycle etc. Inspire of its high strength characteristics, it is restricted to wide scope due to poor corrosion behavior [31-34].

Corrosion is amongst the most important marine complications which causes problems in ships, submarines and other marine structures [35]. Metal corrosion depends on various factors like type of metal used, chemical environment, atmospheric condition, humidity, mechanical forces etc. AA6061 can face severe galvanic attack when comes in contact with nickel alloys, copper alloys, titanium, steel and stainless steel. Hence it must be always coated, anodized or catholically protected for marine applications. Aluminum based composites are common now a days since they enhance the structural and electrochemical behavior of the substrate. Aluminum has inherent property of becoming sacrificial anode in corrosive environment. Many researchers have focused their study on coating aluminum alloys with aluminum - based coatings. Al-Si coatings is one such alloy composition which can be used for coating purpose as it exhibits high corrosion resistance and also aids i n improving the mechanical and strength characteristics.

During the last decade, graphene has emerged as the most desirable reinforcement element. It is about 100 times stronger than in proportion to their thickness. Graphene has high surface area and has nonpolar carbon structure which makes it highly hydrophobic in nature. Also graphene derivatives like Graphene Nano sheets are highly chemical inert, thermals and impermeable to gases and fluids. These properties make them good candidates to be used as reinforcements for protective coating. But, a uniform dispersal of Nano size graphene into the composite powder is very much challenging. Various techniques for mixing the powder like wet mixing, ball milling, etc. have been used for uninform dispersion without forming agglomeration. Another challenge is to obtain a uniform coating of the substrate which would act as barrier against corrosive environment.

Although AA6061 shows excellent strength characteristics, it is limited to much wider applications due to its poor corrosive resistance & poor formability .Hence it must be always coated, anodized or be catholically protected marine applications. Several researchers have focused their interest to enhance the corrosive resistance of AA6061 alloy. Dhanish et al. have developed a protective layer of corrosion resistive for AA 6061 by enhancing simultaneously anodization & sealing parameters of MnVO. Electrochemical behavior of coatings developed using Electro Impedance spectroscopy and potentiodynamic polarization tests was reported.

Mohan D et.al. Have used high Nd: YAG laser power to accomplish shielding of Al-Si powder on Al-6061substrate. Since Al-Si powder is highly corrosion resistant material, it is best fit to be applicable during repairing work as a filler material [36]. Also impurities like Si improves castability and fluidity of aluminum alloy [37] Car et al. laser cladded Ti/TibCN coatings on 6061 aluminum alloy. It was expressed that corrosive potential of AA 6061 improved tobe1.271V. Also, one order magnitude was used to reduce the corrosion current density [38]. Jing et al. investigated electrochemical behavior by modifying aluminum 6061 alloy surface by depositing alumina coating using PEO (Plasma Electrolytic Oxidation) process. Excellent reduced corrosion current density and wear rate was observed [39]. Hussein et al. developed non- fluorinated super hydrophobic surface face of aluminum 6061 alloy by high vacuum process for 4 hrs and laser patterning [40]. Asif et al. developed AA6061/SiC MMC for better electrochemical behavior. This led to improved corrosion rate under different corrosive environment [41].

2.2 Al-Si Coating

Aluminum based coatings proved to be very good barrier against corrosion as it passivates and forms a dense oxide layer. However, it results in sacrificial anodic protection elements like silicon, magnesium, graphene can be used to overcome this problem as it would help in lowering corrosion potential and decrease inter metallic layer thickness [42]. Al-based composite coatings to reduce corrosion damage using surface engineering principle shave been commonly used for marine structures. Harshavardhan et al. developed plasma spray coated aluminum alloy reinforced with Silicon carbide and graphene which proved to have enriched wear resistivity and resistance to corrosion [43]. Huang et al. have deposited electrode Ni-SiC composite coating on A356 aluminum alloy [44].

The corroded parts of structural air frames were repaired using Al-Si alloy filler material due to its high corrosion resistive properties. Several researches have focused their interest on using Al-Si alloy as coating materials to enhance the

Corrosive resistance of the substrate [45]. Cho et al. coated 22MnB5 press hardened steel with Al-10Si alloy and studied its significance on its microstructural characteristics and the mechanical properties of the substrate [46]. Couto et al. have applied Al-Si coating to coat 22MnB5 steel for better electrochemical behavior and estimated the impact of process of hot stamping on the corrosive property of the coated substrate. It was reported that local galvanic couple formed highly depended on the hot stamping process [47]. While, Yunying used Al-10Si-Zn composite coating to coat 22MnB5 steel to enhance the corrosive resistance [48]. Riquelme et al. applied laser cladded Al- 12Si composite coating on Al 6082 to enhance the corrosive resistivity of AA6082 [49-50]. Su et al. applied thermal spray coating process for coating aluminum alloy using Al-Si-ND composite Lower current density during corrosion and Superior potential during corrosion because of coating deposition was reported [51]. Jun et al. have developed Al-12Si reinforced with Al_3Ti particles & TiB2 alloy to coat Al 6028 using GTAW [52].

2.3 GRAPHENE REINFORCEMENT

Graphene is most popularly used reinforcement material to develop ALMMC. It is known designated as one of the hardest and thin nest material with extraordinary mechanical, electrical and thermal properties [53-54]. Graphene is about 100 times much stronger than steel in proportion to its thickness. [55]. Also, it is one of the promising corrosion-resistive coating material because of its super hydrophobic nature. This is due to the fact that, it is thermally and chemically stable and inert under varying environmental conditions [56]. AMCs are reinforced with various graphene derivatives i.e., Graphene Nano-platelets (GNPs), Graphene Nano sheets (GNSs) Graphene Nano flakes (GNFs), etc. Several researchers have developed AMC with reinforcement with various graphene derivatives [57] as described in Table 2.1.

Table 2.1 Review on AMCs developed using Graphene derivatives

Base Material	Graphene Derivative	Wt.% reinforcement	Year	Reference
Al7050	Graphene	0.33,0.55,0.77	2000	[58]
Al	Graphene	0.1	2013	[59]
Al	GNP	1,2,3	2011	[60]
Al	GNS	0.3	2010	[61]
Al	GNP	1, 3, 5	2017	[62]
Al2124	Graphene	2, 4, 6	2014	[63]
Al6061	Graphene	1	2016	[64]
Al	GNP	0.25, 0.5, 1	2017	[65]
Al-	GNF	0.15, 0.5	2018	[66]
Al	GNP	0.3	2011	[67]
Al5052	GO		2014	[68]
Al	Graphene	0.25, 0.5	2018	[69]
Al	GNF	0.5, 1, 1.5, 2	2006	[70]
Al7050	Graphene	0.3, 0.5, 0.7	2017	[71]
Al	FLG	0.3, 0.5, 0.7	2019	[72]
Al	rGO	0.1, 0.25, 0.5	2015	[73]
Al	Graphene	0.05	2016	[74]
Al6061	Graphene		2015	[75]
Al	GNP	1	2015	[76]
Al356-5wt%SiC	Graphene	1, 3, 7	2017	[77]
Al	Graphene	1, 2	2016	[78]
Al6063	Graphene	2, 4, 6	2014	[79]
Al	Graphene	0.5	2006	[80]
Al6061	Graphene	2	2017	[81]

Al	rGO	0.2	2012	[82]
Al	GNP	0.5, 1	2013	[83]
Al	FLG	1	2014	[84]
Al	Graphene	0.3, 0.6, 0.9, 1.2	2006	[85]
Al	Graphene	0.5, 1, 2	2015	[86]
Al	MLG		2019	[87]
Al	GNP	0.5, 1, 3, 5	2010	[88]
Al	GNS	0.25, 0.5, 1	2013	[89]
Al/Mg	GO	1	2018	[90]
Al	FLG	0.05, 0.2, 0.4, 1	2013	[91]
Al	Graphene	0.5, 1, 2.5	2018	[92]
Al	Graphene	0.1, 0.2, 0.3	2017	[93]
AA6061	Graphene	0.5, 1, 1.5, 2	2016	[94]
Al	GNP	0.2	2015	[95]

From the review, it is observed that low graphene content is used as reinforcement to AMCs. This is due to difficulty and complexity in homogeneous dispersion of graphene within Aluminum matrix without making any agglomeration [97]. Because of Graphene’s surface area and because of Vander Waals forces among Al-matrix and graphene, there is formation agglomerates which leads to the deterioration of desired properties and results in inferior outcomes. [98]

2.4 BALL MILLING OF GRAPHENE

Numerous researchers have adopted ball milling process for production of graphene reinforced Al matrix. Table 2.2 describes review on Ball Milling parameters adopted by researchers.

Table 2.2 Review on Ball Milling Parameters adopter for Al/graphene composites

Sl. No	Base material	Wt.% of graphene	Milling type	BPR	Rotational speed (in rpm)	Milling atmosphere	PCA	Milling time (in hrs.)	Ref.
1.	Al	Graphene with 0.1wt. %	Attritor with high energy r	-	-	Argon	-	1	[99]
2.	Al	0.3wt % graphene	Attritor		325	-	-		[100]
3.	Al2124	graphene	Turbulent mixer	15:1	400	Argon	-	2	[101]
4.	Al6061	1wt% graphene	SPEX	2.5:1	-	Ambient	-	0.18, 0.6,1.0, 1.6	[102]
5.	Al	0.26,0.6, GNP with 1wt.%	SPEX	6:1	-	Argon	-	1, 5, 7	[103]
6.	Al-3.8 Cu-1.6 Mg	0.6 wt.% GNF	Roller Milling tank	11:2	76	Ethanol mixed with wet	-	14	[104]
7	Al	GNF with 0.6 wt%,1.0 wt%,1.5 wt%,2.0 wt%	Attritor	45:2	190	Stearic acid	-	4	[105]
8	Al	FLG with 0.8wt. %	Planetary ball mill	20:2	250	-	-	2	[106]

9	Al	Graphene with 0.05wt%	Planetary ball mill	25:2	200	Ambient	-	8.6	[107]
10	Al2024	FLG with 0.05,0.1 vol%	High en ergy ball mill	20:2	700	Ar	-	8	[108]
11	Al	1wt%GNP		20:2	600	-	-	8	[109]
12	Al6061	Graphene decorated with 0.8 wt% Ni	Planetary ball mill	15:2	380	Ar	-	2	[110]
13	Al	0.5wt. % rGO		18:2	250	-	-	4	[111]
14	Al2219	Graphene with 0.5, 1,2wt. %	Planetary ball mill	5:2	250	-	Toluene	8	[112]
15	Al	Graphene with0.25,0.5,1, 2wt.%		15:2	300	Ar	-	6	[113]
16	AlMg5	1wt.%GO	Planetary Ball Mill	15:2	380	Ar	-	30	[114]
17	Al	0.5,1, 2.5 wt.% graph ene	Planetary ball mill	6:1	250	Ambient	-	4	[115]
18	Al	1 wt.%	SPEX	-	-	-	Wet mixing	0.18	[116]

19	Al-1.5wt% Sn	1wt% FLG	-	-	380	Argon	Wet mi xing3+ in ethanol	6	[117]
20	Al-Si alloy	1wt%GNS	Planetary Ball Mill	20:1	300	Argon	-	25	[118]
21	Al	5wt%GNP	-	-	380	-	-	6	[119]

2.5 REVIEW OF MECHANICAL PROPERTIES

Purpose of development of composites is to improve the desired properties of conventional materials for an extensive variety of applications. Regarding this aspect, many research works at both institution and industries level have been documented for various properties such as mechanical / tensile, fatigue, impact, compression, bending, buckling, moisture absorption, etc.

Srivyaset al. **[120]** scrutinized the significance of orientation of fiber on the tensile behavior of Kevlar and glass fiber based Composites with aluminum under static in plane loading condition and concluded that there is found to be increase in ultimate tensile strength with 0° orientation by 32% and 110% when compared with 45°and 90° fiber orientation respectively. Zhao et al.[121] have observed Al 2024 grade with GFPP as composite layer incorporating a interlayer based on maleic-anhydride modified copolymer between the metal layer and composite to enhance its Young's modulus of 25 MPa to 75 MPa and tensile strength of 200 MPa to 500 MPa. Hashmi et al [122] characterized tensile properties on the aluminum matrix samples with 0°/90°and ± 45° SRPP samples along with (Al±45°) composites samples. They demonstrated that composites offered a higher strength (120MPa) than that of matrix composites (60MPa). In the same way, the strain to failure of (Al±45°) was noticed to be superior than that measured on the matrix aluminum alloy. Arif et al. [123] developed a composite laminates comprised of aluminum, steel & epoxy/glass fiber for performing tensile tests and concluded that the composites whose specific strength is found to be greater than that of monolithic aluminum (by 46 to 103%) and steel (by 38 to 91%) layers even though GRP's specific strength is higher than the developed composites. Vijaya Ramnath et al. [124] noted that the tensile properties of composites is affected by its individual components. Composite laminates under tension have exhibited an inelastic behavior because of its plasticity nature of aluminum layers. Panizam et al [125] documented that the addition of composite to the metal layer serves to increase the tensile strength of the component i.e. 350 MPa (40%VF), 400 MPa (60%VF) and 420 MPa (70%VF). The elastic modulus of GLARE is found to be lesser than that of monolithic aluminum because of its lower elastic modulus of epoxy/glass layers. Since epoxy/glass has a lesser modulus, the layer of metal in laminate will exhibit a better stress and thus decreases significantly the yield strength of the laminates. Krishna et al.[126], noticed that aluminum carbon fiber laminate offers a better resistance of 220 MPa compared to 135 MPa of monolithic aluminum and 145 MPa for aluminum glass fiber laminate under tensile loading.

2.6 REVIEW OF TRIBOLOGICAL PROPERTIES

Tribological properties deal with friction, wear and lubrication behavior against the rubbing body in various applications such as bearing, IC engines, power transmission etc. Although it deals with all the three properties, but industries are more focused on wear since it leads to premature failure, increasing operating temperature and over lubrication consumption. One of the major disadvantages of wear is phase out of the material on solid surface during dynamic conditions. Hence many researchers focused on improving the wear resistance by adding hard particles into matrix materials which are used as bearing properties.

In this context, the research has been proved that the incorporation of hybrid reinforcements such as graphite and B_4C into aluminum metal matrix leads in decreasing the wear rate drastically because of the existence of supporting reinforcements within the base material. The reinforcements act as an intermediate materials between the discs and pin at normal speed during wear test. The B_4C reinforcement act as a load barriers and graphite act as solid dry lubricants. Hence the researchers have claimed that both wear and friction simultaneously reduced by incorporating hybrid particles.

The wear test to understand the behavior of an Al /SiC composites has been conducted and the same is reported in the research papers. Researchers claimed that percentage of SiC particles was noted as highest contributing factor on the rate of wear trailed by sliding velocity and sudden jerking load are noted as second and third influencing parameters. The addition of SiC enriches the wear resistance up to 16%, beyond which starts to reduce drastically because of hydrogen embrittlement of material which drops ductility and becomes brittle.

Some researchers focused on the application of Al/graphite composite materials for internal combustion engine chamber and observed longer durability i.e., decrement in rate of wear , reduced coefficient of friction of rubbing surfaces like cylinder wall and piston ring . It is noticed that the incorporation of graphite particulates drastically reduces tribological properties. Some of graphite particulates seen in the lubrication area between the territory of sliding leads to graphite enriched lubricant in the tank Tribological properties becoming poor quality when the % vol of graphite in the composite is high because of the presence of holes in the bunches of graphite particulates [127-128].

2.7 REVIEW OF FATIGUE PROPERTIES

ALMMC is a promising material prominent for several crucial uses because of its extraordinary enriched specific stiffness [129], fatigue strength [130] wear resistivity [131] and alterable coefficient of thermal expansion [132-134]. Ancillary methods like as turning,milling,drilling, etc. its physical and mechanical properties , microstructure which entirely amends the components fatigue life [135] . Generally, hard reinforcement particles incorporated into the metal matrix shows inconsistency in its physical, mechanical and thermal properties and developed cracks for the period of fatigue loading [136]. The inconsistency amongst the reinforcement and the matrix enriches the residual stress which is induced resulted in drastic reduction in fatigue life at its crucial operating conditions [137]. It is essential to enhance the fatigue strength of aluminum composites; simultaneously, required to understand thoroughly during alternate methods of heat treatment [138]. The fatigue strength found to be influenced by its intrinsic properties of alloys. Viz, reinforcements & microstructure and also ancillary methods like heat treatment or aging attended by the consequences of fatigue life [139]. Defects found in matrix materials during ageing process, can be overcome by heat treatment which alters microstructure especially grain size to improved fatigue life [140]. Carbon Nano tubes made up of aluminum metal matrix composites exhibited greater elastic modulus, fracture toughness, coefficient of thermal expansion and hence further more attention is required [141]. Because of its expensive, several authors [142-144] have explored the consequence of graphite and carbon black nano powder to enrich several mechanical properties and fatigue properties of ALMMC. Exhaustive review [145-147] conducted on aluminum composites incorporated with graphite disclosed that ageing process has a significant influence exclusively on hardness. The significant effect of reinforcements on microstructural property and fatigue strength of numerous aluminum composites is explored by previous research literature; but inadequate review is presented for without heat treatment. Since, a clarity is needed on the importance of graphite reinforcement and heat treatment on the fatigue strength of aluminum composites and hence an exertion is exercised for exploring the significance of incorporation of graphite particulates as reinforcement and ageing on the fatigue properties of aluminum composites by using stress life (SN) & reliability stress life (RSN) methods.

2.8 REVIEW OF CORROSION BEHAVIOR

Corrosion is amongst the most important marine complications which adverse problems in ships, submarines and other marine structures. Metal corrosion depends on various factors like the type of metal used, chemical environment, atmospheric condition, humidity, mechanical forces etc. Surface barrier coatings, organic coatings and heat treatment are the most common methods used for protecting aluminum alloys during corrosion [148].

There is a need of corrosion protection of aluminum alloys used in marine structure when operating in sea water medium. Estimations revealed that that corrosion costs are as high as & it accounts for 3.6% of global GDP according to NACE report 2016. Apart from this, another issue of concern is the catastrophic failures and environmental damage occurring due to corrosion [149].Appropriate corrosion resistive material selection; organic and metallic coatings; sacrificial anodes; corrosion inhibitors sue, etc. are some of common methods to prevent and protect the materials against corrosion [150].

Several researches have focused on improvement of corrosion resistance of base substrate matrix metals using reinforcements and coatings. Devaneyan et al., found improved corrosion resistance of AA6061alloy using TiC reinforced Polyurethane PMC coating by conventional spraying process [151]. Fabricated TiCN coated 6061 aluminum alloy using PVD for protection of the aluminum alloy against corrosion. [152]. Dhanish et al., generated a corrosion resistance protective layer for aluminum 6061alloy by simultaneously optimizing the variables during sealing of MnVO and anodization. Electro Impedance spectroscopy (EIS) is used to study the electrochemical behavior of the developed coatings reported by [153].Couto et al, have used Al-Si coating to coat 22MnB5 steel for better electrochemical behavior. They estimated the influence of the process of hot stamping process on the corrosion property of coating on the substrate. It was observed that local galvanic couple formed highly depended on the hot stamping process [154]. While, Yunying used Al-10Si-Zn composite coating to coat 22MnB5 steel to enhance the corrosion resistance. Requelme et al.

coated composites using laser cladded Al-12Si on AA6082 alloy to enhance the corrosion resistivity property of AA6082 [155]. Deposition of Al-Si-ND composite coating on aluminum alloy with the help of thermal spray process was explored by Fu et al. Lower corrosion current density with improved corrosion potential was reported with coating deposition [156]. Table 2.3 discusses the Al-based coatings used for protection of substrate metal against corrosion with different spray techniques in varying electrolyte medium

Table 2.3 Al-based coatings as barrier against corrosion

Substrate	**Coating material**	**Electrolyte**	**Spraying method**	**Method for evaluation of electrochemical behavior**	**Year**	**Ref.**
22% Cr duplex stainless steel	Al99.5%	Artificial Seawater	Electric Arc	Linear Polarization resistance(LPR)	2016	[157]
Glass	Al99.5%	Artificial Sea Water	Electric Arc	Linear Polarization resistance(LPR)	2014	[158]
Steel	Al99.6% AlMg5%	Natural Sea water	Electric Arc and flame	Linear Polarization resistance(LPR)	2020	[159]
Carbon Steel	Al99.5%	Natural Sea Water	Electric Arc	Polarization resistance and polarization curves	2022	[160]
Carbon Steel	Al99.5%	Natural Sea Water	Electric Arc	Polarization resistance and Polarization curves	2013	[161]

Mild steel	Al99.0%	3.5%NaCl	Electric Arc	Tafel EIS	2021	[162]
Carbon Steel	AlMg5%	Natural Sea Water	Electric Arc	Polarization Curves LPR	2016	[163]
Carbon Steel	Al1100	Natural Sea Water	Electric Arc	LPR Polarization curves	1999	[164]
Stainless Steel	Al99.7%	Natural Sea Water	Electric Arc	Polarization Curves	2017	[165]
Carbon steel	Al99.5%	Artificial Sea Water	Electric Arc	LPR	2021	[166]
Mild Steel	Al99.99%	3.5%NaCl	Electric Arc	Polarization curves EIS	2011	[167]
SS316L	Al $Al-Al_2O_3$	Artificial Sea Water	Electric Arc and Plasma spray	Polarization curves EIS	2021	[168]
Mild steel	Commercially available Al powder	3.5%NaCl	Cold spray	Polarization curves EIS	2011	[169]
Mild carbo steel	$Al-Al_2O_3$	0.02%NaCl 0.2%NaCl 1.0 NaCl	Cold spray	Mass change	2021	[170]
Carbon steel	Al99.5%	Artificial Sea Water	Electric Arc	LPR	2022	[171]

2.9 REVIEW OF AGEING PROCESS

The application of components made up of aluminum alloys in automobiles is in focus because of various critical especially, to reduce weight. The necessity of materials which can tolerate an elevated operating temperature in an oxidizing atmosphere has become crucial in recent years. Demand in materials for various applications in defense, missiles, space and nuclear sectors which can operate at a high temperature 1200°C. 7xxx series of Al- Mg-Si alloys having heat treatable property are often considered for the above mentioned applications, as they had demonstrated an extra ordinary combination of formability, weldability and corrosive resistivity [172]. The precipitation hardening process is the factor considered in strengthening Al-Mg-Si alloys. The process of age hardening enriches the hardness and strength of aluminum alloys by developing a nanoparticles and have dissolved homogeneously within a secondary phase of matrix. The heat treatment processes like natural ageing or artificial ageing processes for which natural ageing requires longer time to alter the mechanical properties and hence, it is more important to substitute it with artificial ageing during which both ageing temperature & ageing time are considered as influential parameters [173]. The desired properties of aluminum can be enriched by the heat treatment process during which a small amount of hard precipitates as alloying elements are incorporated [174]. Al 7075 is extensively applied in structures due to its substantial properties like lower density, ductility, higher toughness and strength [175-178].

Al 7075 is widely used to develop aircraft structural components which operate under high induced stress [179-183] and they revealed during their studies that an optimal ageing could be obtained for a duration of 2 – 6 hours under its operating temperature with arrange 170°C to 190°C. Alaneme and Aluko [184], during their studies validated that, the process of ageing plays a critical role in enhancing the material's fracture toughness than its strength. Small man and Nigan [185] have noticed a reduction in solubility limit during their revisions, because of an artificial age hardening of AA 6061 – T6 tempered when there is drop in ageing

Temperature. An improvement in stress, fracture toughness of aluminum alloys is noticed by Abarghouie Lumley et al. [186] when compared with conventional T6 alloys tempered during ageing process. Akhteret al. [187] have conducted tensile test on AA 6111 at different artificial ageing processes to explore the influence of precipitation on its work-hardenability and yield stress. Anthony K et al. [188] have studied the consequence of ageing process on the tensile property and microstructure of AA 6063 by conducting experiments at different pre-ageing conditions at 170°C, 180°C and 200°C for a duration of 24 to 72 hours. Kalkani et al. [189] have noticed reduced yield stress value under larger aging temperature. During their studies on the significance of aging duration and temperature on Al 7075 and hence have concluded that T6 tempered Al 7075 under dissolved condition is an evidence for higher value of hardness during brittle fracture. Kim et al. [190] have made water quenching on Al 7075 specimens for a duration of 8 seconds and aging at 140°C for 10 hours. Hanumanth et al. [191] have noticed reduction in ultimate strength, hardness and enhancement in impact strength during their studies on the impact of quenching during solution heat treatment and pre-strain on the mechanical properties of AA7075 specimens at 460°C for a duration of 4 hrs and then pre-strained for 6% during tensile test. Leng et al. [192] have noticed an enhancement in yield strength and hardness of AA7075 at different durations during age heat-treatment at 150°C. Miracle et al. [193] have deliberated the significance of different heat treatment processes on an aluminum alloy for a specific temperature of 550°C. Prasanna Kumar et al. [194] have conducted experiments on solutionized AA 6061 at 100°C, 150°C and 200°C and observed an increased toughness and reduced strength when the temperature during artificial ageing under the impact of precipitation. Seah et al. [195] have performed experiments on solutionized heat treated specimens during water quenching 1050°C for 5 minutes of duration and noticed a highest elongation and lowest yield strength, higher fracture toughness and impact strength. The specimens at their fully aged condition during solutionized treatment and aged for 18 hrs. at 580°C have shown maximum

Hardness and strength, but displayed lower values of toughness and ductility. They observed a steady mechanical properties during solutionized treated temperatures by controlled cooling technique. For the solution treated fracture specimens, micro void coalescence was noticed and for the fractured specimens at aged condition, microstructure produced cleavage fracture or brittle grain boundary. The instantaneous increment in strength and drop in impact toughness was noticed because of the development and gathering of the κ-carbide and cleavage .The specimen that had been cooled controlled did not shown any fracture. Prasad et al. [196] have conducted their experimental studies on the structures functioning at larger temperatures and tempered with T4 & T6 processes and discovered that mechanical and physical properties of alloys tempered with T6 have lower ductility with higher strength than that of T4 tempered alloys, Yu et al, [197] have deliberated the significance of aging time, aging temperature & pre-strain on mechanical properties for Al7075 & noticed an improvement in the strength during the uniform dispersion of $MgZn_2$ and also observed brittle fracture failure of T6 tempered Al7075 . Bindumadhavan [198] have articulated that quench-induced precipitation and aging temperature played a vital parameter in enhancing mechanical properties which is noticed under electron microscope. Ames et al. [199] have deliberated the consequence of aging processes & solutionized on the mechanical properties and its microstructure of AA7000 series fabricated by powder metallurgy & observed decrease in the phase which is undissolved under increased aging time and temperature. Vishwanath et al. [200] have explored the significance of precipitation throughout the cooling process after post-homogeneous and assessed its influence of composition and rate of cooling on the reaction during precipitation. Rohatgi et al. [201] have explored during the microstructure studies & properties of an extruded Al6082 at 170°C for a duration of 8 hours during aging precipitation process which exhibited an enriched mechanical properties & maintained a stable microstructures of an alloy to enhance alloy's properties. It is essential for undertaking number of stages along with intermediate processing stage prior to age hardening. At first, micro segregation need to be removed and inter dendritic particles having low melting point need to be dissolved and the dispersoids need to be precipitated with the help of a homogenization heat treatment. When the strengthening particles undergoes precipitation, the metal need to be treated with solution to allow it to reach to super saturated solid solution before process of aging. Each time, after processing at high temperature, cooling at room temperature need to be done. Hence, microstructure after quenching is considered as an initial stage for the subsequent supplementary processing. The transition of brittle-to-ductile which is occurred in metals was documented since many years which resulted in a rapid revolution in its transitional behavioral changes from brittle to ductile along a narrow range of temperature.

2.10 REVIEW OF PROCESS

Recently numerous manufacturing processes were used for fabrication of aluminum composite materials like stir casting [202], powder metallurgy [203], pressure less infiltration, and in-situ methods [204]. These methods are used for fabrication of Al MMCs at different weight or volume percentages of the reinforcement. During these fabrication processes, it is very hard to avoid porosity and clustering of particles in the matrix base material. Ancillary processes like forging, rolling and extrusion is essential to decrease porosity [205] and to increase interfacial bond between the matrix-reinforcement phases in MMCs.

W.C. Shi et al. [206] and Pradeep Kumar et al. [207] made their study on hot forging and revealed that surface cracking is a problem during the forging operation with Al MMCs, because of which, the crack generated on the surface of billet and reduces the quality of production. Authors observed that, during the forging process, cracks appeared in the cluster of silicon carbide particles & at interfaces of reinforcement & matrix material and the cracks which emerged starts to enlarge when percentage weight of SiC increased. Further increased forging [208] deformation ratio, can cause the reduction in the porosity and the dispersal of SiC particles inside the molten aluminum metal found to be more homogeneous. Ceschini L. et al. [209] published a article on the forging process of an Al-Al_2O_3p composite and have demonstrated that, because of forging operation, it is there is a slight enhancement in tensile strength, hardness, elongation & young's modulus during tensile test. Further, they studied the morphologies of fracture surface by using SEM analyses and demonstrated similar morphologies for cast and forged Al-Al_2O_{3P} composite material, at both room temperature and high temperature.

Arrhenius-type constitutive equation is formulated to understand the constitutive flow behavior during the hot rolling operation of Al and SiC_p composite material as demonstrated by Meola et al. [210]. This specimen is then studied further to find the stresses in all three directions which is damaged due to reduction in the hot rolling process of Al-SiCp material. The damage value was increased by increasing the reduction ratio. Further El-Sabbagh et al. [211] discussed that, when the size of the silicon carbide reinforcement particle and its percentage weight increased, It is found that the crack/damage near the edges increased drastically during the hot rolling of Al-SiCp material plate.

Ainhoa Riquelme et al. [212] demonstrated the production of MMCs from aluminum and copper alloy chips through hot extrusion processes and investigated various properties like tensile, impact, wear and micro-hardness. Further, it was noted that improvement in all mechanical properties except ductility. Ezatpour et al. [213] studied microstructural properties of extruded Al-Al_2O_3 composite material, and have noticed that Al MMCs are more uniform in nature for as cast and extruded components. Cao et al. [214] examined an extrusion operation on micro pins which gave mathematical results on the extrusion process and established a possible process for micro-forming. Further it was noted that, effect on grain size was investigated with the help of heat treated specimens to produce different sizes of grain. A new technique RKEM was implemented to analyze the process of micro-extrusion to compare with the results of both experimental and FEM.

Since, all the above primary processes of casting are costly and difficult to fabricate, stir casting process is used as primary process. Since rolling and extrusion considered as a secondary processes which are costly and difficult to operate, the forging process is used for secondary operation.

2.11 REVIEW OF ANALYTICAL MODELLING

Many researchers have developed analytical and numerical modelling to find the stress, strain, velocity of material flow, deformation and damage during the forging operation. Authors used a DEFORM 3D [215] FE tool for finding stress, damage, and velocity, but they considered an aluminum matrix phase as more plastic rather than elastic. A secondary operation or forming operation proposes and develops new FE tools [216] such as DEFORM 3D, QFORM, FORGE and MSC SUPER FORM. Y. Shen et al. [217], Mohan et al. [218] and Behrens et al. [219] have demonstrated FE and experimental methods to observe an initialization and transmission of crack/damage in hot forging operation based on the damage model of Gurson Tvergaard Needleman (GTN). Further, they compared them with FEM and experimental values. Since, only limited researchers have explored the simulation of forging operation on Al-SiC composite material and examined the damage values by using the FE method, Analytical software ABAQUS is used for analyses of constitutive flow behavior in hot rolling operation on the Al MMCs material which helped the user to improve the present system. The effect of cold and warm forming operation of MMCs material is simulated in MSC-Super Form software and an investigated forming property were demonstrated by Behrens et al. [218]. The FORGE-3 code [89] is used for simulating hot forging processes on the industrial parts and its evaluation of thermo mechanical and numerical solutions. Maity et al. [220] demonstrated the extrusion process in the Deform 3d tool and gave a mathematical evaluation of contoured die. They noted that both contour dies are important parameters in the development of surface reliability of extruded components. Also, there is a continuing reduction through the extrusion operation which gives the homogeneous microstructure of materials in the current analysis by using 3D-upper bond method at different extrusion ratios. That was calculated as the dimensionless parameter such as pressure required for the extrusion process and approximated die length. Many researchers have made numerical simulation of the forging process by using constitutive analysis with an Avrami-Type equation and Manto Carlo simulation method applicable for the most forming processes [221-224].

2.12 REVIEW OF APPLICATIONS

Application of secondary operation such as forging on Nano MMCs shows that the MMCs with an ion Nano sized particle imparted excellent & assurance for the application of aerospace, electronics and automotive companies [224, 225]. Forged and extrusion on Particulate MMCs are the new composites which found their application in marine, aerospace, motor, electronics products, sports industries [226,227]. Forged Al MMCs applicable for the production of automotive and aerospace components like crankshaft, disk brake, cylindrical head, valve, piston, combustion chamber, propeller shaft, turbine, wings, etc. Hyo Lee and Jae Yeo [228] demonstrated the properties of Al-SiC MMCs material for the compressor pistons of air-conditioners and have calculated during the hot forming process like hot forging, pressing, and extrusion. Y Zhang et al. [229] demonstrated the mechanical properties & its microstructure of Al-SiC composites during cold forging on gears and investigated properties such as tensile strength and micro hardness of forged gear and noticed an increment by 40% and 50% respectively. Cui Yuan et al. [230] have demonstrated the multi-functional aerospace applications of forged Al/SiCp composite material. They revealed that silicon carbide particles are Al/SiCp composite were used in place of Tungsten particles to create substrates with optical mirror in a satellite which is expected to reduce its mass by 10 kg, which further reduced the weight of supporting structures in saving the fuel. Shao-Yi Hsia et al. [231] examined the wear properties of cold forging operation on the hexagonal bolt and nuts. They noticed that, due to the cold forging operation, a small improvement in wear of the nuts and bolts was observed.

CHAPTER 3
SCOPE OF RESEARCH WORK

This chapter presents the problem definition, research gaps objectives of the research methodology and techniques adopted to develop and to test the aluminum graphite composites.

Research Gaps

Few researchers successfully worked on development of composite based structures; but limited work has been performed to develop graphite composite for structural applications and optimization of wear parameters.

Hence the objectives of the present research is to develop an aluminum composites incorporated with graphite for various mechanical structural applications and to `conduct experiments to reveal the consequences of various factors on the performance of composites during adhesive wear and to optimize the wear parameters using design of experiments and to find out the effective resultant combinations to optimize the parameters which could be resulted in reduction in the rate of wear of composites.

3.1 OBJECTIVES OF RESESRCH WORK

1. To fabricate Aluminum composites with different percentage and size of Graphite as reinforcement particles.
2. To investigate the effect of reinforcement on the mechanical properties of Aluminium composites.
3. To investigate the effect of heat treatment on the mechanical properties of Aluminium composites.
4. To optimize the tribological properties of aluminum composite using Taguchi technique and ANOVA method.

- Optimization of the process parameters, % wt. of graphite and duration of ageing for studying mechanical properties and fatigue analysis.
- Fabrication of graphite reinforced composites specimens with the help of liquid metallurgical technique.
- Characterization of aluminum graphite composite specimens for tensile, hardness, fatigue tests for various ageing processes.
- To conduct experiment to understand the wear behavior of ALMMC reinforced with graphite particles in accordance with ASTM standards.
- Optimizing the results obtained during experiments for number of iterations using design of experiments (DOE).
- Developing correlation for wear rate based on experimental results with analytical model results.
- Analyzing the morphology of worn out & fractured surfaces with the help of Scanning Electron Microscope (SEM).

3.2 SCOPE AND LIMITATION OF PRESENT WORK

This research work represents a profile of the research under taken with respect to graphite reinforced composites, objectives of the research work and methodology of the experimental studies.

An exhaustive literature survey and market survey was performed to identify the topic for research and the parameters to focus on. Once the topic was chosen and materials selected, DOE was done using Minitab tool in order to minimize the number of trails during the experiments without compromising on the quality of the data collected. Taguchi orthogonal array L-18 was used for DOE. Then, the specimens were fabricated using liquid metallurgical technique and are fabricated as per the required dimensions using turning and milling machining operations based on ASTM standards which were obtained during literature survey. Artificial sea water was prepared in a tank which controls the temperature, in which the specimens allowed to corrode for 90 days at a constant temperature of 50°C. The aged composite specimens were characterized by tensile test and flexural fatigue test. Established on the experimental data, the process parameters and reinforcement-to-resin ratio, were optimized using Grey-Taguchi analysis.

3.3 METHODOLOGY

The Fig 3.1 describes the methodology adopted to discover the various mechanical and tribology properties and various equipment & tools which were employed at various stages of research to complete the research work.

The objectives of all the tasks under taken in the report are as follows:

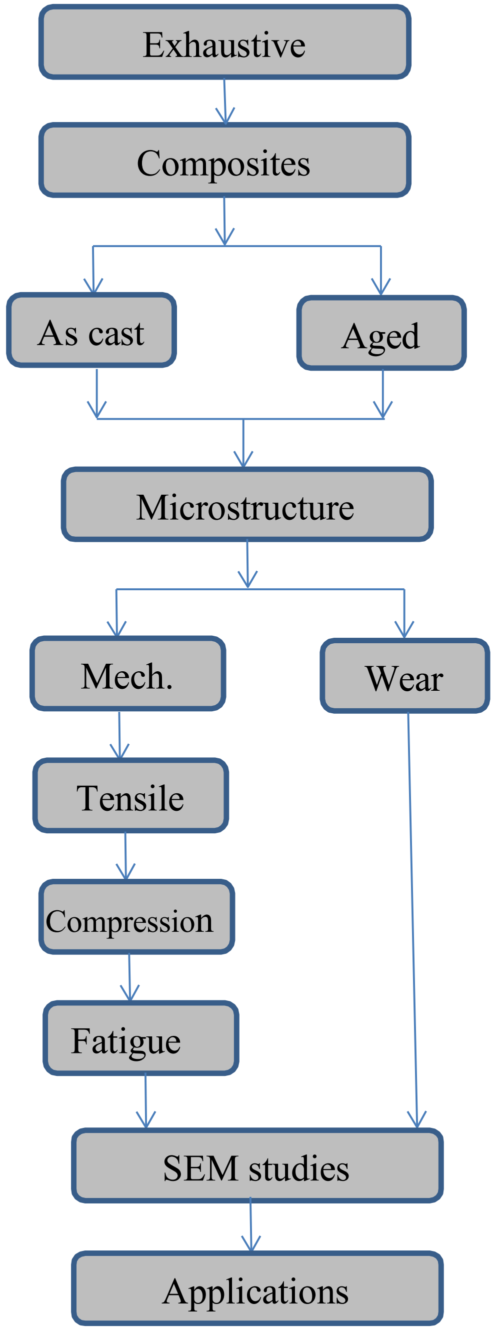

Fig. 3.1 Flow chart for the research

3.3.1 STUDYING THE EXISTING ALUMINIUM COMPOSITES TO IDENTIFY THE GAPS

An exhaust literature survey made on the fabrication and characterization of MMCs of Aluminum alloys and its composites, fabrication technology, end applications, thermal properties like residual thermal stresses, thermal coefficient of expansion, residual deformation and dislocation density around the particles and their effects is also studied in detail.

Mechanical properties, wear studies, corrosion properties, microstructure studies, Fractographical studies, worn surface studies, corroded surface studies and machinability studies also made thoroughly.

3.3.2 DEVELOPING, FABRICATING AND TESTING OF MMCS

1. Selection of Materials

a) Matrix metal

Aluminum is considered as matrix base material because of its superior cast properties, exceptional strength and its flexibility in adjustment during mass production of lightweight casted products.

b) Reinforcement

Graphite generally referred to as "intercalates" in patent literature. Hence graphite of size 30 to 70 nm in the varying proportion of 5,10,15,20 wt. % is used as reinforced material.

c) Fabrication

Steps involved in fabricating graphite reinforced metal matrix composites

- Exercising Pre-casting precautions
- Flushing pure argon gas in order to avoid oxidation by creating an inert atmosphere making degasification of molten metal.
- Supplying the pre requisite quantity of super-heated liquid molten metal into the mixing chamber.
- Supplying a pre requisite quantity of preheated Nano clay particulate into the mixing chamber.

- Creating an instant vortex and pouring it into the die.
- Specimens, at the end were taken out from the split die.
- Extra and unwanted material from the specimen is removed by cleaning Process.

d) Testing the quality of casting

- Macro-cracks and voids on the surface of the specimen were inspected visually and detected.
- Microscopic observation was performed to confirm the uniform distribution of the reinforcement particles.
- The density of the composites is found practically and simultaneously compared with its theoretical density.

e) Heat treatment

- Specimens were treated with a solution in a protective atmosphere (Nitrogen)
- Specimens were subjected to homogenous heat treatment for a fixed time duration and were then water quenched at room temperature.
- Specimens were subjected to natural ageing at operating temperature.
- Specimens subjected to aging at 175°C at different duration of times and finally solidified at room temperature.

f) Microstructure studies

- Specimens were fabricated by sectioning/turning, grinding and then polishing operation which in turn followed by etching for microstructural studies as per ASTM F2450-04 standards
- Testing for mechanical properties
- Tensile test is conducted in accordance with ASTM E8-82 standards using UTM at room temperature.
- Compression test was conducted in accordance with ASTM E9 standard using UTM.
- Hardness test is conducted as per ASTM E384 standards with the help of Leitz Wetzlar micro hardness tester which is equipped with Vickers

diamond pyramid indentor.

g) Fracture studies

SEM examinations of the specimens which were fractured during tensile and fatigue tests for different wt. % and with different sizes of Nano clay particulate was performed.

h) Wear studies

- Dry sliding wear test is conducted with the help of Pin-on-disc machine on each reinforced and non-reinforced specimens at room temperature.
- Specimen having size 8 mm dia x 15 mm length were fabricated for the test purpose.
- The test was performed at various applied loads and rotating speeds.

Design of experiments and Taguchi gray method

The Taguchi method is widely used to design various industrial components to enhance their quality and rectify the problems found during production. This approach is very effective in enhancing the efficiency of experiments. Only less number of experiments are required based on an orthogonal array. Gray rational analysis (GRA) method is suitable in solving complex problems depend on the interrelationship between several factors and variables of response by analyzing the similarity among the sequences using the grey relational analysis. Later, the Grey-Taguchi method was formulated to optimize accurately and effectively various processing parameters in investigating the effect of each factor on the response variables Hence,Grey-Taguchi method is applied to optimize various process parameters by combining the Taguchi method with Grey Relational Analysis (GRA) which involves the following steps :

Taguchi method is used to design an experiment by designing the orthogonal experiments.

Analysis of variance (ANOVA) and signal to noise ratio (SNR) methods are used to analyze the data.

GRA is used to convert the response targets into a single GRG that can be quantified.

GRG is used to optimize the parameters.

The Taguchi method uses orthogonal test and signal-to-noise ratio technology to optimize parameters. It' is a powerful tool for in optimizing the quality of components during manufacturing processes.

Here are some of important features of the Taguchi method:

It decreases the sensitivity of the system to noise changes by choosing a combination of levels of controllable variable factors.

It splits the quality characteristics as smaller-the-better, nominal-the-better, and larger-the-better.

It adopts a design of orthogonal arrays in studying the entire parameter set with a less number of experiments.

It defines a functional loss in calculating the deviation among the desired values and experimental values.

The Full Factorial Design requires a large number of experiments to be carried out and hence it becomes complex and laborious since there in increase in the number of factors. Hence Taguchi suggested an exclusive method of using orthogonal array to study the entire set of parameters by conducting lesser no of experiments to be conducted. In regard this, Taguchi recommended the use of functional loss to measure the performance characteristics that are getting variation from the desired target value. The value of this functional loss is transformed further into signal-to-noise (S/N) ratio. Usually, there are three types of the performance characteristics for analyzing the S/N ratio namely nominal- the-best, larger-the-better, and smaller-the-better.

Steps Involved in Taguchi Method

a. Recognize the main function and its side effects.

b. Recognize the noise factors, quality characteristics and testing condition.

c. Recognize the functional objective to be optimized.

d. Recognize the control factors along with their levels.

e. Choose a suitable Orthogonal Array to construct the Matrix

f. Conduct the Matrix experiment.

g. Analyze the data; inspect the levels of optimum control factors and its performance.

h. perform the experiment for verification.

SN) STB=−10∗log10 (1n∑i=1ny2i) (1)

(SN)NTB=10∗log10 (y¯2 s2) (2)

(SN)HTB=−10∗log10 (1n∑i=1n1y2i) (3)

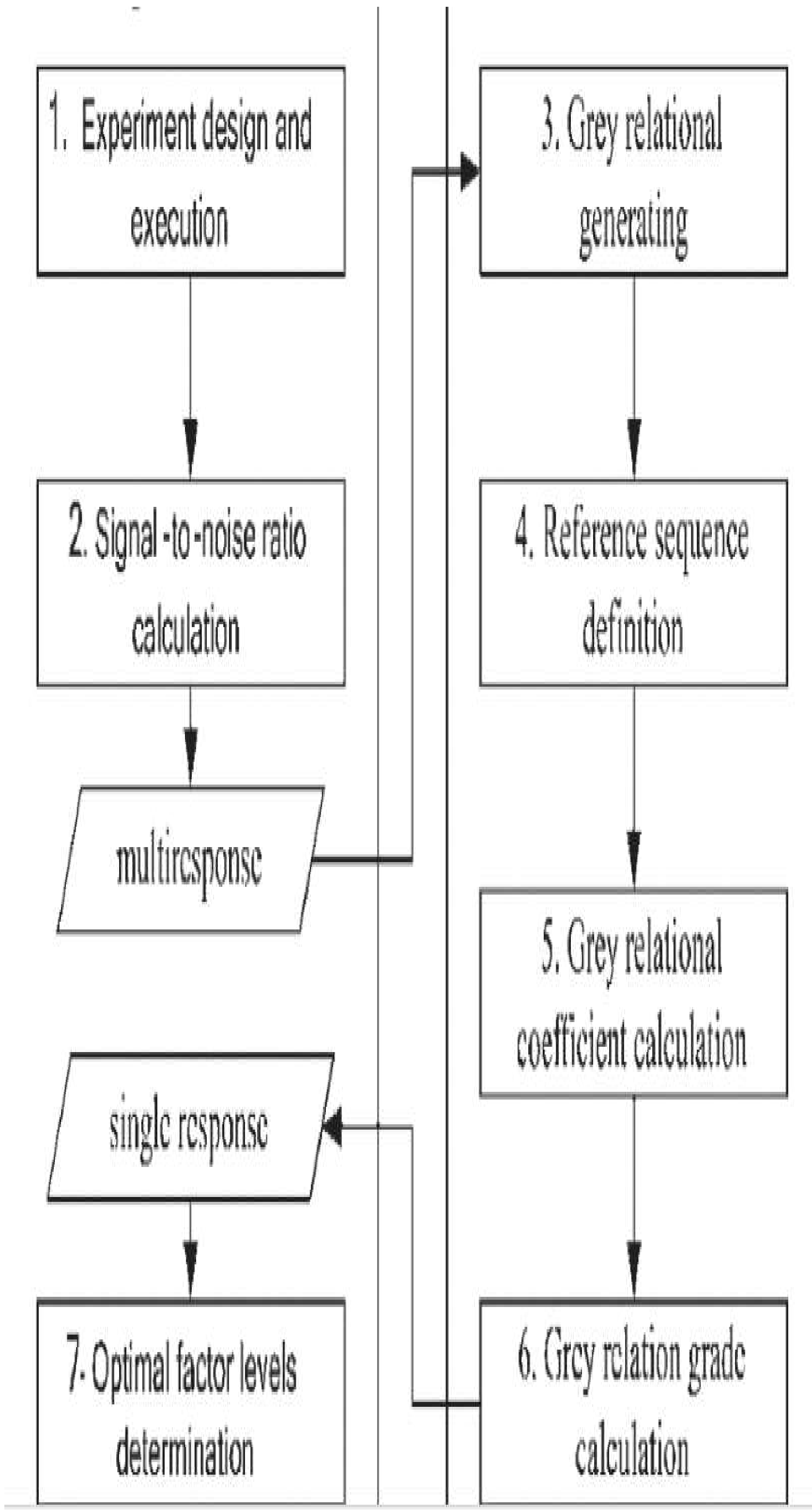
1. Experiment design and execution
2. Signal -to-noise ratio calculation
multiresponse
3. Grey relational generating
4. Reference sequence definition
5. Grey relational coefficient calculation
6. Grey relation grade calculation
single response
7- Optimal factor levels determination

CHAPTER-4

EXPERIMENTAL STUDIES

This section contains a detailed study of the selection of relevant matrix material to develop composites and the characterization for further investigation. It gives an information about the experiment associated with stir casting, extrusion operation, mechanical characterization of composite material, and microstructural characterization of the casted and extrusion MMCs specimens at different weight percentage of graphite.

4.1 MATERIALS USED

4.1.1 MATRIX MATERIAL

It is the major phase of composite having a continuing character and usually more ductile and less hard phase. MMCs are generally made up of Al or Mg alloys having low density and reinforced with a hard ceramic particulates, like silicon carbide, titanium, zirconium, etc. In this work, Aluminum alloy of 6061 series is chosen as matrix material and need is fulfilled by "Ferrite metallurgical Pvt. Ltd. Bengaluru". Al 6061 series material is selected as a base material as shown in Fig 4.1 to form composite. Both chemical compositions and the mechanical properties of Al 6061 is shown in Tables.4.1 & 4.2 respectively. Element with higher percentage in Al 6061 is Mg and other lesser percentage elements are, copper, and magnesium. Al 6061 melts at around 650-750 ºC flows free in molten state.

Fig. 4.1 Ingots of 6061 Aluminum Alloy

Table 4.1: chemical composition of Al 6061						
Elements	Al	Mg	Si	Fe	Cu	Zn
%	Rest	0.85-1.10	0.45 – 0.8	0.6	0.20-0.35	0.25

Al-6061 series has their initial mechanical properties as shown in Table 4.2 which were observed to be improved after casting further

Table.4.2 Mechanical properties of Al 6061

PROPERTIES	VALUES
Density	2.78 g/cc
E	70-80 GPa
Yield point	275 MPa
Tensile point	350 MPa
Poisson's ratio	0.33

For MMCs planned to be used at prominent temperatures, a further consideration is that variation in melting point between matrix and reinforcement phase. Because of the large melting temperature difference in MMCs may result in creep generated in phase of matrix while the phase in reinforcement remains in elastic condition, even though temperatures close to the melting point of matrices.

4.1.2 REINFORCED MATERIAL (GRAPHITE)

Graphite is a reinforcing material used in this research as needed to form composite. This reinforcing material is less expensive as compared to other reinforcements. Graphite is selected as reinforcement material since it possesses highest hardness and low thermal coefficient of expansion. Graphite is highly resistant to wear &also possesses good mechanical properties like resistance to high temperature and thermal shocks.

4.2 SET UP FOR FABRICATING COMPOSITES

The stir casting method which is of liquid processing route has been chosen in this research work during which, the selected matrix material initially is heated in an incubation chamber (furnace) until it reaches to its melting point and simultaneously, the reinforcement material is also added after a saturation point is attained inside the chamber and stirred slowly using a mechanical stirrer arrangement provided on equipment till it disperse uniformly. Hence, it is used as

a) Aging bath furnace

b) Furnace controller

c) Motor stirrer

d) Clay graphite crucible

Fig 4.2 Facilities used during casting process

the most suitable method in this research. Once the constant stirring is done, the mixture is then poured into the mold cavity to get final cast specimen with better directional solidification.

The fabrication of composite specimen is performed with the help of a setup of machinery and tools to be used. The main equipment and tools used here are as a furnace, mold cavity, stirrer, tong, and crucible shown in Fig. 4.2. The furnace is cleaned and adjusted to the required temperature & then the aluminum ingots were placed in a crucible which are further kept in the furnace [55]. The aging bath furnace has a maximum of 1200°c temperature which has a chamber capacity of 12”x12”x8”. The power rating of the furnace is 9 KW. The thermocouple used here is Cr/Al with SS and the heating element is Kanthel Aluruinal with the accuracy ranging closely to 1°c.

The set up for the furnace equipment used during the conduct of experiment is shown in Fig. 4.2. The controller has a voltage meter which shows the voltage across the heating coils and ampere meter which indicate the amount of current passing through it. It has the temperature indicator and also has a adjustable regulator to set the required temperature. Fig. 4.2 (c and d) shows electric stirrers and clay graphite crucible used here. A crucible is a refractory container which can hold up very high temperatures to melt or otherwise modify its reinforcements. It is used for melting of the materials such as glass, metals and pigments during production. The motor assisted stirrer equipment is used for uniform mixing of the liquid molten metal to speed up the reaction. Stirrer was designated for the purpose of uniform mixing of all solutions, liquid, oilment, viscous material and solid-liquid homogeneously

4.3 COMPOSITE FABRICATION

- ✓ The Gr reinforcement was in amorphous form and hence wrapped in aluminum foil to ensure uniform dispersion.
- ✓ Same as that of reinforcements are weighed carefully as per the selected strategy of forming different casting composition. Also safe handling of these particulate was made with proper maintenance.
- ✓ Main process now begins with setting up the arrangement for casting equipment. Initially graphite crucible is placed inside the induction chamber at proper center.
- ✓ Later a vertical rod holding graphite plug at one end is inserted in the chamber. It ensures that the bottom opening of the crucible is closed properly.
- ✓ With complete setup, Al-6061 cut pieces (1kg) are fed into the crucible without disturbing any arrangement. Later the combustion chamber is closed with the help of lid cover at top of the chamber
- ✓ Induction chamber is then started with a power supply and also temperature indicator is made on to set the required temperature (850ºC)
- ✓ The temperature setting device is then adjusted to read melting point value of aluminum alloy.
- ✓ The System is left to operate until the temperature reaches its preset value and material in the crucible melts completely.
- ✓ Simultaneously, while operating with Al6061 and reinforcements ash are set to preheat at 400ºC for about 1 hour of time.
- ✓ Now metal in molten state is made slag free by adding coverall flux-6 and degasification powder and soon the reinforcements are fed carefully in to the crucible containing molten metal.
- ✓ Instantaneously stirrer immersed in the molten metal is started to rotate at 300 rpm as displayed in Fig. 4.3.

Fig 4.3 Setup for Stir casting technique

- ✓ To obtain a uniform dispersion of reinforcement particles, stirring action is performed for almost 25-30 minutes is carried.
- ✓ After finishing the stirring the motor is stopped and the graphite plug placed over the bottom opening is lifted to allow the molten mixture to pour in the mold arranged at bottom.
- ✓ Funnel arrangement is done to provide a correct path to flow the material in mold.
- ✓ Finally after pouring complete material in to the mold the bottom opening is then closed and flow is terminated.
- ✓ Mold with molten mixture in it is left at room temperature to solidify.
- ✓ After being cooled at room temperature the material inside the mold is removed carefully and is obtained.
- ✓ Alike procedure is followed to obtain all other composites for respective compositions.
- ✓ Results for every casting are obtained by testing the specimens for each casting, prepared with precise size configurations.
- ✓ Different tests and methods are explained in next sub-section
- ✓ Once the casting got solidified after 24 hours, they are taken out from the mold cavity and fabricated according to the desired shape and sizes of dia 60 mm and width 50 mm for extrusion operation. The casted aluminum rods obtained after cooling as shown in Fig. 4.4.

Fig. 4.4 Aluminum castingrods after solidification

4.4 MACHINING OPERATION

Once casting is completed, the turning operation is performed on the rod which is taken out from the mold cavity to the required dimensions of 55 mm diameter and a length of approximately 50 mm using lathe machine to get a smooth surface finish. The turning is done at a slow speed so as to get the desired optimum surface finish. The lathe used is shown in Fig. 4.5.

Fig 4.5 Lathe Machine: Kirloskar Turnmaster-45

The turning operation performed on the lathe is shown in Fig. 4.6 with an auto fed setup so that an even surface finish can be obtained. With an optimum speed of 600 rpm, the whole turning process is carried out. Finally the dimension of 55 mm is achieved and a hacksaw blade is used to cut the specimen for length of 50 mm. The Fig. 4.7 shows the final output of the specimen after turning on lathe machine.

Fig 4.6 Specimen preparation for extrusion

Fig 4.7 Specimen after turning Process

4.5 MECHANICAL CHARACTERIZATION

Details of data is collected during the experiments conducted on Al6061 composite which is herewith presented and is further compared before and after the extrusion.

The following tests are conducted as per ASTM standards

1. Brinel hardness test of heat treated Al6061 matrix alloy and its composite specimen is carried out as per ASTM E10.
2. Tensile test of heat treated Al6061 matrix alloy and its composite specimen is conducted in accordance with ASTM E8/E8M-15a standards.
3. Compression tests of Al6061 matrix heat treated alloy and its composite specimen are carried out as per ASTM E9.
4. Wear test of Al6061 matrix heat treated alloy and its composite specimens is performed as per ASTM G99 Standards.

4.5.1 HARDNESS TEST

The Brinel hardness test is performed for both non-heat treated and heat treated specimens as shown in Fig. 4.8. The ball indentation with a minor load of 31.50 kg applied on specimens at a dwell time of 20-30 sec. The hardness test is performed along the direction of extrusion operation and its value is assessed with the help of a formula of applied load divided by the surface area under the indentation.

Fig 4.8 Vickers and Brinell hardness testing machine

Brinel hardness test is conducted at three different positions to assess the possible influence of ball indentation on metal matrix composites and an average of all the three readings is considered to calculate BHN of the specimen. The load to be applied depends on the material and a P/D^2 ratio which is constant for Aluminum

$$\frac{P}{D^2} = 5 \text{-------------- } 1$$

Because of the limitation of testing machine, we have selected 2.5 mm ball indentor. At D=2.5 and mm P = 31.25 kg

The BHN is obtained by the dividing applied load to the indentation surface area:

$$\therefore \text{BHN} = \left[\frac{2P}{\pi D\left[D-\sqrt{D^2-d^2}\right]}\right] \text{kg/mm}^2\text{----------}2$$

Where, P: Load Applied to specimen (kg)

D: Ball indentor diameter (mm)

d: Mean diameter of indentation (mm)

4.5.2 TENSILE TEST

It is a simple test for testing the property of a material during which, the test sample is subjected to tension until it get failure/ breaks. The tension test results is commonly used for the selection of a proper material as based on an application, such as aerospace, automobiles and to forecast how the materials will respond under different types of loads/forces.

Tensile test is conducted at room temperature with an Instron-5500 R UTM as shown in Fig.4.9 (a). Fig. 4.9 (b) demonstrates the tensile samples for tensile test fabricated in accordance with ASTM.

Fig.4.9 (a) Universal Testing Machine

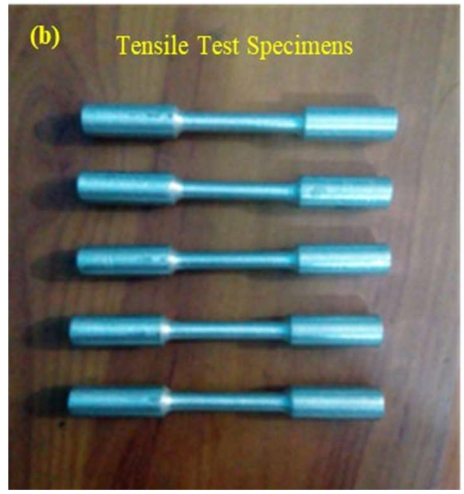

Fig.4.9 (b) Tensile specimens of Al composites

E8 standard with 20 mm gage length, 6 mm gage diameter and the total length is 60 mm. These specimen are machined from composites of both casted and heat treated in the ratios of 2.66 and 5.32 with a tensile axis which is perpendicular to the direction of extrusion.

Tensile tests of fabricated composites were performed as per ASTM E-8 standards using universal testing machine of Model: TUE-C-400.The test was performed at Advanced Metallurgical Laboratory (AML), Peenya, Bangalore. Fig. 4.9(a) demonstrates tensile testing machine setup. The specimens were machined in accordance with ASTM standards as displayed in Fig. 4.9 (c). Continuous strain rate of 0.4 mm/min was retained throughout all the tests to evaluate the ultimate tensile strength.

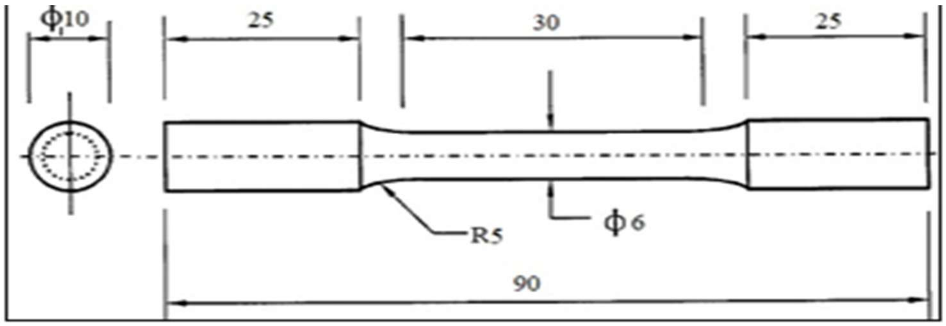

Fig. 4.9 (c) Dimension of the Tensile specimens

4.5.3 COMPRESSION TEST

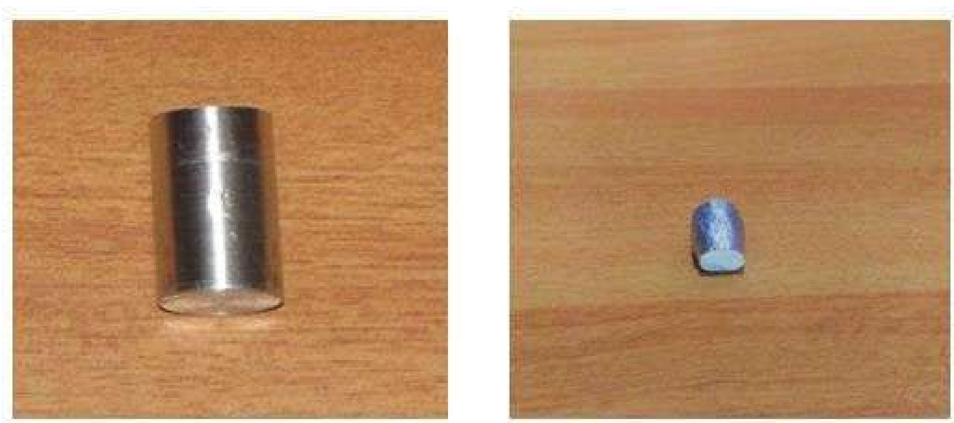

a) b)

Fig. 4.10 Specimen for compression test a) initial testing condition b) Final condition after testing

The compression test is carried out as per ASTM E9 standards and the specimens of ϕ15 mm and 20 mm length were taken for the test. The tests are carried out with the help of Universal testing machine with an attachment to make slow movement of cross head. Compressive strength for each specimen for respective composition is obtained directly from the test results. Universal testing machine is operated for this test. Loading each specimen until its fracture point gives the results for compressive strength. An Increasing load is applied vertically downwards on the specimen surface. Figure 4.10 shows compression test specimens prepared under ASTM standards of E9 series. A Dimensional ratio of 1:2 is followed for diameter to length ratio, which prevents bulging and buckling. A dimensional specification for specimens is diameter is 15 mm and length is 30 mm. While testing the specimen, it is held firm in the grips at bottom to withstand the applied load. Hydraulic actuator is operated to apply on the upper surface of the specimen. Analog pointer with scale for load applied is used to measure the compressive strength. The point at which the specimen breaks are tabulated and is a measure of compressive strength of the material.

4.5.4 WEAR TEST

Dry wear test is performed on both the specimens of heat treated and un-heat treated using pin on disc set up which consists of a rotating disc of EN 4 materials against the cylindrical specimens with various loads and speed shown in Fig. 4.11.

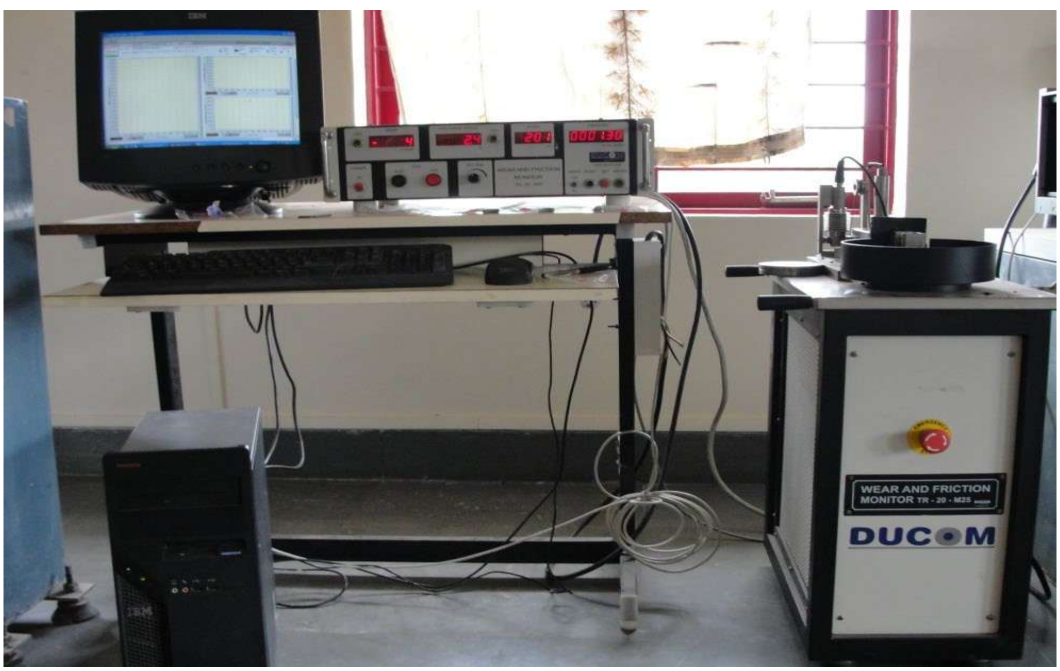

Fig 4.11 Pin-on-disc set up for wear test

The monitor adjacent to the set up displays the wear and friction force which will be noted down for further calculation. The DUCOM pin-on-disc wear tester of model TR-20-M25 is used here.

4.5.5 GRAVIMATRIC CORROSOION TEST

The required size of the specimen for Corrosion test is of Φ10mm X 25mm length are prepared and kept in a three different normality's of HCl solution. The required specimens for experiments were machined from heat treated rods as per standards, then polished with a series of emery papers and washed with water and then with acetone. Gravimetric corrosion test was conducted for a duration of 24, 48, 72 96 and 120 h in 250 ml of 1M HCl solution. After exposure, corroded specimens were cleaned with Clark' solution and soft brush then dried. The weight loss after corrosion tests is determined by measuring the difference in weights before and after test up to accuracy of 0.1 mg. The diameter of the specimen is measured and placed in HCl solution as shown in Fig. 4.12. The weight loss occurred due to corrosion is noted by measuring the difference in weights of specimens of initial and final condition.

Fig 4.12: Specimens immersed in Hcl Solution for three normality's

4.5.6 FATIGUE STUDIES

Al/Graphite composites were fabricated with the help of stir casting process by varying the % of graphite nano particles. The dust particles on surface of aluminum ingots and acidic impurities were cleaned with the help of acetone. An inert atmosphere is created by a nitrogen gas during the melting process. Calculated quantity of pre-heated graphite along with 1% of Mg powder is added with the molten metal during stirring itself and this slurry of molten metal is then poured into the preheated metallic die. After solidification, the specimens were taken out and machined as per the dimensions given Fig.4.13 (a). Then, the specimens are subjected to grinding with precision grinding machine and finally polished in longitudinal direction on its surface using an emery paper of finest grade. A proper care need to be considered to make sure that no undercut happens at the transition of cylindrical cross section and fillets occurred during the process of machining. A non-corroding grease must be applied on the surface of the testing specimen to protect against an undesirable corrosion which may occur at any time. The

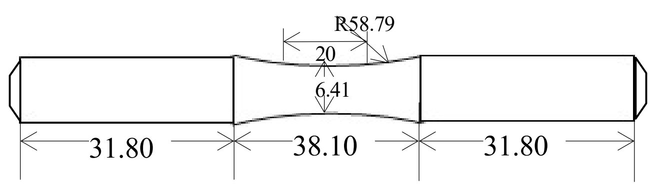

Fig. 4.13 (a) Specimen dimensions for rotating beam fatigue test

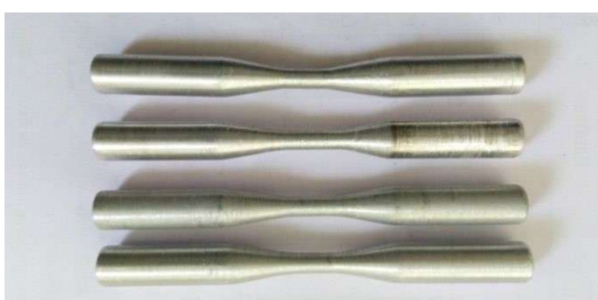

Fig. 4.13 (b) Prepared specimens for fatigue studies

Specimens for conducting the fatigue test were fabricated according to drawing 4.13(b).

Al/graphite composite specimens were solution heat treated by keeping them in a muffle furnace for a duration of 1 hour, at a temperature 550°C and then water quenched. Heat treatment for artificial ageing was conducted by keeping the specimens in a muffle furnace for a period of about 2 hrs and at a temperature of 180 °C, followed by air cooling. Heat treatment for over ageing was also conducted by placing the specimens in a muffle furnace at 280^0 C, for a period of 2hrs and then followed by air cooling. The specimens were polished as per standard metallurgical procedure for the purpose of microstructure analysis. The samples were analyzed using Neophat optical electron microscope (OEM) after etching with Keller's regent.

Fatigue tests were conducted with the help of rotating beam cantilever type fatigue machine as displayed in Fig. 4.14. The specimen made to fix rigidly onto the collets of the machine and a poise weight is loaded in accordance with pre requisite bending stress. The fatigue machine is subjected to rotate at a continuous speed of 700 rpm and its number of rotation is noted with the help of a cycle counter. The radial load is measured by pasting the load cell between the specimen holders .The fractured specimens were collected by a part catcher fixed below the bearing support. Specimens which were tested at various loads considered as sufficient data for developing Stress vs. Number of cycles (S/N) curve. The fracture surface were studied under TESCAN scanning electron microscope.

Fig. 4.14. Rotating beam fatigue machine used For testing the specimen

4.5.7 MICROSTRUCTURE ANALYSIS

The coarse grit formed during the previous processes which was carried forward is prevented by washing the cloth used for cleaning the specimens. After the fine polishing of the specimens, then they were etched with Keller's reagent (1.75 ml HCl, 2.0 ml HNO_3 1.25 ml HF, 90.0 ml water) and dried with an electric dryer. In addition, the microstructure's images were captured for both as cast and heat treated specimens from Optical microscope in accordance with IS: 7789 PART II - 1978 (RA) at Raghavendra Spectro Metallurgical Laboratory, Bangalore shown in Fig. 4.15.

Fig 4.15 Optical microscope

Also, the images were captured with using JEOLJSM-6840LVSEM at RV College of Engineering, Bangalore which is displayed in Fig. 4.16. The grain size of both casted and forged composites was found with the help of grey threshold technique with the help of an optical electron microscope.

Fig. 4.16 JEOL JSM-6480LV scanning electron microscope

CHAPTER 5

RESULTS AND DISCUSSION

The results and discussion are divided into two categories of experimental results and Statistical results.

5.1 MICROSTRUCTURAL STUDIES

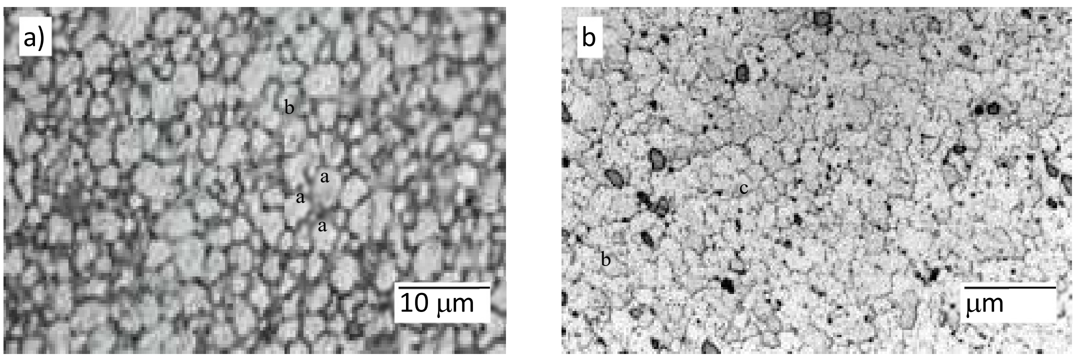

Fig. 5.1 Optical micrographs of a) as cast Al6061 b) 170°C aged Al 6061

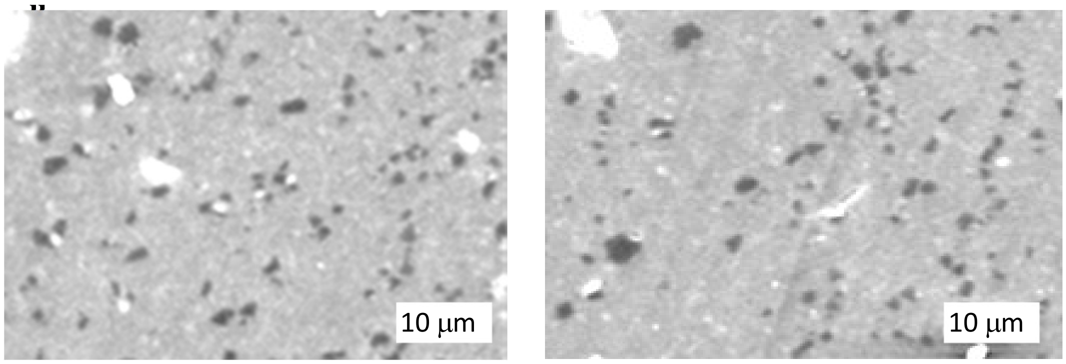

Fig. 5.2 Optical micrographs of a) as cast Al/5% b) 170°C aged Al/5% composites

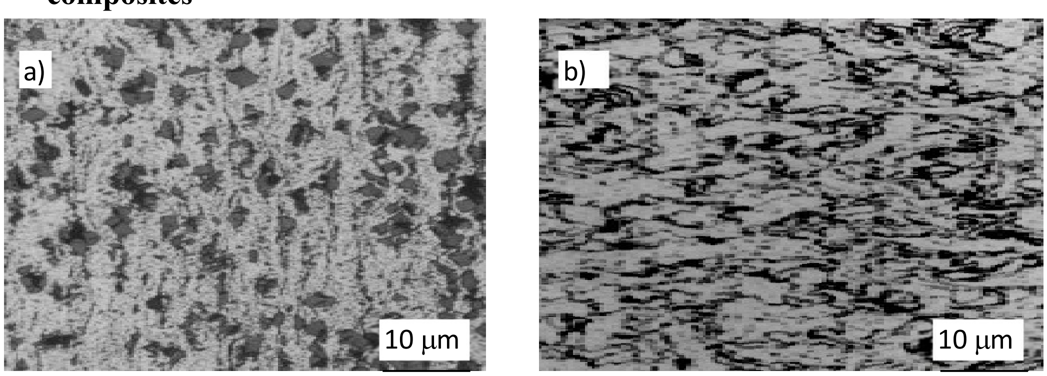

Fig. 5.3 Optical micrographs of a) as cast Al/10% b) 170°C aged Al/10% composites

Scanning electron microscopes used to investigate the morphology of Al 6061/graphite composites.

The optical microscopic images of both as cast and aged Al 6061 specimens at 170 °C are displayed in Fig. 5.1(a) and (b) respectively. There are three phases which are observed clearly in the microstructure like Eutectic Si phase (a), as α-Al phase (b) and Mg_2Si Phase(c) which are shown in above figures. The α-Al Eutectic phase formed at the grain boundaries due to combination of Si and Al element. The eutectic nucleated initiated during solidification of Al alloy [232].

Fig. 5.2 (a) and (b) show the OM of as cast and 170 °C aged Al/graphite 5% composites respectively where in the graphite distribution seems to be uniformly and this even dispersion of the particles enhances its physical strength of the materials. Only few porous and defects are seen in between particles and matrix alloy. The graphite particles lead the perturbation inside the solute and hence it changes the grain boundaries during ageing until changes to dendrite structures.

The Fig. 5.3 (a) and (b) OM of Al6061 alloy and its 10% graphite reinforced composites for both cast and aged condition composites Fig. 5.1(a) shows an uniform grain boundaries without dimples and cracks in the surface. Some small patches which are in white color were noticed in the form of polishing materials which is found to be sticked on to the specimen surface. Fig. 5.1(b) displayed some cracks on the surface in the form of black colored lines due to aged conditions besides with small pit type structure which are formed because of reshaping of aluminum metal matrix alloy. During the microstructure analysis, a typical ductile behavior is noticed during work hardening process. Due to age hardened heat treatment, some foreign particles stuck on to the surface which initiated several small cracks which were observed under microscope. Since there were irregular cracks developed, hence surface cracks alone were noticed under microscope. At increased % of graphite (>15%) which is not displayed in figure, several blow holes were noticed due to agglomeration. The occurrence of tiny openings in the nature of shallow pits were noticed on the surface of specimens.

5.2 HARDNESS OF THE COMPOSITES

Table 5.1 Hardness of the both as cast and aged Al 6061 matrix and Al/Gr composites

As cast condition	**Hardness (BHN)**	Aging Condition	**Hardness (BHN)**
Al 6061	94.4	Al 6061	97.6
Al/5% Gr	111.9	Al/5% Gr	113.3
Al/10% Gr	118.4	Al/10% Gr	120.9
Al/15% Gr	105.5	Al/15% Gr	110.0

The average values of hardness for all the specimens obtained during the by experimental study are listed in Table 5.1 and the hardness result of composites is grouped into three categories such as grain boundary, effect of graphite and condition of ageing on the properties of hardness of aluminum composites. The above table represents the influence of % of graphite and heat treatment on the composites.

5.2.1 INFLUENCE OF PERCENTAGE OF GRAPHITE ON THE HARDNESS OF COMPOSITES

The influence of % of graphite on hardness properties of aluminum composites for both as cast and aged condition is shown in Fig. 5.4. There is a linear increment is noticed in the composites hardness when the % vol of graphite is increased irrespective of ageing conditions. The composites hardness is found to be increased to 18%, 25% and 11% for a graphite with 5%, 10% and 15% respectively. Hence, just adding small proportion of graphite which also act as impurity, is enough to increase the hardness because of the development of residual stress during the casting process and because of the grain refinement process. Also, an addition of hard reinforcement particulates into the soft ductile matrix leads to improvement in hardness. The hardness of metal matrix composites increased initially up to a certain 10% wt., and then it decreases with the % wt reinforcement. Another reason is higher difference in coefficient of expansion amongst graphite (− 8.717 × 10−8 K^{-1}) and Al alloy (26 x 10^{-6} K^{-1}) results higher density of dislocation leading to higher hardness

5.2.2 INFLUENCE OF AGEING ON THE HARDNESS OF COMPOSITES

The influence of ageing operation is generally proportional to the mechanical properties viz yield strength, tensile strength and hardness due to the enhancement in grains found during microstructure studies[232-233]. The enrichment of composite's hardness is as a result of resistance to deformation. Ageing provides directional alignment to enrich desirable directional properties found in ductility, strength and resistance to impact resistance and fatigue resistance. In summary, the ageing of composites increases approximately 28% over original casting it was made from. Ageing breaks up the grains which leads to reduce surface porosity to get finer grain structure and hence increases the composite's hardness

.

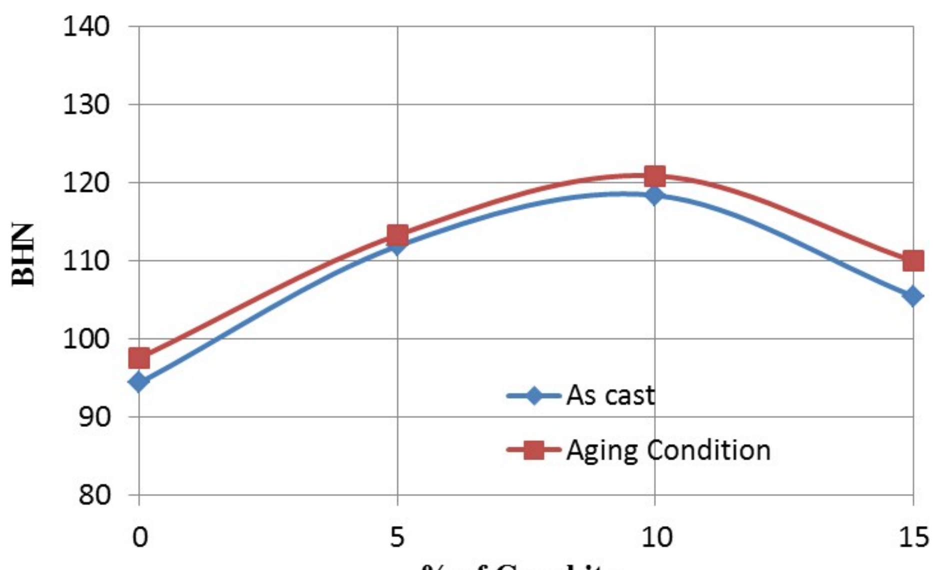

Fig. 5.4 Influence of % of graphite on the hardness of Al/Gr composites for both as cast and ageing conditions.

Similarly, aged composites shown related trends similar to without aged composites. The values of hardness of aged composites were higher and better compared to composites without ageing.

5.3 MECHANICAL PROPERTIES

The mechanical properties such as ductility, ultimate tensile strength and yield strength including the average values for the reference alloy such as Al 6061 and its composites are listed in Table 5.2.

Table 5.2 Mechanical properties of the as cast and aged condition Al/Gr composites

Without ageing condition	**Ultimate tensile strength MPa**	**Yield Strength, (MPa)**	**Elongation in %**	**Aged condition**	**ultimate tensile strength MPa**	**Yield Strength, (MPa)**	**Elongation in %**
Al 6061	239.23	208.12	17.01	Al 6061	252.16	216.85	17.81
Al/5% Gr	257.32	223.86	10.71	Al/5% Gr	266.96	229.58	13.64
Al/10% Gr	270.30	235.16	9.59	Al/10% Gr	292.21	251.29	12.73
Al/15% Gr	255.34	219.55	7.74	Al/15% Gr	264.78	222.32	8.29

5.3.1 ULTIMATE TENSILE STRENGTH

Fig. 5.5 represent the results obtained during the experiments and the consequence of vol % of graphite particles and ageing on ultimate tensile strength of aluminum composites incorporated with graphite particulates. The consequence of each parameter on the composite's tensile strength is deliberated below.

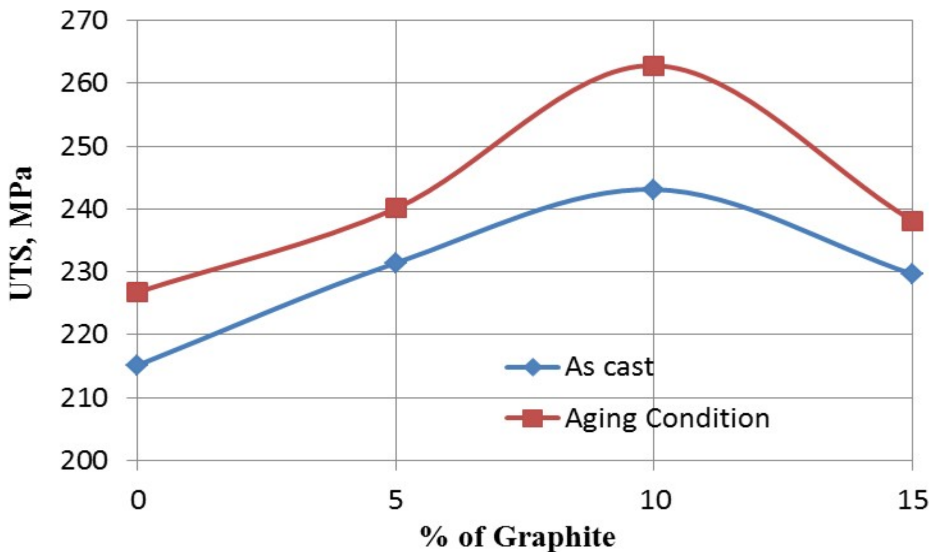

Fig. 5.5 Consequence of % of graphite on ultimate tensile strength of Al/Gr composites for both as cast and ageing conditions.

Fig. 5.5 displays the consequence of graphite content on the composite's ultimate tensile strength which shows an enhancement in the ultimate tensile strength when the graphite is incorporated as reinforcement. The graphite has lower coefficient of expansion in comparison with aluminum matrix alloy and hence there is high localized density, which enhances the tensile strength.

Increase in tensile strength by 13% for without ageing condition and 22% for aged condition of aluminum composites. The tensile strength of graphite (<480 MPa) is much higher than matrix alloy (<250 MPa), which helps to withstand the maximum load from the matrix alloy. One more reason for high strength is, fine grained structure formed due to graphite during solidification. They act as grain refiner due to its specific heat capacity. Graphite acts as contamination in the fabrication process. They are highly sensitive to absorption of environmental gasses, which causes matrix harnessing and brittleness. The dissolved gases are removed by degassing agent but alloying elements are coated on the graphite surface (adhered to the particle) which give higher grip and hence it withstand maximum load.

Results obtained from an experimental study are summarized in Fig. 5.5, which presents the mean value of the tensile strength test conducted on the specimens before and after ageing operations. The ageing induced greater strength to the composite specimens irrespective of reinforcements. This would be because of the effect of the microstructural change after ageing, leading to remarkable increment in yield strength through ageing. A conventional grain boundary was visible but many of that long grain appeared. After ageing the microstructure having aligned a plate and many substructures have formed, they help in the enhancement in composite's tensile strength. Aged specimens exhibited higher amounts of compressive residual stresses than that of matrix allow and this can be endorsed for ageing capability. (56)

5.3.2 YIELD STRENGTH

Fig. 5.6 represents results obtained during the experiments to study the influence of % vol of graphite and ageing on the yield strength of Al/graphite composites respectively. The effect of each parameter on the yield strength of the composites is as follows.

5.3.2.1 CONSEQUENCE OF % OF GRAPHITE ON YIELD STRENGTH

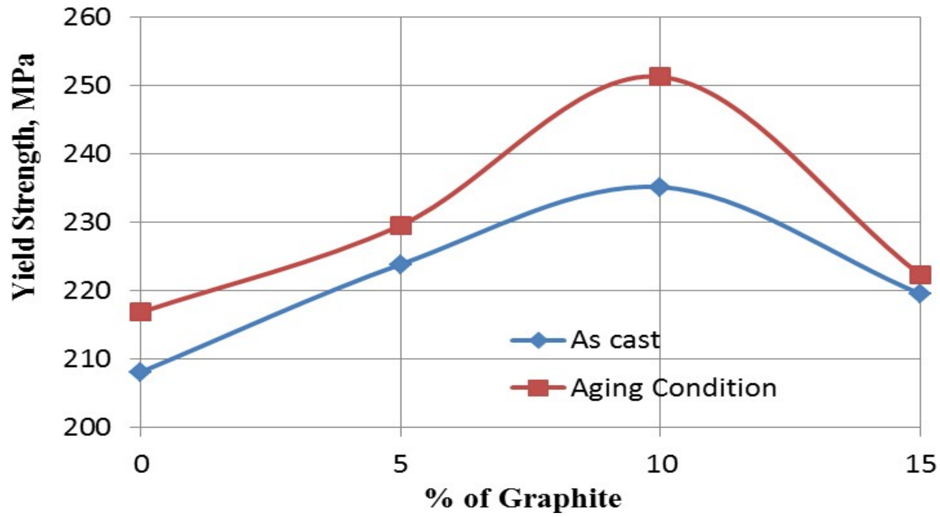

Fig. 5.6 Consequence of % vol of graphite on the yield strength of Al/Gr composites for both as cast and aged conditions.

The results obtained during tensile test are displayed in Fig. 5.6 which revealed that the graphite exhibits a greater yield strength in both without ageing and aged condition of Al composites. The graphite reinforced composites show greater enhancement of yield strength of composites found to be 10- 13%. The variation in yield strength between the materials because of good binding amongst reinforcement and the matrix. An addition of graphite makes stronger bonding between the matrix grain boundaries. . Graphite shows its ability to absorb more energy prior to failure hence yield strength enhances.

5.3.2.2 CONSEQUENCE OF AGEING ON YIELD STRENGTH

The yield strength of an aluminum composites as a function of ageing is displayed in Fig. 5.6 contributes to enhance composite's yield strength due to recrystallization of grains during ageing operation. Also the composite's yield strength with sub-grains is significantly dependent on the grains size. It is concluded that, smaller the grain boundaries, higher is the yield strength and vice versa. In this research work, the grain boundaries size reduction is approximately

10 mm, which influences the yield strength. Aged aluminum composites are definitely lower density compared to other structural materials hence it is an ideal material for aerospace applications.

5.3.3 DUCTILITY OF THE COMPOSITES

The impact of each parameter on its behavior during the composite's ductility is discussed below:

5.3.3.1 EFFECT OF GRAPHITE ON DUCTILITY OF COMPOSITES

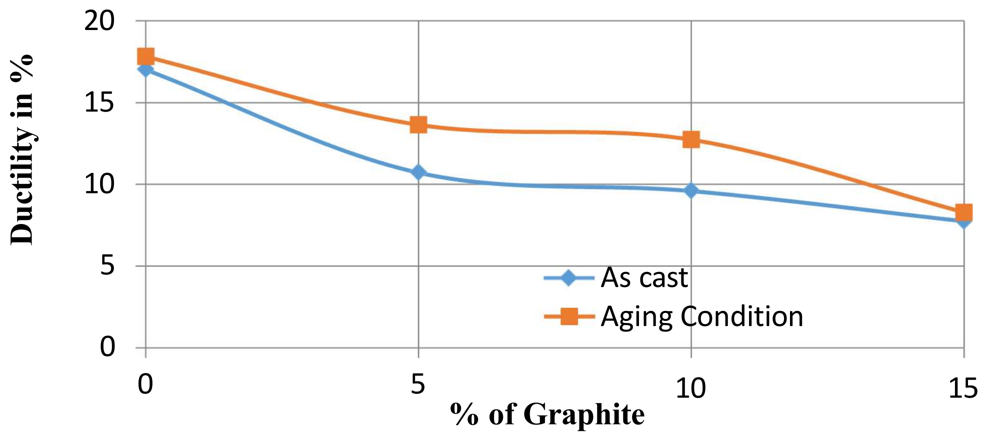

Fig. 5.7 Consequence of % of graphite on ductility of Al/Gr composites for both as cast and ageing conditions.

From Fig. 5.7, it is noticed that the ductility of both as cast and aged composites found to reduce with the increase in % vol of graphite. The reason for this behavior of composites is commonly encountered in particle / dispersed metal matrix composites [234]. Author opinions for this behavior may be void formation during solidification and increase in brittleness due to addition of foreign material into the metal family. Sharma et al. [235] provided solid reasons for reduction of ductility due to non-homogeneous dispersion of the reinforcement and opening of voids amongst reinforcement and the matrix leading to weak interfacial bond. The reduction in ductility in these specimens because of which may get fractured and since sharp corners which are prone to develop localized stresses, initiation of cracks and its propagation. There might be an effect of embrittlement because of the presence of graphite particulates, developing increased local stress concentration regions.

5.3.3.2 CONSEQUENCE OF AGEING ON THE DUCTILITY OF COMPOSITES

Fig. 5.8 displays the influence of an ageing on the ductility of aluminum composites incorporated with graphite particles during which, it is noticed that ageing process causes an increment in ductility irrespective of the % graphite. An increment in ductility is might be due to recrystallization, reduction in casting defects and refinement in grains in matrix base material during the ageing process of alloys and the composites. When these parameters combined together contributes in improving the boundary strength and ductility of both base matrix material and composites. The ductility values of extruded composites were established higher values and better than the composites without ageing. This is because of a uniform distribution of hard particulates in soft ductile matrix which improves the strength at the reduction of the ductility when wt. % of reinforcement is increased. This might be due to the fact that, when wt. % of reinforcement increases which leads intrinsically the formation of brittle phases and presence of inter-metallic phases exhibits potential regions for the initiation of cracks leading to decrease in ductility during quasi-static loading.

5.4 COMPRESSION STRENGTH

Table 5.3 Compression properties of the both as cast and aged condition Al/Gr composites

Without ageing condition	Compression Strength, MPa	Aged Condition	Compression Strength, MPa
Al 6061	313.07	Al 6061	329.08
Al/5% Gr	355.21	Al/5% Gr	367.44
Al/10% Gr	371.22	Al/10% Gr	390.90
Al/15% Gr	351.10	Al/15% Gr	353.54

Fig. 5.8 displays the plots for values of compression strength (UCS) of Al6061 MMC before and after ageing (Complete data is given in the Table 5.3). The

Composites after ageing have a better compression strength compared to MMCs before ageing. From the figure, it can be observed that, the highest UCS was found for 10% graphite reinforcement. Meanwhile, aged composites showed similar trends as that of composites without ageing. The values of yield strength extruded alloy and composites were higher and better compared to composites without ageing. This is due to the uniform distribution of hard particulates in soft ductile matrix which leads in enhancement in strength which further leads to development of bulky residual stress during cooling and formation of density dislocation of density because of mismatch of coefficient of thermal expansion amongst soft aluminum matrix & hard ceramic particle. Grain refinement is one of the factors for improved strength in extruded alloy and its MMCs.

5.4.1 CONSEQUENCE OF GRAPHITE ON ULTIMATE COMPRESSION

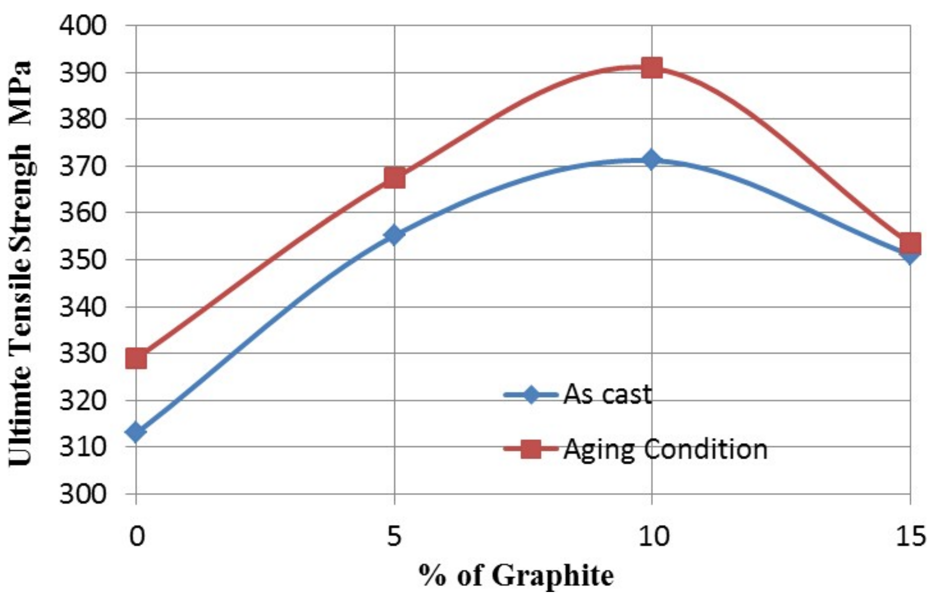

Fig. 5.8 Consequence of % of graphite on UCS of Al/Gr composites for both as cast and aged conditions.

The influence of addition of wt. % of graphite in aluminum composites on compression strength of the without ageing and aged samples are given in the Fig. 5.8. The curves of the without ageing and aged composites samples shows that the compression strength is increasing with addition of up to 10% graphite. The graphite used in composites suppressed the local micro-cracks which improves the composite's compressive strength. One of the reason for improvement in confinement effect on the binder aluminum alloy of graphite reinforcement, which improves its stiffness of the composites under the axial compression. Graphite reduces the proliferation of cracks by arresting mechanism and reduces the stress concentration at the crack-tips and diverting stress concentration other direction.

5.4.2 EFFECT OF AGEING ON ULTIMATE COMPRESSION

The results obtained during ultimate compression strength test are shown in Fig. 5.8 for all composition as a function of ageing condition. Ageing operation enhances the tensile strength (UTS) because of strong interface and diffusion bonding which is observed amongst the Al matrix alloy and graphite reinforcement that produced a very tough structure composites. There is no de-bonding at the interface between Al and graphite particles.

5.5 FATIGUE STUDIES

In fatigue studies, only three samples were selected due to availability of fatigue facility in lab and also because of its expensive. Those three samples are as cast, 5 % graphite and 10 % graphite specimens for two type fatigue properties.

5.5.1 FATIGUE LIVES OF ASCAST ALUMINUM SPECIMENS.

Analysis of as cast Al matrix alloy specimens and the results of fatigue to predict the average life of fatigue with 10% error that means 90% confidence level is shown in the Table 5.4.

Table 5.4: As cast Al alloy fatigue lives						
Stress level	**63 MPa**		**47 Mpa**		**40 Mpa**	
	Life		**Life**		**Life**	
No	**Cycles**	**log**	**Cycles**	**Log**	**Cycles**	**Log**
1	18426	4.2654	37513	4.5742	98906	4.9952
2	23563	4.3722	68224	4.8339	149650	11.1751
3	40238	4.6046	70932	4.8508	156335	11.1941
4					219905	11.3422
Average life	27409	4.4379	58890	4.7700	131199	11.1179
Standard Log deviation		0.1759		0.1564		0.1575
C.O.V (%)		3.9636		3.28		3.08

The variation in life at stress levels I, II, III is less than expected 4%, 5%, and 7% respectively. Hence there is no need of testing additional specimens at level I, II, III so as to maintain the same percent error (10%) in the life estimated for same degree of confidence for both as cast and heat treatments is shown in Table 5.4. This is calculated as follows, the acceptable percentage error as assumed in section is 10% and co-efficient of variation was found in level I is 3.9636% .therefore,

$$\frac{\text{Percenterror }\%}{\%\text{ co}-\text{efficient of variation}} = \frac{10}{3.9636} = 2.5228$$

Now, from Table 5.5 with ordinary value of 1.214 at 90% confidence, the number of samples required is to read off. Since, 4 specimens were already tested at level I, hence there is no need of additional specimens to test at level I, and then same method is repeated for all values of fatigue results for both specimens which are of as cast & heat treated..

Table 5.5: Revised test plan for as cast Al alloys			
Stress(MPa)	**C.O.V**	**%Error/ C.O.V**	**Revised Sample Size**
63	3.9636	2.5230	3
47	3.28	3.0488	3
40	3.08	3.2468	4

Table 5.6: Revised average fatigue life for as cast Al alloy.		
Stress Level	**Average Log Life**	**Average Life**
63	27409	4.4379
47	58890	4.7700
40	131199	11.1179

Tables 5.5 and 5.6 show the results corresponding to this revised test plan, revised average fatigue life for as cast Al matrix alloy specimens respectively.

5.5.2 FATIGUE LIVES OF AGING AND OVER AGING HEAT TREATED ALUMINUM SPECIMENS.

Experimental results used for the analysis of aging and over aging heat treated specimens to calculate the fatigue life in average within 10% error and 90% confidence as per the primary estimate.

For aging and over aging heat treated specimens, the co-efficient of variation was found to be 3.98, 2.08% % at I stress level, 3.76%, 1.77% at II stress level II and 3.60%, 0.98%at III stress level respectively.

The co-efficient of variation in the lives at I, II& III stress levels is less than the expected 4%, 5%, and 7% respectively. Hence there is no need of additional specimens testing at level I, II, III for both type of heat treatment. Table 5.7 and 5.8 show the fatigue test data of aging, over aging heat treated specimens respectively.

Table 5.7 Revised test plan for aging heat treatment Al-GR specimens (5% of GR).			
Stress Level (MPa)	**C.O.V**	**%Error/ C.O.V**	**Revised Sample Size**
63	3.98	2.542	3
47	3.76	2.656	3
40	3.60	2.778	4

Table 5.8: Aging heat treated Al-graphite specimens fatigue lives(5% of GR).		
Stress Level (MPa)	**Average Log Life**	**Average Life**
63	28226	4.4506
47	69270	4.8405
40	218947	11.3403

Table 5.9: Revised test plan for over ageing heat treatment Al/GR specimens			
Stress Level (MPa)	**C.O.V**	**C.O.V(% error)**	**Sample Size after revision**
63	2.08	4.807	3
47	1.77	11.649	3
40	0.98	10.121	4

Table 5.10: Revised average life for over aging heat treatment Al-GR specimens.		
Stress Level (MPa)	**Average Log Life**	**Average Life**
63	22318	4.3487
47	49167	4.6917
40	90702	4.9576

Tables 5.9 and 5.10 show the results corresponding to this revised test plan for as aging and over aging heat treated Al-GR specimens respectively.

Cantilever type rotating beam fatigue test set up is used to develop stress amplitude v/s number of cycles during fatigue test until it gets fractured at room temperature. Throughout the process of exploring the influence of ageing on the properties of fatigue life of as cast aluminum, aluminum with 5% GR& aluminum with 10% GR composites and their data were displayed in Fig. 5.10 – 5.11 (a), (b) &(c) respectively.

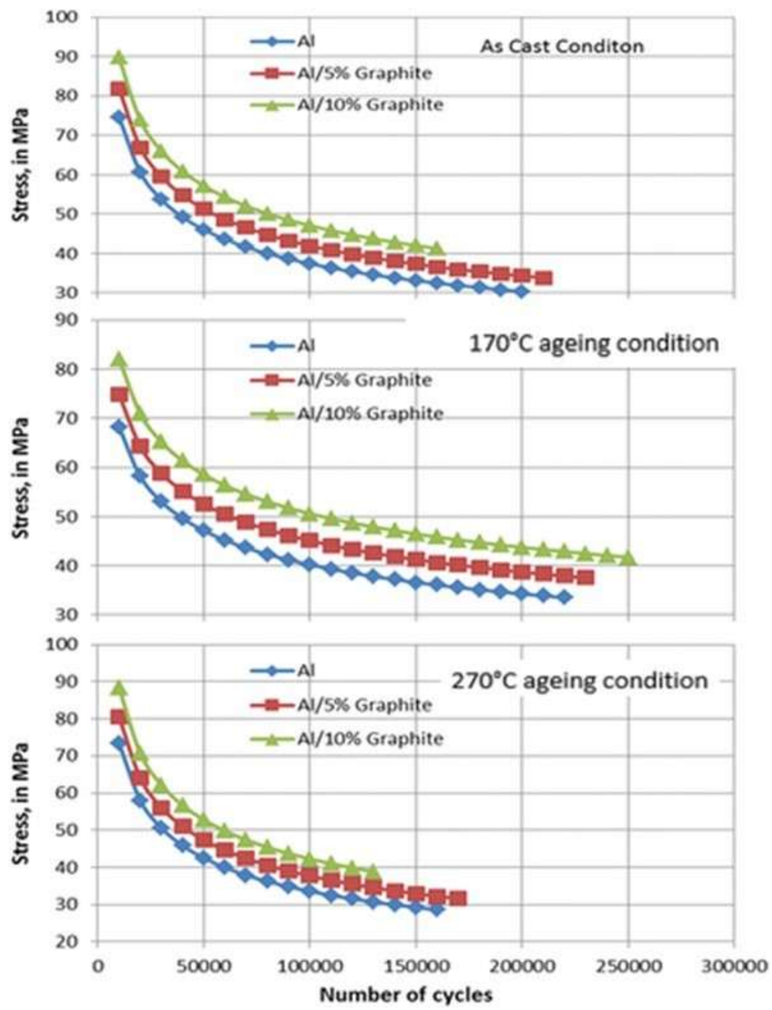

Fatigue 5.10 fatigue life of a) as cast, b) aged at 170 °C and aged at 270 °C ageing condition for Aluminum alloy, aluminum alloy with 5% graphite and aluminum alloy with 10% graphite composites.

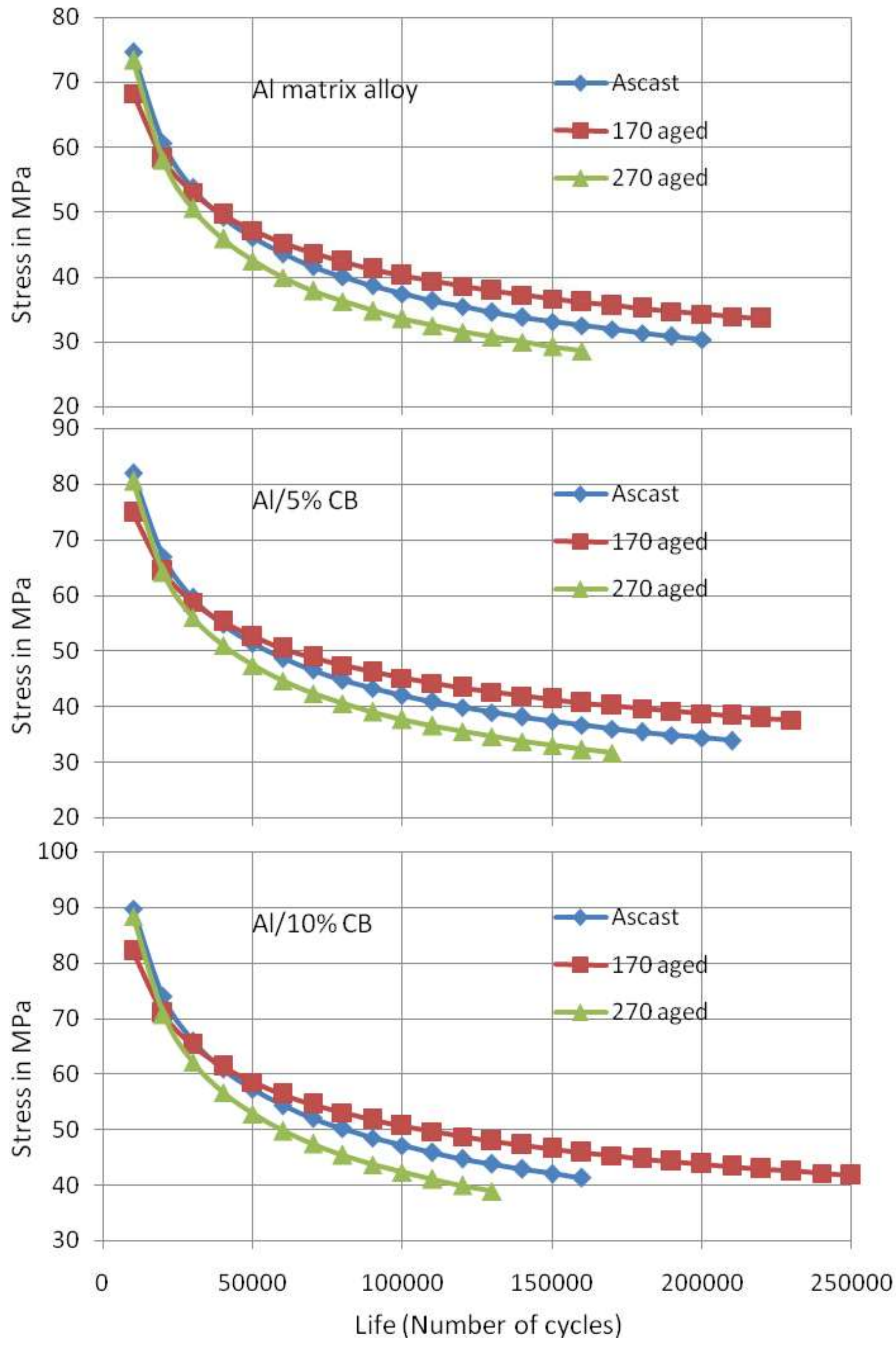

Fig. 5.11. Fatigue S–N curves of a) as casted aluminum b) aluminum with 5% GR and aluminum with 10% GR composites for as cast, 170 °C and 270 °C aged condition

The experiments conducted during fatigue test on aluminum metal matrix composites incorporated with graphite to know its life and if found to be more as compared to as cast matrix alloy regardless of ageing conditions. In other words, the life of fatigue of an aluminum metal matrix composites reinforced with graphite displayed high stresses converge value against an as cast aluminum alloy. Fig. 5.10 (a, b, c) and 5.11(a, b, c) displayed lives of fatigue of aluminum matrix in place of three various conditions viz as cast, aged at 170 °C and aged at 270 °C. Specimens aged at 170 °C condition have validated for longer life during fatigue trailed by as cast condition specimens, whereas specimen at 270 °C ageing demonstrated poorer life under fatigue because of its over ageing state. The lives of fatigue limit displayed at 160000 cycles for specimens with as cast conditions, nearly 220000 cycles for aged specimens at 170 °C; whereas only 140000 cycles for over aged specimens at 270 °C. Same type of tendency is noticed for aluminum with 5% GR and aluminum metal matrix composite with 10% GR which is displayed in Fig. 5.10(b) and 5. 10(c). Usually, aluminum and its alloys don't behave a stable fatigue strength but have demonstrated constantly reducing fatigue resistivity. As per the results of previously published research paper [236], the fatigue limit of an aluminum metal matrix is noted to be 70 N/mm^2 . While aluminum alloy and aluminum composite reinforced with graphite were artificially aged at 170 °C, the fatigue life found to be enhanced to 95 N/mm^2. At lesser cycles, the fatigue resistivity of the composites at aged condition found to be significantly enhanced. By incorporating only 5% of graphite with aluminum metal matrix at aged conditions, the limit of fatigue life attains beyond 95 N/mm^2. The average limit of fatigue stress is found to be 60 N/mm^2 in aluminum metal matrix reinforced with 10% graphite and for the pure matrix alloy, it is found to be 50 N/mm^2 as displayed in Fig. 5.12.

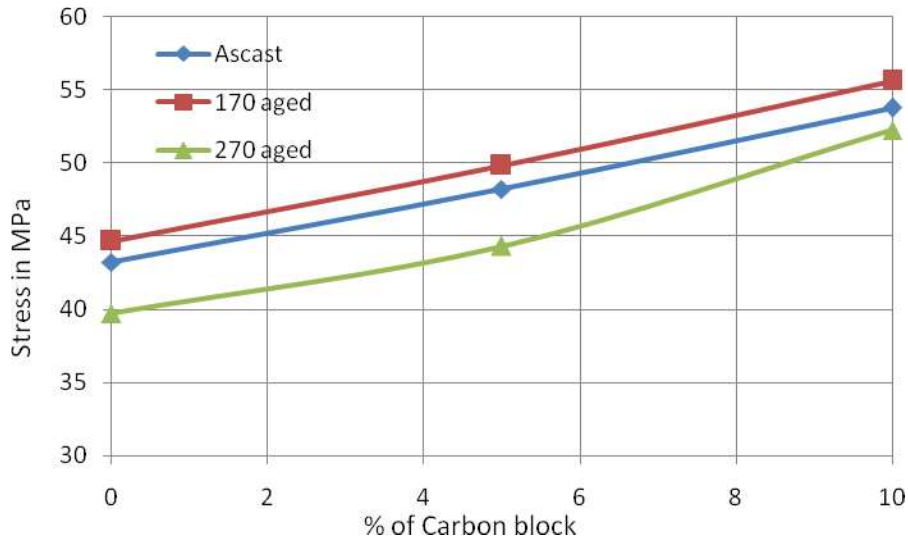

Fig. 5.12 Effect of GR on an average fatigue stress of an Aluminum metal matrix composites at different ageing conditions.

The dislocation of substructure in an aluminum alloy matrix influences the strengthening effects during the formation of precipitates. An indication for the concentration of valences clusters attained by increasing the temperature of solution, enhancing quenching rate& storage duration at operating temperature was demonstrated by its previously published papers. Needle shaped precipitates were developed during aging possess at 170°C which can be treated as an intermediate phase. Increasing the temperature of solution and enhancing the quenching rate endorses the process of clustering resulted in the formation of a precipitation with finer scale leads to higher concentration of vacancy. It is now estimated that formation of β-Mg2Si can develop a remarkable hardness levels in Al-6061. However, these levels depends upon the spacing and size of β precipitates. The later one is organized by its temperature and appearance of β nuclei in the form of GP zones during formation. The absenteeism of formation of GP zone in composites is therefore has a remarkable significance on its morphology and the size β precipitates and its resultant age hardening. Many researchers noticed a homogeneously nucleated precipitates in materials at its peak aged condition in material contained β-Mg2Si with the help of a coarse Widmanstatten morphology of non-reinforced alloys.

5.5.3 Fracture Surface

The substantial variations in microstructure of particles precipitated during second phase in aluminum metal matrix composites which are subjected to aging at 170°c and over aging at 270°c conditions distressing the fatigue life is revealed during fractography analysis as shown in Fig. 5.13 .The voids which are considered as cast defects were noticed in the fractured surfaces of aluminum alloy is displayed in Fig. 5.13(a), simultaneously develops few blocks on the surface of as cast condition aluminum alloy during fracture. There is no formation of voids found; instead, least number of cracks are noticed its surface at aged condition as displayed in 5.13(b) and the size of voids and primary cracks found to be reduced. The surfaces of the specimens fractured during rotational fatigue beam test machine exhibited the cast defects along with graphite cluster near the origin at its operating temperature as shown in Fig. 5.13(c)-5.13 (f). Since, it is hardly challenging to trace out the origin of the fracture, since radiative lines are not found on the surface of the composites. At some regions, the cavitations responsible for occurrence of multiple fractures in aluminum metal matrix composites were found as displayed in Fig. 5.13(c). Due to ageing, the cavitation as a damage decreases which is dominated by a diffusion controlled process. In general, an initiation of different cracks because of stress concentration sources like graphite inclusions during aged condition were reported i n Al MMC's. In other words, graphite responds with magnesium which is existing in an alloy during ageing is a confirmation for strengthening the significance of graphite is revealed in the present work.

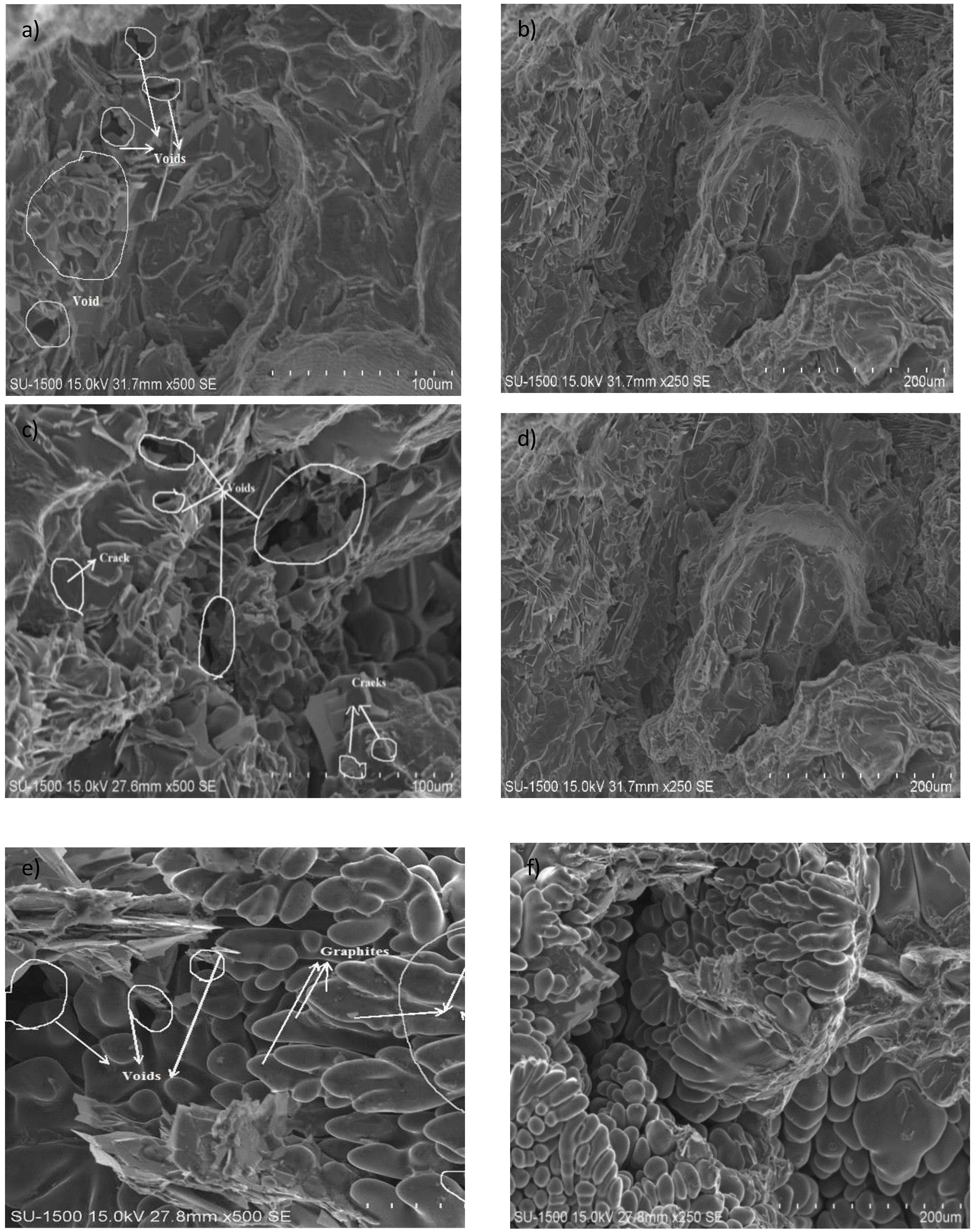

Fig. 5.13. Fracture surface of a) Aluminum alloy b) over Aged aluminum c) Aluminum alloy with 5% graphite, d)Aged aluminum with 5%graphite e) Aluminum with 10%graphite and f) Aluminum with 10% graphite at aged condition displaying the origin of fatigue fracture at its whiskers of cluster .

5.6 RELIABILITY STRESS LIFE ANALYSIS

5.6.1 EXPERIMENTAL PLANS TO DEVELOP R-S-N CURVES

Because of the scattering noticed among each of the fatigue tests, the relation between the stress levels cannot be articulated in single curve, but might be deliberated as the group of curves, each denoting a certain probability of failure. Thus, for a particular material, there is a group of S-N curves with a failure probability among one of the factor. In this work, aluminum with 10% graphite is considered because of its highest fatigue life.

At each stress level, sufficient number of tests were conducted to plot the above S-N curves experimentally. It was chosen to test five specimens to obtain the estimated variability during replicate test and the % of repetition was established as follows:

% repetition =100[1-(TL/TN)] .... (5.1)

Where,

TL= total number of different levels of stress during testing.

TN= Total number of tested specimens.

Hence,

Repetition percentage = ([1(3/15)] x100)

=80% which aggress with valued given in Table 5.13

Table 5.11: Guidelines to estimate replication and selection of sample size for the purpose of testing

Test type	Minimum % of replication	Minimum no of specimens
Primary& Exportability	18-34	7-13
R&D testing	34-51	7-13
Data for design allowance	51-76	13-25
Reliability data	76-89	13-25

Table 5.11 gives guidelines for estimating repetition and selection of sample size of the sample for the purpose of testing to get data for reliability analysis.

5.6.2 RELIABILITY EXPERIMENTS

For reliability experiment as indicated in Table 5.12, it is required to test 12-24 specimens including three stress levels. In the present work, 15 specimens are tested, out of which 5 specimens at each stress level. Already during fatigue test, we have tested 3 specimens at each stress level and hence now 2 more specimens need to be tested at I, II, III stress level to fulfil the necessity to test 5 specimens at each stress level.

5.6.3 RELIABILITY STRESS LIFE ANALYSIS OF AN AS CAST AND HEAT TREATED AL/GR COMPOSITES.

Least square can be conveniently used to setup a linear correlation amongst a dependent and an independent parameter which is applicable to linear data. Linearization conversions are accomplished to use least square method since the fatigue details usually corresponds to Log-Normal applicable to these distributions. The failure probability for the test data obtained can be determined by the concept of median rank. The test data of lives of fatigue is initially arranged in order of ascending and then assigned with median rank. Then, the regression analysis is done with the help of linearizing transformation and thus, the relationship amongst failure probability and life of fatigue is calculated. The following correlations can be used to develop R-S-N curves:

$$\text{Median ranks} = \frac{(J-0.3)}{(n+0.4)} \qquad \ldots\ldots\ldots\ldots\ldots\ldots\ldots\ldots \text{(5.2)}$$

Where, J= Failure's order number.

n =sample size

If it is Normal log distribution of a fixed data, then, the correlation amongst dependent & independent parameter can be articulated with the following expression:

$$Y=aX+b \quad \ldots\ldots\ldots\ldots\ldots\ldots\ldots\ldots\ldots\ldots\ldots\ldots \text{(5.3)}$$

Where Y and X are linear variables of corresponding x & y in which;

$$Y= \ln y \ldots\ldots\ldots\ldots\ldots\ldots\ldots\ldots\ldots\ldots\ldots\ldots \text{(5.4)}$$

$$X= \ln x \ldots\ldots\ldots\ldots\ldots\ldots\ldots\ldots\ldots\ldots\ldots\ldots \text{(5.5)}$$

Y denotes a % of failure& x denotes failure life of fatigue.

Median ranks = $\frac{(J-0.3)}{(n+0.4)}$ Where J= 1, 2, 3, 4, 5 and n=5

Median ranks = $\frac{(1-0.3)}{(5+0.4)}$ = 0.1296

Table 5.12: Linearizing transformation of failure percentage and lives of fatigue of an as cast Aluminum composite with 10% GR at stress level I level stress

SL no	% Failed(y_0)	y= ln(y_0)	Life of Fatigue (x_0)	x= ln(x_0)
1	0.1287	-2.04280	37513	10.5324
2	0.3208	-1.16682	43224	10.6742
3	0.500	-0.69315	52669	10.8718
4	0.6652	-0.37804	68224	11.1306
5	0.8704	-0.13880	70932	11.1695

Table 5.13: Linearizing transformation of failure percentage and lives of fatigue of an as cast Aluminum composite with 10% GR at II level stress.

SL no	% Failed(y_0)	y= ln(y_0)	Life of Fatigue (x_0)	x= ln(x_0)
1	0.1287	-2.04280	37513	10.5324
2	0.3208	-1.16682	43224	10.6742
3	0.500	-0.69315	52669	10.8718
4	0.6652	-0.37804	68224	11.1306
5	0.8704	-0.13880	70932	11.1695

Table 5.14: Linearizing transformation of failure percentage and lives of fatigue of an as cast Aluminum composite with 10% GR at III level stress

SL no	Percent Failed(y_0)	y= ln(y_0)	Fatigue Life(x_0)	x= ln(x_0)
1	0.1287	-2.04280	37513	10.5324
2	0.3208	-1.16682	43224	10.6742
3	0.500	-0.69315	52669	10.8718
4	0.6652	-0.37804	68224	11.1306
5	0.8704	-0.13880	70932	11.1695

Tables 5.12, 5.13 and 5.14 displays x and y values after linear conversion for each test levels. Then, the constants in equation 5.3 can be calculated as shown below:

Level I: $Y_1=a_1X_1 + b_1 a_1= 2.0732, b_1=-22.2474$

Level II: $Y_2=a_2X_2 + b_2 a_2= 2.5822, b_2=-28.9657$

Level III: $Y_3=a_3X_3 + b_3 a_3= 2.4685, b_3=-30.4121$ (From appendix)

The above equation which is related to probability of percentage failure to fatigue life. With the help of above calculations and considering logs of X & Y, lives of fatigue equivalent to different probability of failure at each levels of stress is assessed using the data shown in Tables 5.15, 5.16, and 5.17. [Reliability =1-Probability of failure]. It can now be related to fatigue life and the values of fatigue life corresponding to different reliabilities at stress levels I, II and III respectively.

Table 5.15: Probability of failure - fatigue life of as cast Al/10%GR composite at stress level I.

SL no	Percentage of failure(y_0)	y= ln(y_0)	Fatigue Life(x_0)	x= ln(x_0)
1	0.1297	-2.04331	18426	9.8215
2	0.3149	-1.16682	23563	10.0674
3	0.500	-0.69315	32456	10.3876
4	0.6652	-0.37804	40238	10.6026
5	0.8704	-0.13880	42338	10.6534

Table 5.16: Probability of fatigue life-failure of as cast Al/10%GR composite at level II stress.

SL No	% Failed(y)	Y= ln(y)	X, Projected from Equation	Antilog(X)= x, life (Cycles)
1	0.01	-4.605	8.5096	4963
2	0.1	-2.303	9.6200	15064
3	0.5	-0.693	10.3966	32748
4	0.75	-0.228	10.6209	40982
5	0.99	-0.010	10.7260	45526

Table 5.17: Probability of fatigue life-failure of as cast Al/10%GR composite at level III stress.				
SL No	% Failed(y)	Y= ln(y)	X, Projected from Equation	Antilog(X)= x, life in Cycles
1	0.01	-4.605	9.4341	12508
2	0.1	-2.303	10.3256	30503
3	0.5	-0.693	10.9491	56902
4	0.75	-0.228	11.1292	68129
5	0.99	-0.010	11.2136	74131

Table 5.18: Number of cycles to failure of ageing heat treated Al/10%GR composite corresponding to median ranks.					
SL No	% Failed(y)	Y= ln(y)	X, Projected from Equation	Antilog(X)= x, life in Cycles	Reliability
1	0.02	-4.805	10.4546	34703	0.99
2	0.2	-2.603	11.3871	88179	0.95
3	0.6	-0.683	13.0393	169285	0.55
4	0.75	-0.228	12.2277	204345	0.25
5	0.99	-0.010	12.3160	223245	0.01

Number of cycles to failure of ageing heat treated Al/10%GR composite corresponding to median ranks is shown in table 5.18. The results of R-S-N analysis of as cast specimens are denoted in the terms of actual R-S-N curves shown in Fig 5.14. The lines in Fig. 5.14 denoted the relation among stress life's reliability and indicate fatigue life of fatigue of the test specimen which is getting failed between Reliability of 99% life and Reliability of 1% life at any given stress level.

Table 5.19: Linearizing transformation with percentage of failure and lives of fatigue of composites with 10%GR under ageing heat treated condition at stress level I.				
SL no	Median Rank	Level I (63MPa)	Level II (47MPa)	Level III (40MPa)
1	0.1296	20153	41559	112356
2	0.3148	22012	45236	123960
3	0.500	32581	73228	170236
4	0.6652	42513	85236	242710
5	0.8704	45652	93021	338882

Table 5.20: Linearizing transformation with percentage of failure and lives of fatigue of composites with 10%GR under ageing heat treated condition at level II stress.

SL no	% Failed(y_0)	y= ln(y_0)	Life of fatigue(x_0)	y= ln(x_0)
1	0.1297	-3.04331	20153	8.9111
2	0.3149	-2.15583	22012	9.9993
3	0.500	-0.69315	32581	10.3915
4	0.6652	-0.37804	42513	10.6576
5	0.8704	-0.13880	45652	10.7288

Table 5.21: Linearizing transformation with percentage of failure and lives of fatigue of composites with 10% GR under ageing heat treated condition at stress level III.

SL no	% Failed(y_0)	y= ln(y_0)	Life of fatigue(x_0)	x= ln(x_0)
1	0.1297	-3.04331	41559	10.6349
2	0.3149	-2.15583	45236	10.7196
3	0.500	-0.69315	73228	11.2013
4	0.6652	-0.37804	85236	11.3532
5	0.8704	-0.13880	93021	11.4406

x and y values after linear conversion for each testing levels are shown in tables 5.19, 5.20 and 5.21. Then, the constants in equation 5.3 are estimated for ageing heat treated Al (6061) composite with 10%GR as below:

Level I: $Y_1=a_1X_1 + b_1 a_1= 1.8928$, $b_1=-20.5338$

Level II: $Y_2=a_2X_2 + b_2 a_2= 1.9092$, $b_2=-22.0171$

Level III: $Y_3=a_3X_3 + b_3 a_3= 1.4753$, $b_3=-18.7430$

Where a_1 and b_1 can be found by equations

$$_1 = \frac{n\,\Sigma\,(xy) - \Sigma\,x\,\Sigma\,y}{n\,\Sigma(x^2) - (\Sigma x)^2} \& b_1 = \frac{\Sigma\,y\,\Sigma\,(x^2) - \Sigma\,x\,\Sigma\,(xy)}{n\,\Sigma(x^2) - (\Sigma x)^2}$$

Table 5.22: Probability of fatigue life-failure of ageing heat treated Al/10%GR composite at level I stress.					
SL No	%t Failed(y)	**Y= ln(y)**	X, Projected from Calculation	Antilog(X)= x, life(Cycles)	Reliability
1	0.02	-4.606	8.4155	4517	0.99
2	0.2	-2.304	9.6317	15240	0.91
3	0.6	-0.694	10.4928	36056	0.50
4	0.75	-0.228	10.7279	45612	0.25
5	0.99	-0.010	10.8431	51180	0.01

Table 5.23: Probability of fatigue life –failure of ageing heat treated Al/ 10%GR composite at level II stress					
SL No	%Failed(y)	Y= ln(y)	X, Projected from Calculation	Antilog(X)= x, life (Cycles)	Reliability
1	0.02	-4.606	9.1201	9138	0.99
2	0.2	-2.304	10.3258	30512	0.91
3	0.6	-0.694	11.1691	70908	0.50
4	0.75	-0.228	11.4127	90463	0.25
5	0.99	-0.010	11.5269	101405	0.01

Table 5.24: Probability of fatigue life-failure of ageing heat treated Al/10%GR composite at level III stress.					
SL No	% Failed(y)	Y= ln(y)	X, Projected from Equation	Antilog(X)= x, life in Cycles	Reliability
1	0.02	-4.805	9.6831	14518	0.99
2	0.2	-2.803	11.2435	69113	0.95
3	0.6	-0.683	12.3348	205829	0.50
4	0.75	-0.228	12.550	282093	0.25
5	0.99	-0.010	12.3978	327014	0.01

Table 5.25: Number of cycles to failure of over ageing heat treated Al/10%GR composite corresponding to median ranks.				
SL no	Median Rank	Level I (63MPa)	Level II (47MPa)	Level III (40MPa)
1	0.1296	17346	37527	78880
2	0.3148	24258	39523	88325
3	0.500	25348	50457	90702
4	0.6652	28128	57527	92150
5	0.8704	31682	61238	103450

Table 5.26: Linearizing transformation of failure percentage and lives of fatigue of over ageing heat treated Aluminum composite with 10%GR level I.				
SL no	% Failed(y_0)	y= ln(y_0)	Fatigue Life(x_0)	x= ln(x_0)
1	0.1297	-3.04331	17346	8.7611
2	0.3149	-2.15583	24258	10.0965
3	0.500	-0.69315	25348	10.1405
4	0.6652	-0.37804	28128	10.2445
5	0.8704	-0.13880	31682	10.3635

Table 5.27: Linearizing transformation of failure percentage and lives of Fatigue of over ageing heat treated Al/aluminum composite with 10% GR level II.				
SL no	% Failed(y_0)	y= ln(y_0)	Fatigue Life(x_0)	x= ln(x_0)
1	0.1297	-3.04331	37527	10.5328
2	0.3149	-1.15583	39523	10.5846
3	0.500	-0.69315	50457	10.8289
4	0.6652	-0.37804	57527	10.9600
5	0.8704	-0.13880	61238	11.0225

Table5.28: Linearizing transformation of failure percentage and lives of fatigue of over ageing heat treated Al/ aluminum composite with 10%GR level III.				
SL no	% Failed(y_0)	y= ln(y_0)	Fatigue Life(x_0)	x= ln(x_0)
1	0.1297	-3.04331	78880	11.2757
2	0.3149	-1.15583	88325	11.3888
3	0.500	-0.69315	90702	11.4153
4	0.6652	-0.37804	92150	11.4312
5	0.8704	-0.13880	103450	11.5468

x and y values after linear conversion at each testing levels is shown in tables 5.25, 5.26, 5.27 and 5.28. Then, the constants in equation 3 were estimated for over ageing heat treated Al (6061)-GR composite as shown below:

Level I: $Y_1 = a_1 X_1 + b_1 a_1 = 3.2792,\ b_1 = -34.0704$

Level II: $Y_2 = a_2 X_2 + b_2 a_2 = 3.1945,\ b_2 = -311.3366$

Level III: $Y_3 = a_3 X_3 + b_3 a_3 = 7.2960,\ b_3 = -84.1435$

Where a_1 and b_1 can be found by equations

$$1 = \frac{n\,\Sigma\,(xy) - \Sigma\,x\,\Sigma\,y}{n\,\Sigma(x^2) - (\Sigma x)^2} \;\&\; b_1 = \frac{\Sigma\,y\,\Sigma\,(\;)^{2} - \Sigma\,x\,\Sigma\,(xy)}{n\,\Sigma(x^2) - (\Sigma x)^2} \text{(From Appendix)}$$

x and y values after linear conversion at each testing levels is shown in tables 5.29, 5.30, 5.31.

Table 5.29: Probability of fatigue life-failure of over ageing heat treated Al/10%GR composite at level I stress.					
SL No	% Failed(y)	Y= ln(y)	X, Projected from Equation	Antilog(X)= x, life in Cycles	Reliability
1	0.02	-5.606	8.9855	7987	0.99
2	0.2	-2.304	9.6875	16116	0.91
3	0.6	-0.694	10.1785	26332	0.50
4	0.75	-0.228	10.3203	30344	0.25
5	0.99	-0.010	10.3868	32429	0.01

Table 5.30: Probability of failure - fatigue life of over ageing heat treated Al/10%GR composite at stress level II.					
SL No	% Failed(y)	Y= ln(y)	X, Projected from Equation	Antilog(X)= x, life in Cycles	Reliability
1	0.02	-5.606	8.6202	15066	0.99
2	0.2	-2.304	10.3408	30970	0.91
3	0.6	-0.694	10.8448	51266	0.50
4	0.75	-0.228	10.9903	59298	0.25
5	0.99	-0.010	11.0586	63486	0.01

Table 5.31: Probability of failure - fatigue life of over ageing heat treated Al/ 10%GR composite at stress level III.					
SL No	% Failed(y)	Y= ln(y)	X, Projected from Equation	Antilog(X)= x, life in Cycles	Reliability
1	0.02	-4.805	10.9017	54267	0.99
2	0.2	-2.603	11.2172	74398	0.95
3	0.6	-0.893	11.4378	92767	0.50
4	0.75	-0.228	11.5016	98872	0.25
5	0.99	-0.010	11.5315	101871	0.01

5.6.4 AVERAGE FATIGUE LIFE OF AS CAST AL/GR COMPOSITE.

Static tests conducted on as cast aluminum graphite composite whose tensile strength (UTS) is noted to be 78 Mpa. The average fatigue life of as cast aluminum graphite composite obtained at 3 stress levels are tabulated in Table 5.32

Table 5.32: Average life of fatigue of as cast Al/10% GR composite.		
Stress Level	Average Life	Average Log Life
63	27409	4.4379
47	58890	4.7700
40	131199	11.1179

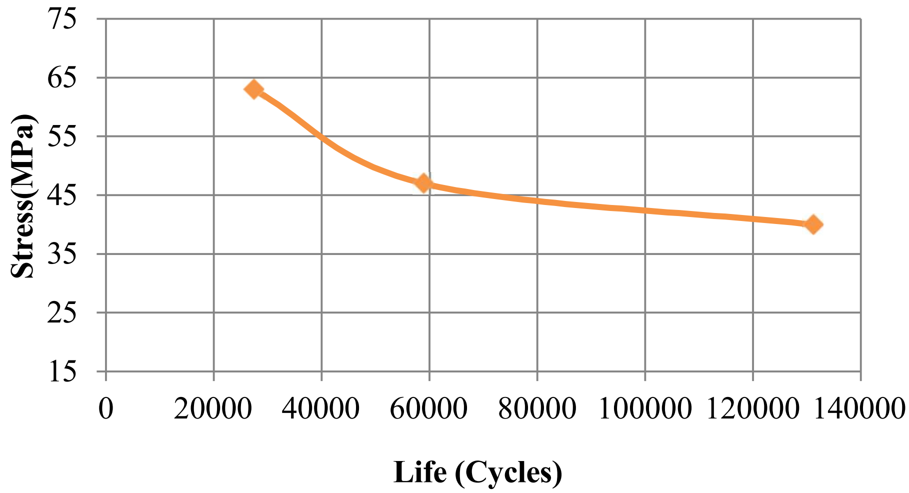

Fig.5.14: S-N Curve of as cast Al/10%GR composite

Fatigue lives of as cast Al/10%GR composite corresponding to different stress level can be read of from the Fig.5.14.

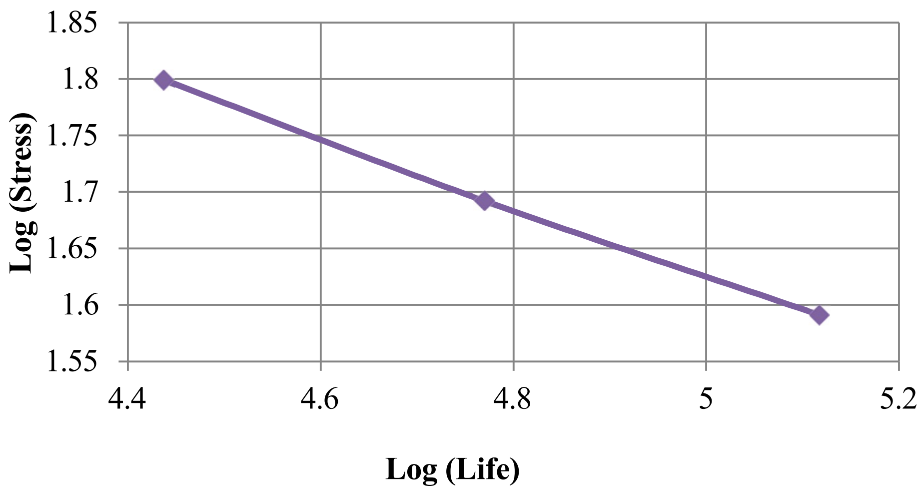

Fig. 5.15: Stress V/s Life in Log-Log Scale of as cast composite

Logarithmic fatigue life's corresponding to different logarithmic stress level of as cast Al/10%GR composite can be read off from Fig 5.15.

5.6.5 AVERAGE FATIGUE LIFE OF AGING HEAT TREATED AL/10%GR COMPOSITE

The average life of fatigue at 170^{0}C aged heat treated aluminum graphite obtained at 3rd stress levels are formulated in Table 5.33.

Table 5.33 Average lives of fatigue of aged heat treated Al/10%GR composite

Stress Level	Average Life	Average Log Life
63	28226	4.4506
47	69270	4.8405
40	218947	11.3403

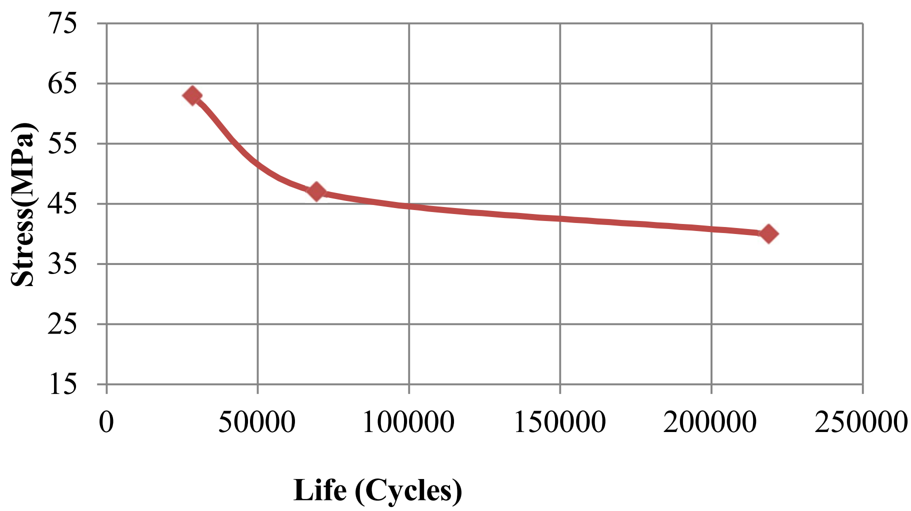

Fig. 5.16: S-N Curve of 170^0 Caging Heat treated samples

Fatigue lives of aging heat treated Al/10%GR composite corresponding to different stress level can be read of from the Fig.5.16.

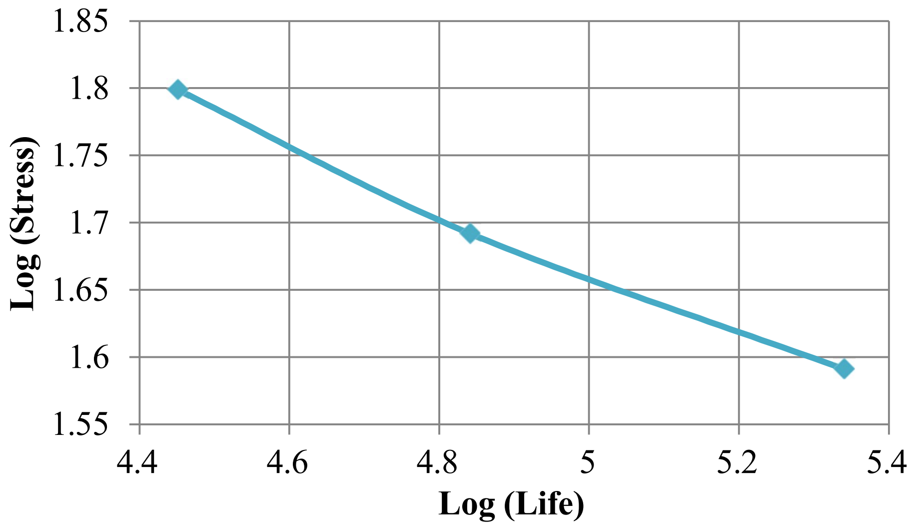

Fig. 5.17: Stress V/s Life in Log-Log Scale (170^0C HT)

Logarithmic fatigue lives corresponding to different logarithmic stress level of aging heat treated Al/GR composite can be read off from Fig 5.17.

5.6.6 Average fatigue life for over aged heat treated Al/GR composite

The average fatigue life of 270^0C over aging heat treated Al/10%GR composite shown in Table 5.34.

Table 5.34: Average lives of fatigue for over aged heat treated Al/10%GR Composite.

Stress Level (MPa)	Average Log Life	Average Life
63	22318	4.3487
47	49167	4.6917
40	90702	4.9576

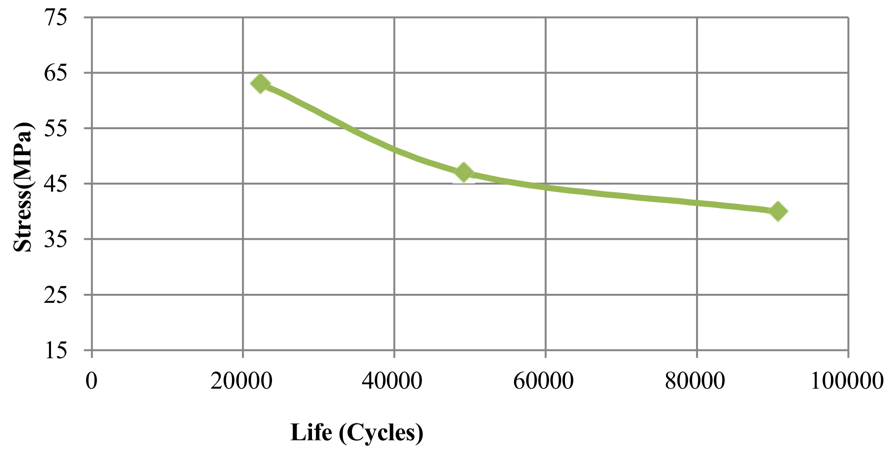

Fig. 5.18 S-N Curve of 270^0 C averaging Heat treated

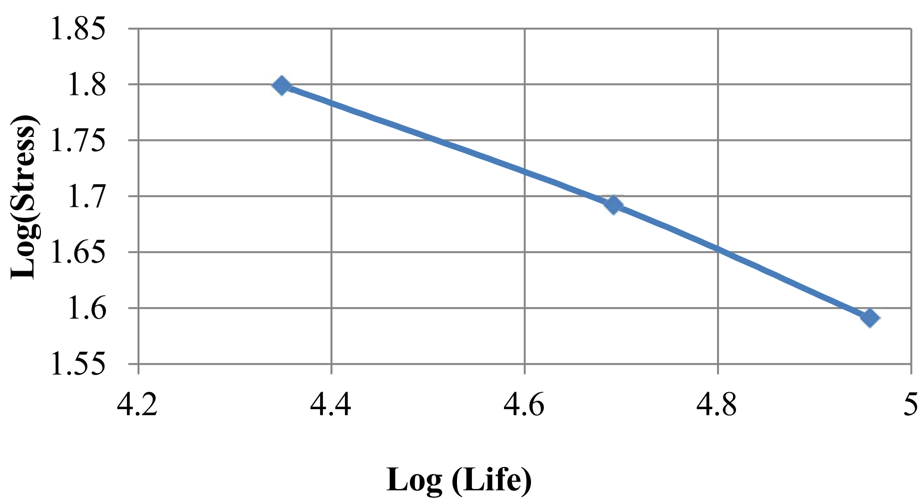

Fig.5.19: Stress V/s Life in Log-Log Scale (270^{0}C HT)

Fatigue lives corresponding to different stress levels of over aging heat treated Al/GR composite can be read of from Fig 5.19. Logarithmic fatigue lives corresponding to different logarithmic stress level of over aging heat treated Al/GR composite can be read off from Fig. 5.20.

5.6.7 ASSESSMENT OF BEHAVIOR OF FATIGUE OF AN ASCAST AL/10%GR COMPOSITES WITH HEAT TREATED AL/10%GR COMPOSITES

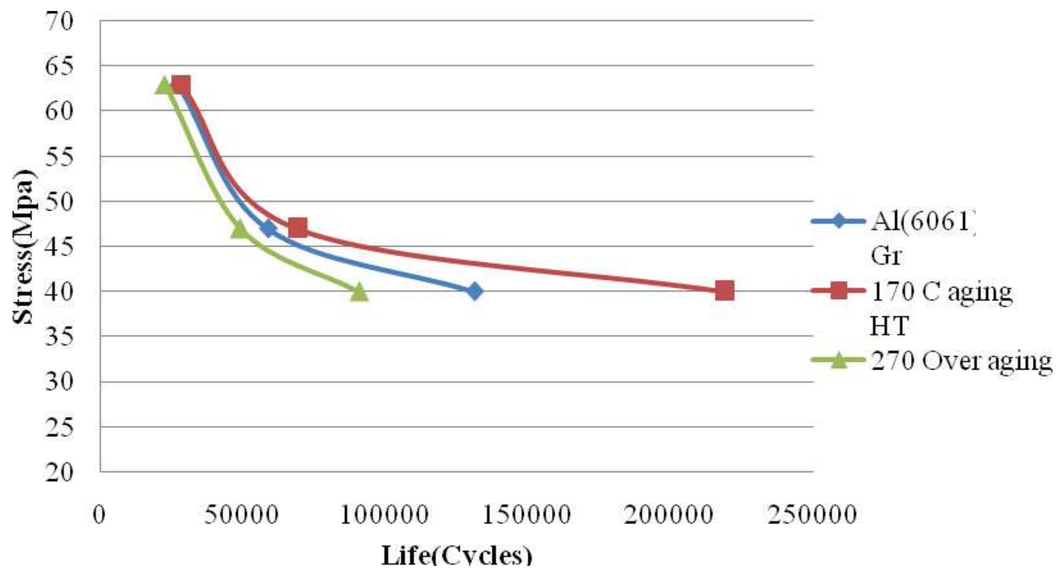

Fig. 5.20: Assessment of behavior of fatigue of an as cast and heat treated samples

Fig 5.20 displays an assessment of behavior of fatigue of as cast, aging and over aging heat treated specimen. Fatigue life of as cast is 2.90% , 17.71% , 66.88% less than aged heat treated specimen at I, II& III stress levels respectively. Whereas fatigue life of as cast is 18.57%, 16.51%, 30.86% greater than over aged heat treated specimen at I, II& III stress levels respectively. Its shows that aged heat treated specimens fatigue life is greater than that of as cast & over aged heat treated specimens.

5.7. RELIABILITY STRESS LIFE ANALYSIS

Reliability stress life curves of as cast, aged heat treated and over aged composite specimens at different reliabilities were plotted at different stress level

5.7.1 THE LIVES OF FATIGUE CORRESPONDING TO DIFFERENT RELIABILITIES AT RESPECTIVE STRESS LEVELS OF AS CAST AL/GR COMPOSITE.

Table 5.35 gives fatigue lives results of as cast Al/10%GR composite at different reliability.

Table 5.35: Fatigue lives of as cast Al/10%GR composites different reliability.

Reliability	level I stress	level II stress	level III stress
0.99	4963	12508	34703
0.90	15064	30503	88179
0.50	32748	56902	169285
0.25	40982	68129	204345
0.01	45526	74131	223245

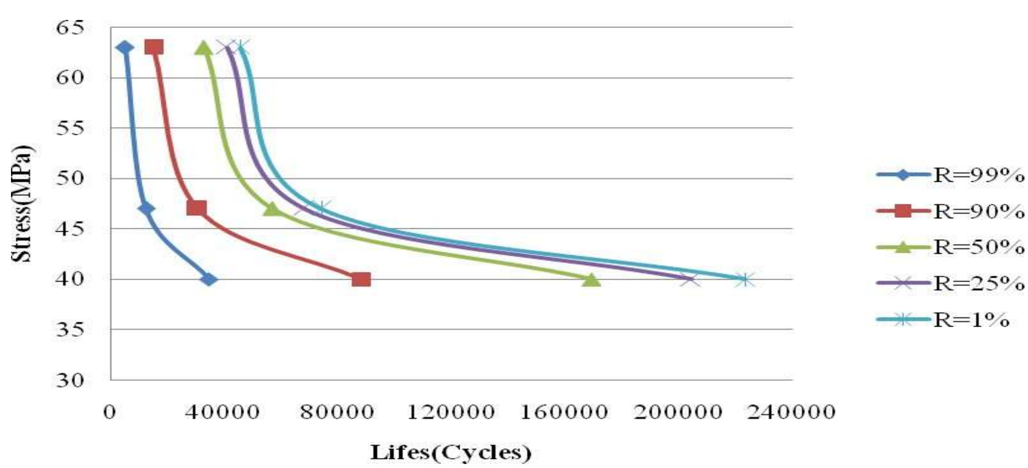

Fig. 5.21 R-S-N Curves of as cast Al/10%GR metal matrix

Fig. 5.21 shows relation between fatigue lives and reliability of as cast composite at different stress levels.

5.7.2 THE LIVES OF FATIGUE EQUIVALENT TO DIFFERENT RELIABILITIES AT RESPECTIVE STRESS LEVELS OF AGING HEAT TREATED AL/GR COMPOSITE.

Table 5.36 gives fatigue lives results of aging heat treated Al/GR composite at different reliability

Table 5.36: Fatigue lives of aging heat treated Al/10%GR composites for different reliability.

Reliability	level I stress	level II stress	level III stress
0.99	4517	9138	14518
0.90	15240	30512	69113
0.50	36056	70908	205829
0.25	45612	90463	282093
0.01	51180	101405	327014

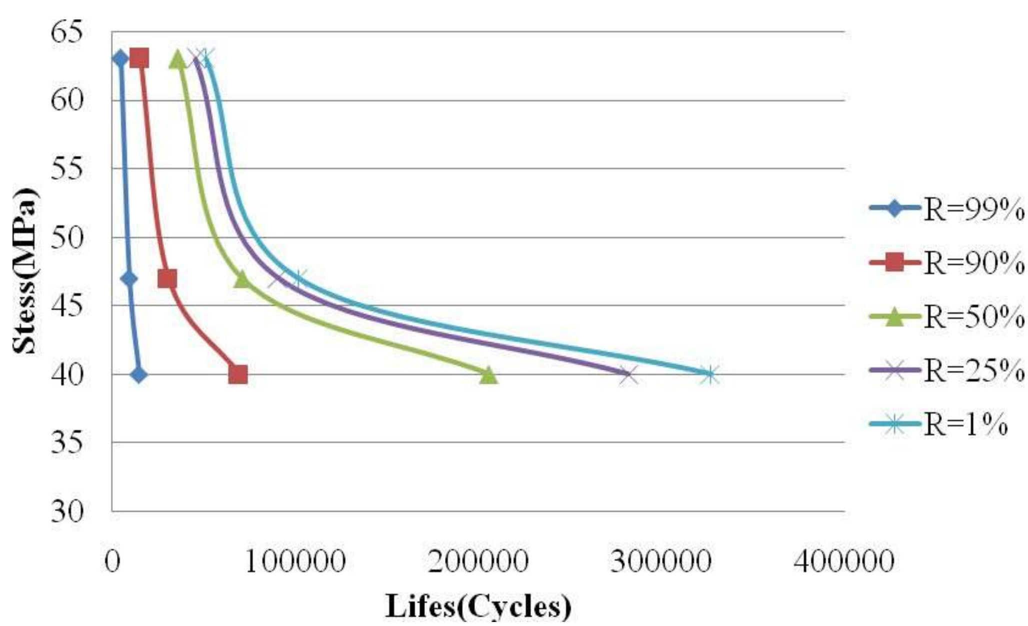

Fig. 5.22: R-S-N Curves of aging heat treated Al-10%GR metal matrix composites

Fig. 5.22 shows relation between fatigue lives and reliability of 170^{0}C aging heat treated metal matrix composite at different stress levels.

5.7.3 THE LIVES OF FATIGUE EQUIVALENT TO DIFFERENT RELIABILITIES AT RESPECTIVE STRESS LEVELS OF OVER AGING HEAT TREATED AL/GR COMPOSITE.

Table 5.37 gives fatigue lives results of over aging heat treated Al/10%GR composite at different reliability

Table 5.37: Fatigue lives of over aging heat treated Al-10%GR for different reliability

Reliability	level I stress	level II stress	level III stress
0.99	7987	15066	54267
0.90	16116	30970	74398
0.50	26332	51266	92767
0.25	30344	59298	98872
0.01	32429	63486	101871

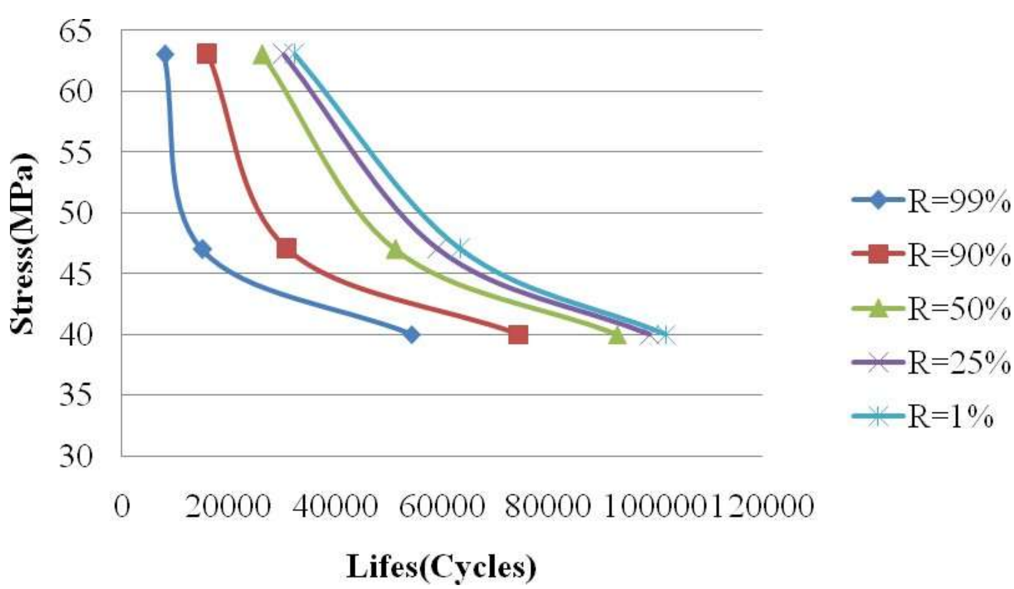

Fig. 5.23 R-S-N Curves of over aging heat treated Al-10%GR metal matrix composites

Fig. 5.23 shows relation between fatigue lives and reliability of 270^0 C over aging heat treated metal matrix composite at different stress levels.

5.8 Wear

The significance of aluminum composites incorporated with graphite particulate on wear resistivity in comparison with the base matrix material is discussed here. The wear volume in the form of weight loss / unit length with respect to material loss during sliding for Al/GR composites having 0, 5, 10,15 & 20% for as cast state is given in the Table 5.41.

Table 5.38 Rate of wear (mm^3/km) of Al/GR composites at various speed &different loading conditions

Load, N	Sliding speed Rpm	% of GR				
		0	5	10	15	20
20	**200**	1.4125	1.3886	1.2366	1.1635	0.9814
300	1.5376	1.4796	1.3098	1.1998	1.0224	
400	1.5569	1.5296	1.3337	1.2112	1.0372	
500	1.8140	1.5433	1.4074	1.2795	0.9929	
30	**200**	1.6036	1.5820	1.3699	1.2339	1.0600
300	1.6173	1.5911	1.3815	1.2454	1.0725	
400	1.6286	1.6206	1.3974	1.2533	1.0872	
500	1.9471	1.6547	1.5192	1.3397	1.1350	
40	**200**	1.7071	1.6502	1.4376	1.2647	1.1282
300	1.7344	1.6730	1.4512	1.2806	1.1168	
400	1.7560	1.7071	1.4827	1.3056	1.1623	
500	1.9993	1.7299	1.5549	1.3249	1.1657	
50	**200**	1.8038	1.7616	1.5208	1.3181	1.1998
300	1.8140	1.7879	1.5337	1.3249	1.2078	
400	1.8220	1.8094	1.5493	1.3352	1.2306	
500	2.1586	1.7879	1.6255	1.3477	1.2078	

5.8.1 SIGNIFICANCE OF GRAPHITE CONTENT ON WEAR

The significance of graphite wt. % on the behavior of composites during wear which are developed to operate at different wear rotational speeds, such as 200, 300, 400 and 500 rpm and for wear loads of 20, 30, 40 and 50 N is plotted in the Figures. 5.24 and 5.25. The data obtained clearly revealed that the improvement in % of graphite increases the wear resistivity of Al/GR composites. In this work, the rate of wear is noticed to be reduced when there is an increase in the % of graphite from 5% to 20%. The minimum material loss is observed for 20% graphite dispersed in the Al matrix alloy. But the same % of GR at a higher velocity and higher load showed higher values. On the other hand at lower loads and speeds the wear rate remains constant and also wear rate is almost constant even at higher speeds. When compared to aluminum matrix material, the wear rate is more steady state and less for composites.

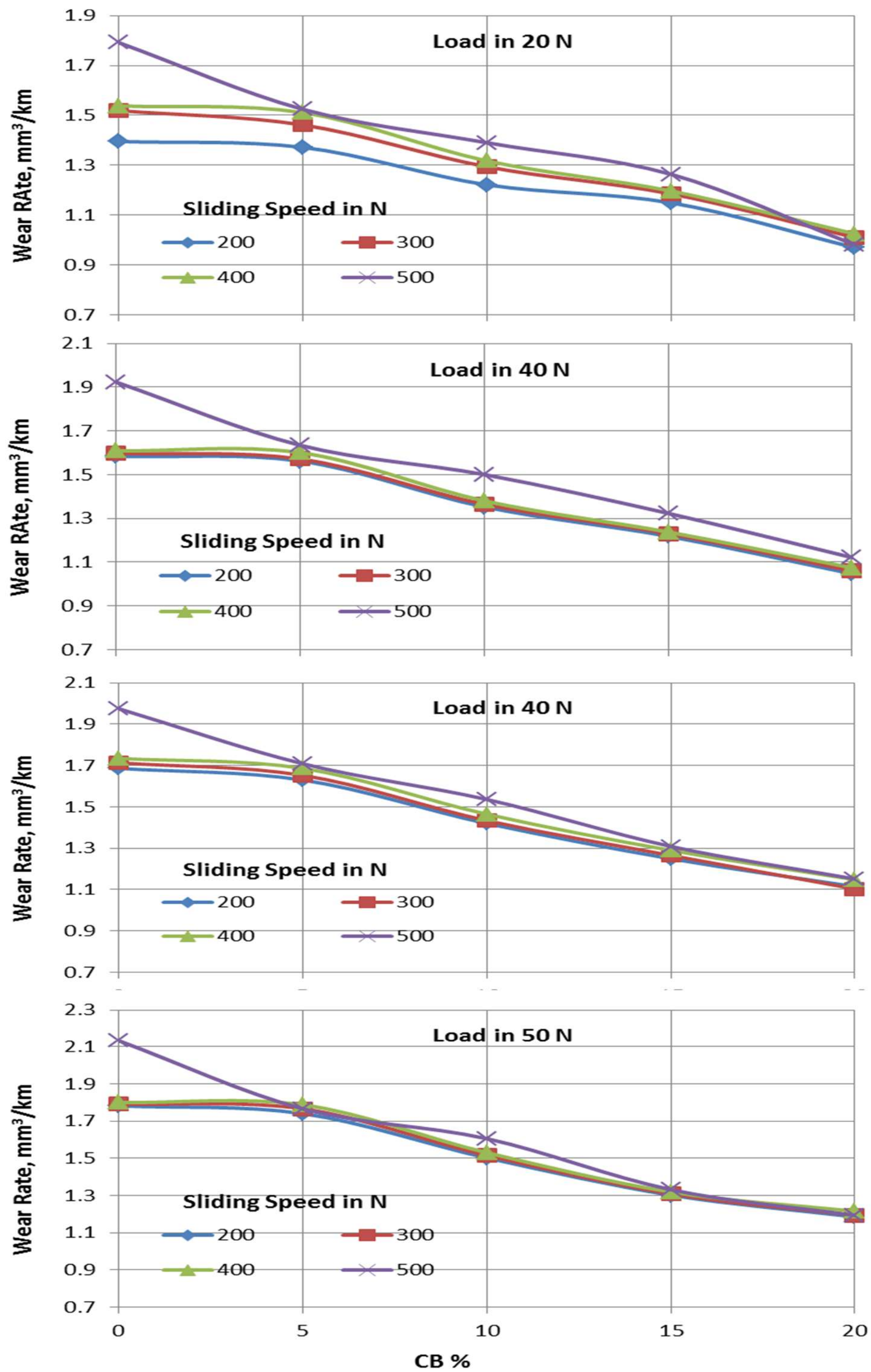

Fig. 5.24. Variation in the rate of wear of Aluminum graphite MMCs for different percentage of graphite, different speeds and different loads.

The dispersal of graphite reinforcement particles in the aluminum base matrix leads to relative attainment of stability in the wear resistance of composites. The contemptuous of graphite particulate probably held with less adherence which attributed to the subsequent wear loss.

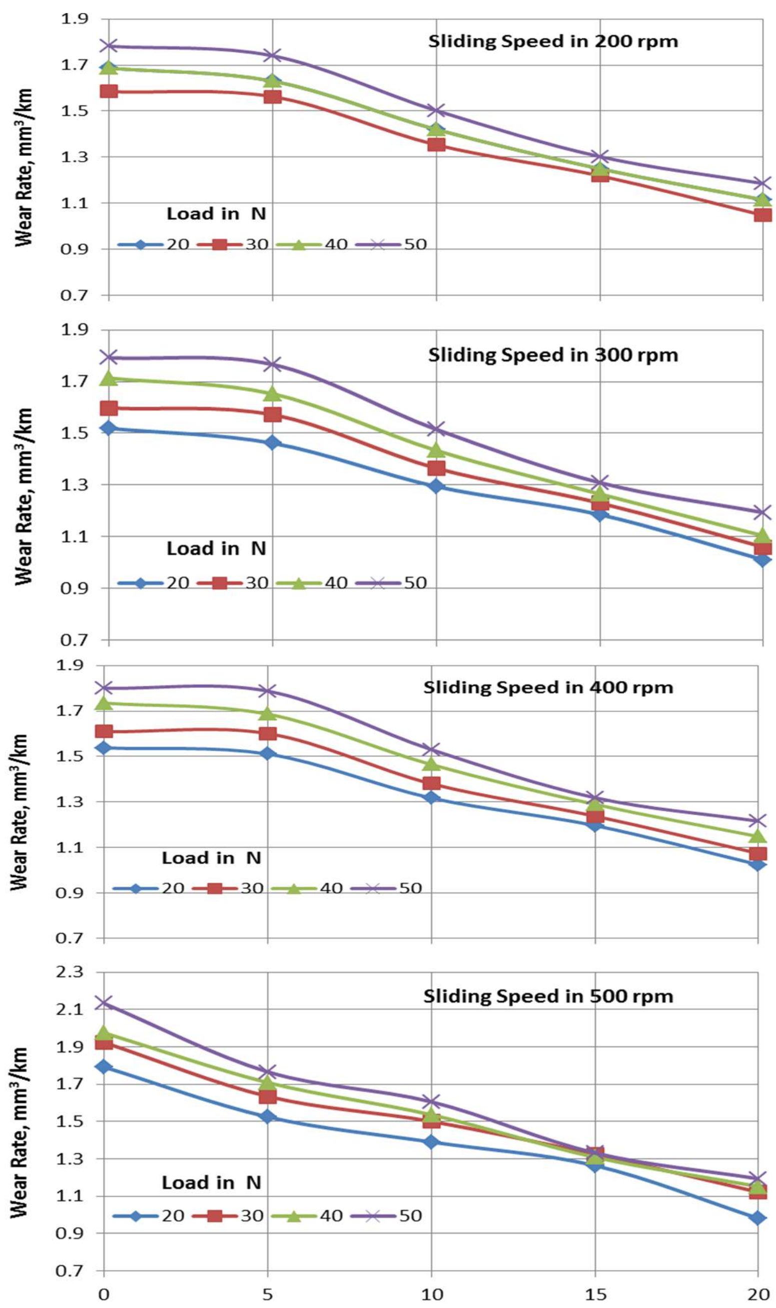

Fig. 5.25 The variation in the wear rate of the GR/ Al MMCs for different percentage of Graphite, different speeds and different loads.

5.8.2 SGINIFICANCE OF SLIDING SPEED ON THE WEAR RATE

The Fig. 5.26 and 5.27 shows rate of wear of the composites as a function of sliding speed for different loads. It clearly shows a small marginal change in wear rate absorbed during changing speeds. Five samples were taken for the single condition and the average wear rate considered to draw the graphs. The sliding speed only contributes a slight change from 3.2 to 3.8% wear rate. A rapid change in the rate of is noticed, when there is an increase in speed from zero to 200 rpm, but subsequently, the rate of wear increased marginally or linearly with the sliding speed. It is followed by a mild wear stat with nearly linear wear rate and speed relationship.

Previous literature shows the experimental result of wear test in removing the material which is proportional to the sliding distance or speed [237] However, the rate of wear increased linearly with its sliding velocity and rest all are kept constant. Sharma [238] have explained a mechanism in their research work: During the sliding process the metal of both disc as well as specimen increases the temperature, it enhances the oxidation which leads to development of oxide layer on the specimen [239]. The oxide layer is generally weak and porous during sliding the more serious damage seen at the tip of the pins due to shear between matrix materials and oxidized layers. The oxide layer does not have a successive contact between the disc and specimens at a lower speed, but the higher speed the formation layer faster and at the same time the mixing debris of both matrix, reinforcement and disc materials. The mechanically mixed debris consists of larger metallic fragments which have been found to be turned away because of its strong adhesive junctions with a proper grade of inter-metallic interaction due to absenteeism of adequate oxide layers. It is noticed that there is an enhancement in the wear resistance in noticed for a corresponding increase in wear velocity.

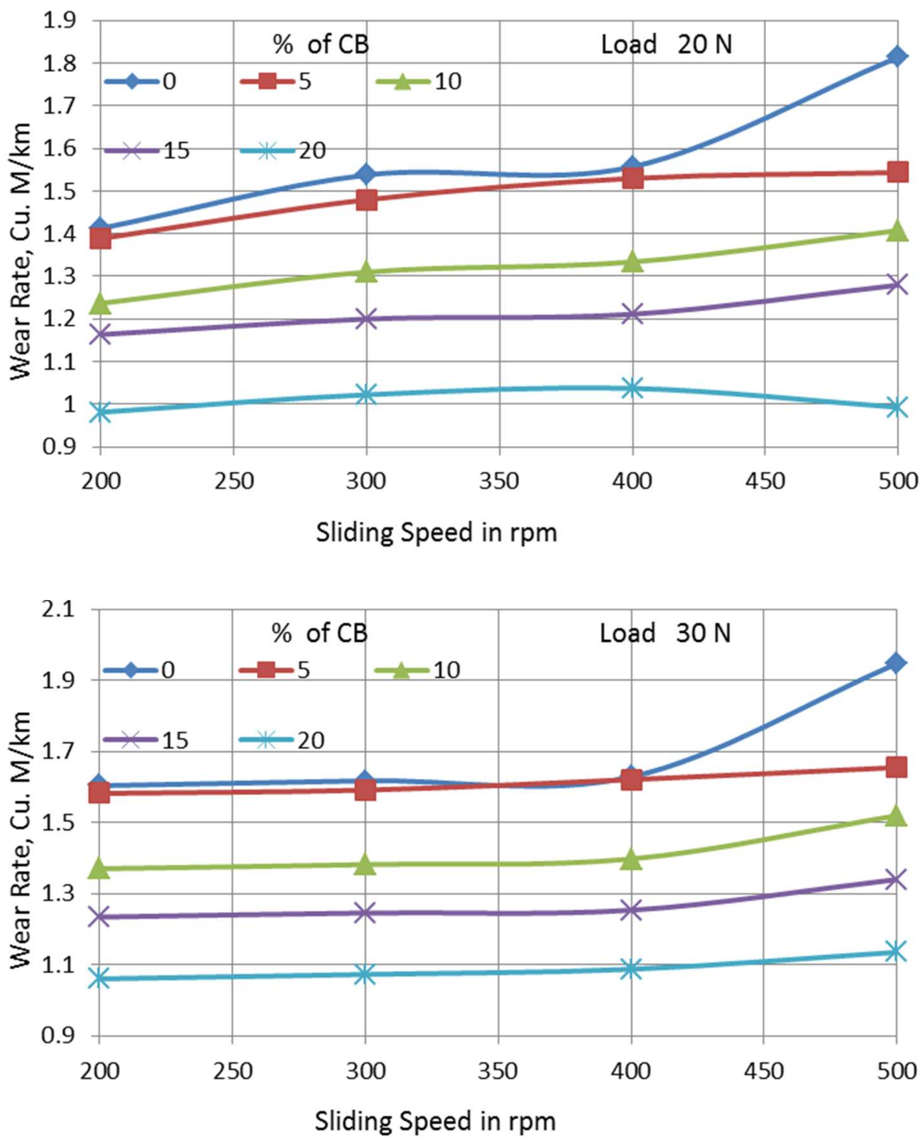

Fig. 5.26. The variation in the wear rate of the ALMMC reinforced with graphite as a function of sliding velocity at different loads.

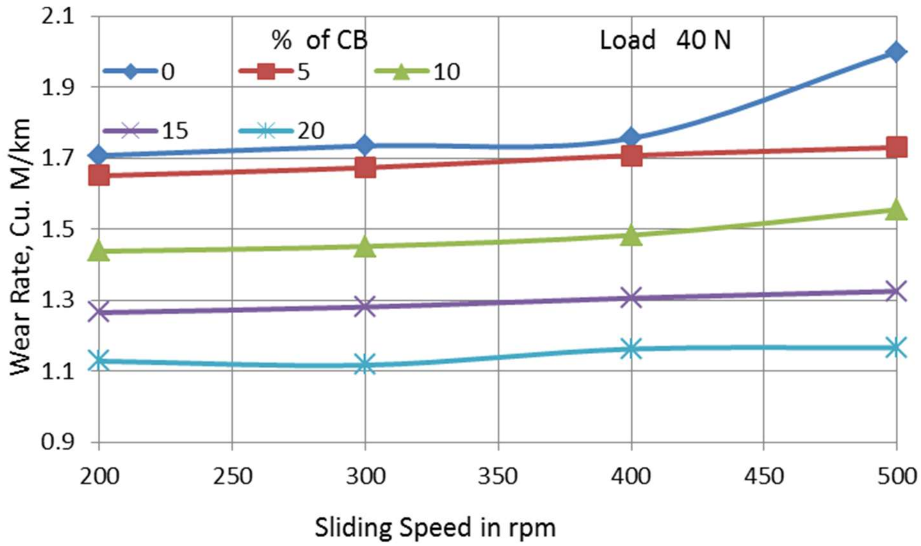

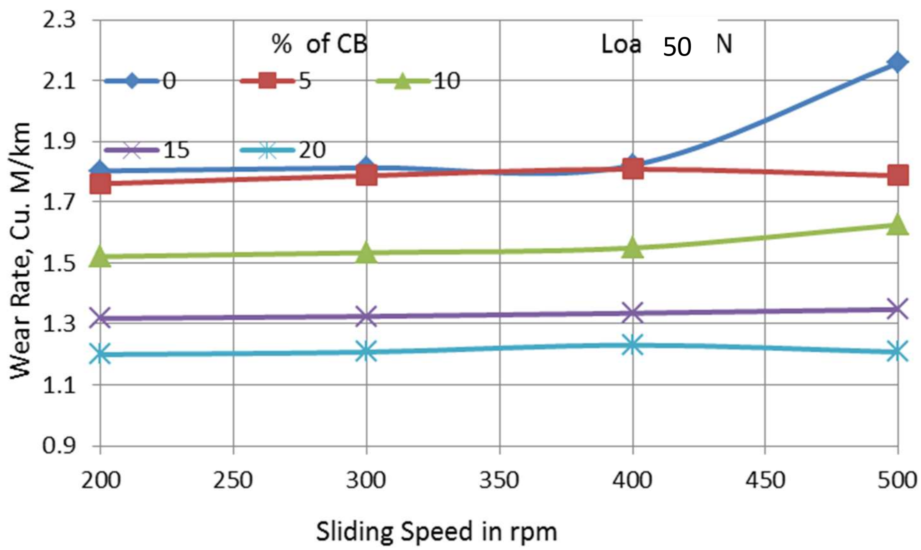

Fig. 5.27. The variation in the wear rate of the ALMMC reinforced with graphite as a function of sliding velocity at different loads.

5.8.3 SIGNIFICANCE OF NORMAL LOAD ON THE WEAR RATE

Fig. 5.28 and 5.29 displays the rate of wear rate of aluminum graphite composites as a function of normal load at different speeds. When the normal load is applied linearly during the wear test, the rate of wear found to increase under the linearly applied normal load; but it can be severe at higher loads. The results showed approximately 8% higher wear for a load of 50 N. At lower loads, the wear can be seen within the mild wear region even though sliding speed is higher. But at higher loads, the harshness is still higher which causes more loss in the material. The debris of both the specimen and disc formed their oxides because of the higher temperature and surplus of plenty of air. At lower load, this mechanical mixed layer acts as a barrier in preventing further material loss due lower shear force. On the other hand, these metallic oxides failed to give protection to base metal due to higher shear loads. This material is removed frequently due to higher shear forces between the host and debris & hence it promotes metal contact between both specimen and disc materials which leads to further wear of material taking place continuously. But for lower load, the wear plot is almost a linear, but in higher loads these curves are almost hyperbolic in nature. These curves are almost the same for both pure and composite materials, but matrix material shown a higher wear rate as compared to composites.

.

.

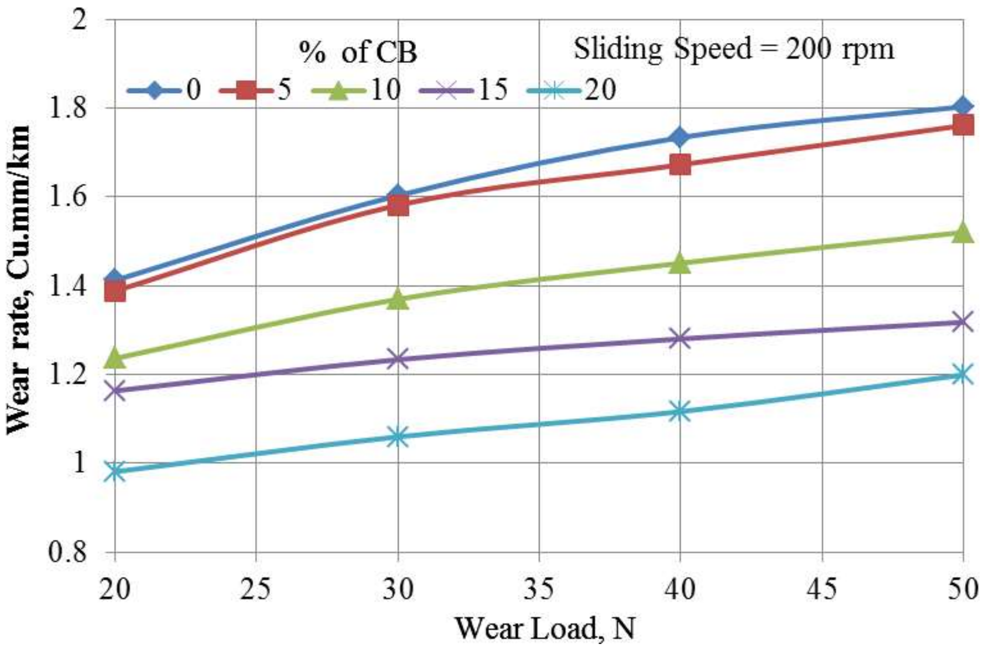

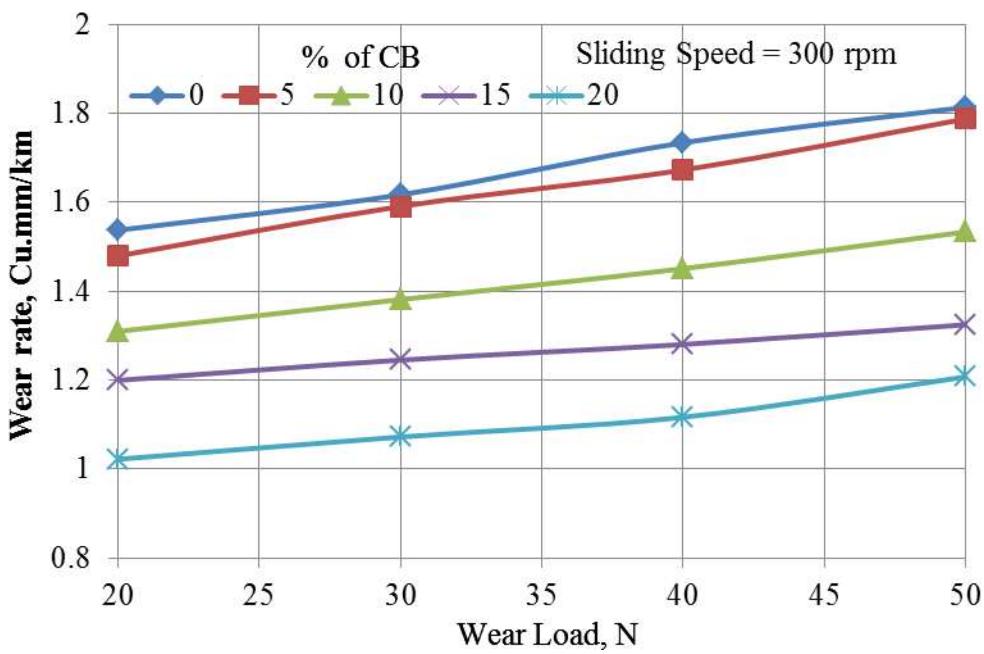

Fig. 5.28 The variation in the wear rate of the ALMMC reinforced with carbon black (graphite) as a function of normal loads at different sliding speeds.

1q

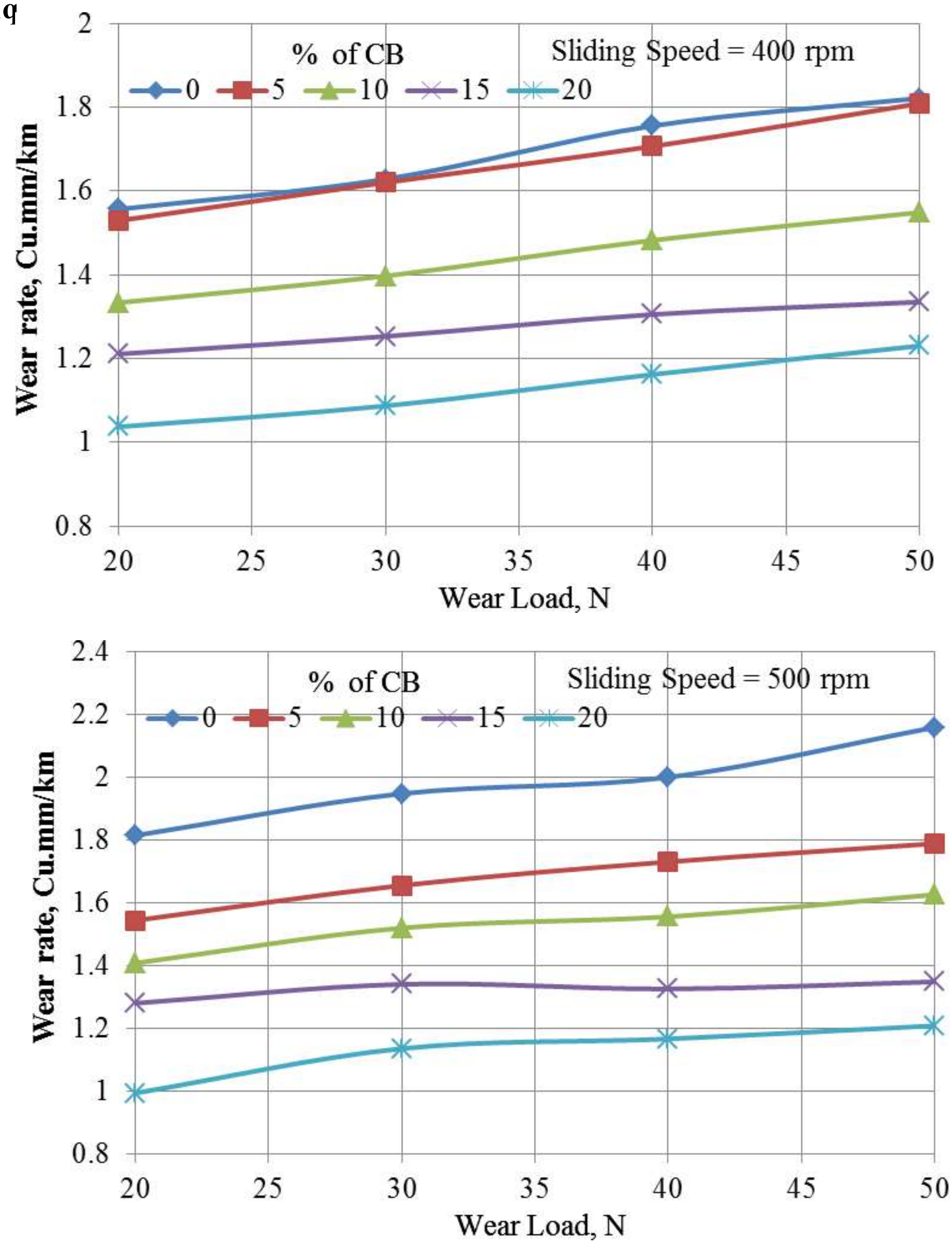

Fig. 5.29 The variation in the wear rate of the ALMMC reinforced with carbon black (graphite) as a function of normal loads at different sliding speeds.

5.8.4 STUDIES OF WORN-OUT SURFACES

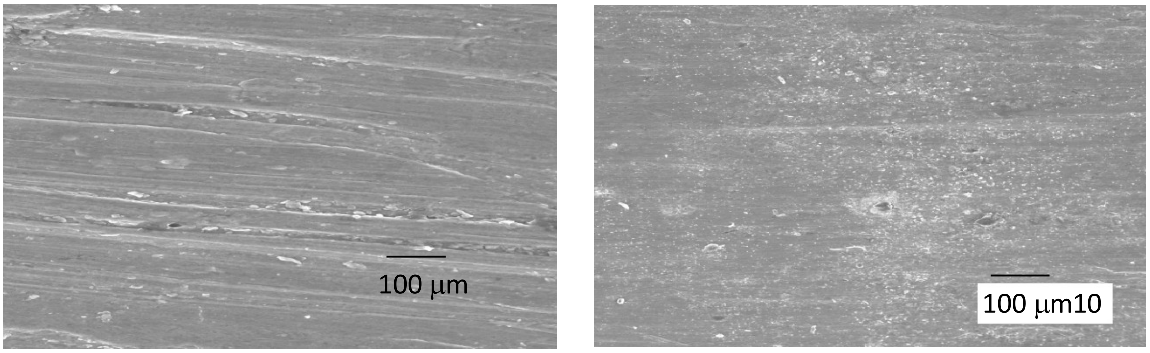

Fig. 5.30 Worn-out surface of matrix metal and composite incorporated with 15 % GR at 100 rpm & 10 N

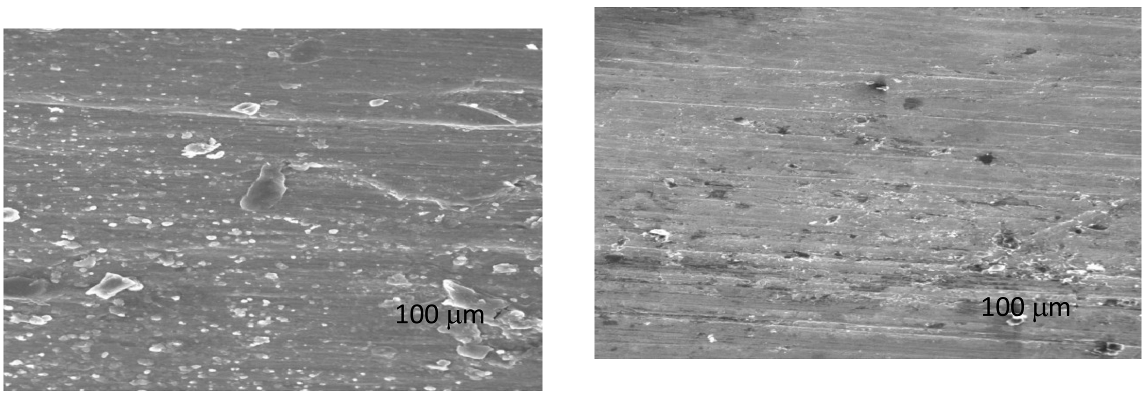

Fig. 5.31 Worn-out surface of matrix metal and composite incorporated with 15 % GR at 300 rpm & 30 N

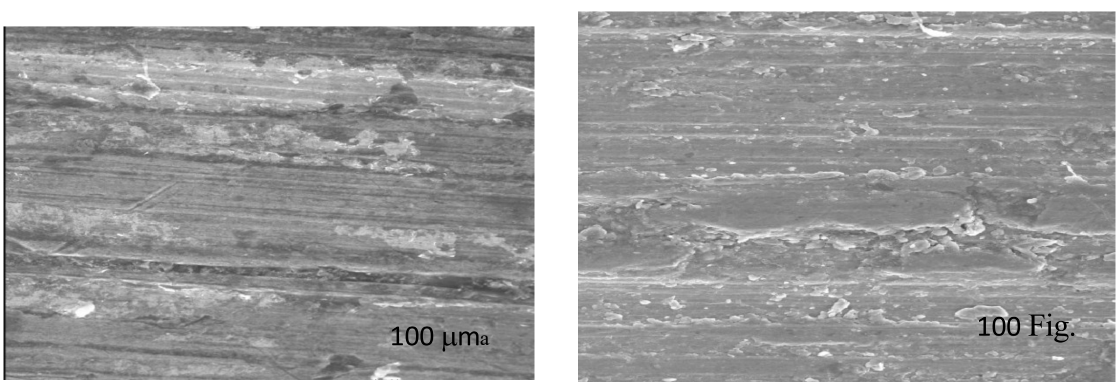

Fig. 5.32 Worn-out surface of matrix metal and composite incorporated with15 % GR at 500 rpm & 50 N

Worn out surfaces of both aluminum matrix and aluminum graphite composites, which are observed under scanning electronic microscope are shown in the Fig. 5.30 to 5.32. Fig. 5.30 shows the worn out surface of both aluminum matrix and aluminum composite incorporated with 15% graphite. At lower speed of 200 rpm and lower load of 20 N, it shows mild damages on both the surfaces of aluminum matrix and aluminum composite. The material removal appears to progress by the fracture of Al alloy and GR particles due to very high frictional load subjected at the wear surface of the specimen. A very low delamination caused by fractured surface which leads to less severe than that of higher loads and speeds. In aluminum alloy, the surface damage can be more severe than that of Al/GR composites.

An intermediate wear load and sliding speed of 30 N and 300 rpm are shown in Fig. 5.31 during which the grooves visible clearly on the surface due to wear, which is not clear at lower wear loads. In this case, it is also realized that matrix materials showed higher damage compared to composite because of its lower mechanical properties of aluminum metal matrix in comparison with its composites. By observing wear surface, it can be considered that groove plays parameter role in the behavior of wear i.e., the wear is caused by the formation and enlargement of groove. In general, the wear grooves are formed with locally metal and a fractured reinforcement. Even though minimum frictional force applied on the worn out surface, the local fractured surface found to occur by larger frictional forces arising from the casting material’s non-uniform surface and defective regions of the wear surface. The depth of grooves is higher due to the fracture of worn out surface both outside and besides the groove. The worn out surfaces revealed that the adherent wear found to be based on the governing wear mechanism during its intermediate loads and speeds. In other words, the worn out surface of aluminum composite with 15% graphite showed almost same behavior but less severe.

Fig. 5.32 showed worn out surfaces of aluminum and aluminum with 15% graphite composites under upper normal load of 50 N &at a speed of 500 rpm. Due to higher speed and load, the melting temperature increased drastically and causes localized melted area which can be observed clearly in the above Figure 5.32. The higher localized melting during sliding wear leads to higher delamination because of its very large plastic deformation of the metal. The fractured GR and some debris of metal reduces the frictional force somewhat at the worn out surface. Larger grooves and smaller grooves may be related to precipitates as displayed in Fig. 5.32 which revealed that the mechanism of wear mechanism at high sliding speeds is because of the wear noticed at melted region& hence the seizure of the matrix occurs.

The wear which is responsible for the damage can be seen in two dimensional and randomly on the surface of specimen because of normal load and pressure due to sliding speed irrespective of matrix and composite materials. The grooves found on the worn out surface parallel to normal loads or in the direction of pressure and hence the graphite particles are emerging out of the surface in the same sliding direction. At higher speed, the orientation of reinforcement is unpredictable, especially in discontinuous composites.

In lower and higher loading conditions, there are highly significant changes in wear mechanism can be seen. In lower loads, the delamination and damage can be seen in only one direction, but in higher loads it can be seen in all three direction changes. Simultaneously, at lower sliding speed, more damage is noticed on the wear surface which is parallel to the direction of pressure applied . It might be due to the higher frictional forces required for making abrasion on the wear surface parallel to the direction of pressure.

5.9 CORROSION STUDIES

The final computed test data of corrosion is given in the Table 5.39 with respect to the corrosion testing variables such as forging condition, normality of the solution, wt. % of the GR and corrosion duration. The individual effect on corrosion loss are explained in next sessions.

Table 5.39 Corrosion loss in grams for Al and Al/Gr reinforced MMCs at different conditions.

Condition	Normality of solution	Wt. % Gr	Corrosion duration in days					
			40	50	60	70	80	90
As cast	1.0	0	2.529	3.338	3.567	4.04	4.326	4.37
		5	2.313	2.909	3.22	3.517	3.61	3.87
		10	1.808	2.571	2.862	3.126	3.291	3.297
		15	1.192	2.18	2.738	2.797	3.074	3.088
		20	0.832	1.797	2.097	2.386	2.503	2.749
	1.5	0	2.714	3.577	3.977	4.007	4.264	4.303
		5	2.451	3.218	3.554	3.728	3.956	4.014
		10	1.949	2.662	2.888	3.1	3.182	3.496
		15	1.315	2.067	2.501	2.869	2.815	2.93
		20	0.933	1.61	1.942	2.328	2.412	2.492
	2.0	0	2.859	4.004	4.165	4.181	4.385	4.559
		5	2.254	3.34	3.386	3.665	4.023	4.035

		10	1.96	2.844	2.981	3.117	3.671	3.696
		15	1.496	2.151	2.526	2.689	2.877	3.051
		20	1.047	1.571	1.934	2.157	2.533	2.607
Heat treated	1.0	0	2.855	3.715	4.185	4.262	4.298	4.546
		5	2.179	3.018	3.145	3.54	3.62	3.825
		10	1.624	2.812	2.914	3.19	3.324	3.567
		15	1.235	2.304	2.659	2.656	2.699	2.967
		20	0.62	1.853	2.021	2.021	2.312	2.48
	1.5	0	2.726	3.591	4.125	4.192	4.409	4.726
		5	2.366	3.046	3.352	3.66	3.711	4.366
		10	1.833	2.788	3.025	3.172	3.287	3.833
		15	1.343	2.331	2.77	2.758	2.807	3.343
		20	0.897	1.93	2.093	2.204	2.386	2.897
	2.0	0	2.597	3.466	4.065	4.122	4.519	4.64
		5	2.552	3.074	3.558	3.78	3.801	4.057
		10	2.041	2.764	3.136	3.153	3.25	3.648
		15	1.451	2.358	2.88	2.86	2.915	3.076
		20	1.173	2.007	2.165	2.387	2.459	2.641

5.9.1 SIGNIFICANCE OF EXPOSURE TIME ON THE RATE OF CORROSION

Fig. 5.33 and 5.34 shows the corrosion loss by weight loss/area of the Al matrix materials and Al/GR composites without heat treatment and with heat treatment respectively at various normalities of corrosion media. The corrosion rate reduced significantly when there is an increase in the duration of corrosion. Initially, boththe matrix and composites experienced a severe corrosion due to which the corrosion rate slowly came to a steady state in nature. The nature of the curves is decreasing with corrosion, exposure time due to corrosion products that could protect further corrosion which is called as passivation of the matrix alloy. The same mechanism holds good even for composite materials. A thin protective layer is developed on the surface of the specimen which prevent the corrosion even in an aggressive corrosive environment.

Henry et al. [240] have noticed a thin protective layer on the surface of corroded specimen during XRD studies which consisted of hydrogen hydroxyl chloride, which in turn further retarded corrosion reaction. The same was confirmed by Moshier et al. [241] and presence of aluminum hydroxide compounds. But the correct chemical composition of corroded thin protective film is yet to know. Mc.Cafferty[242] states that the behavior of thin film due to rich in Al3+ ions in the corrosion media, which acts as a hurdle for corrosion reaction. The reaction continues in the corrosion media depleted rich in hydrogen ions which slow down the corrosion reaction.

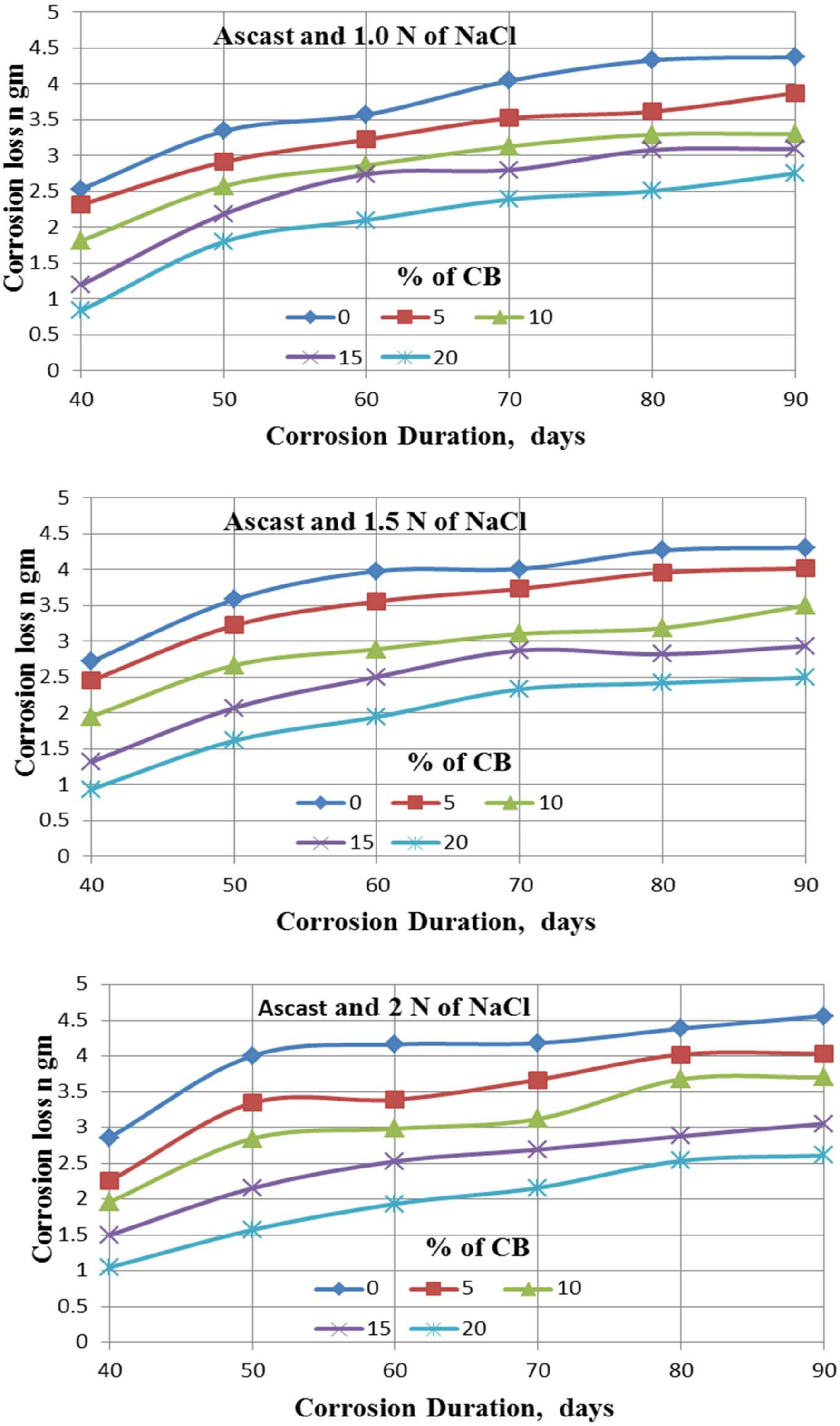

Fig. 5.33 Effect of corrosion duration on aggregated average corrosion wt. Loss of aluminum matrix Al and aluminum composites incorporated with Graphite for different normality of ascast specimens without heat

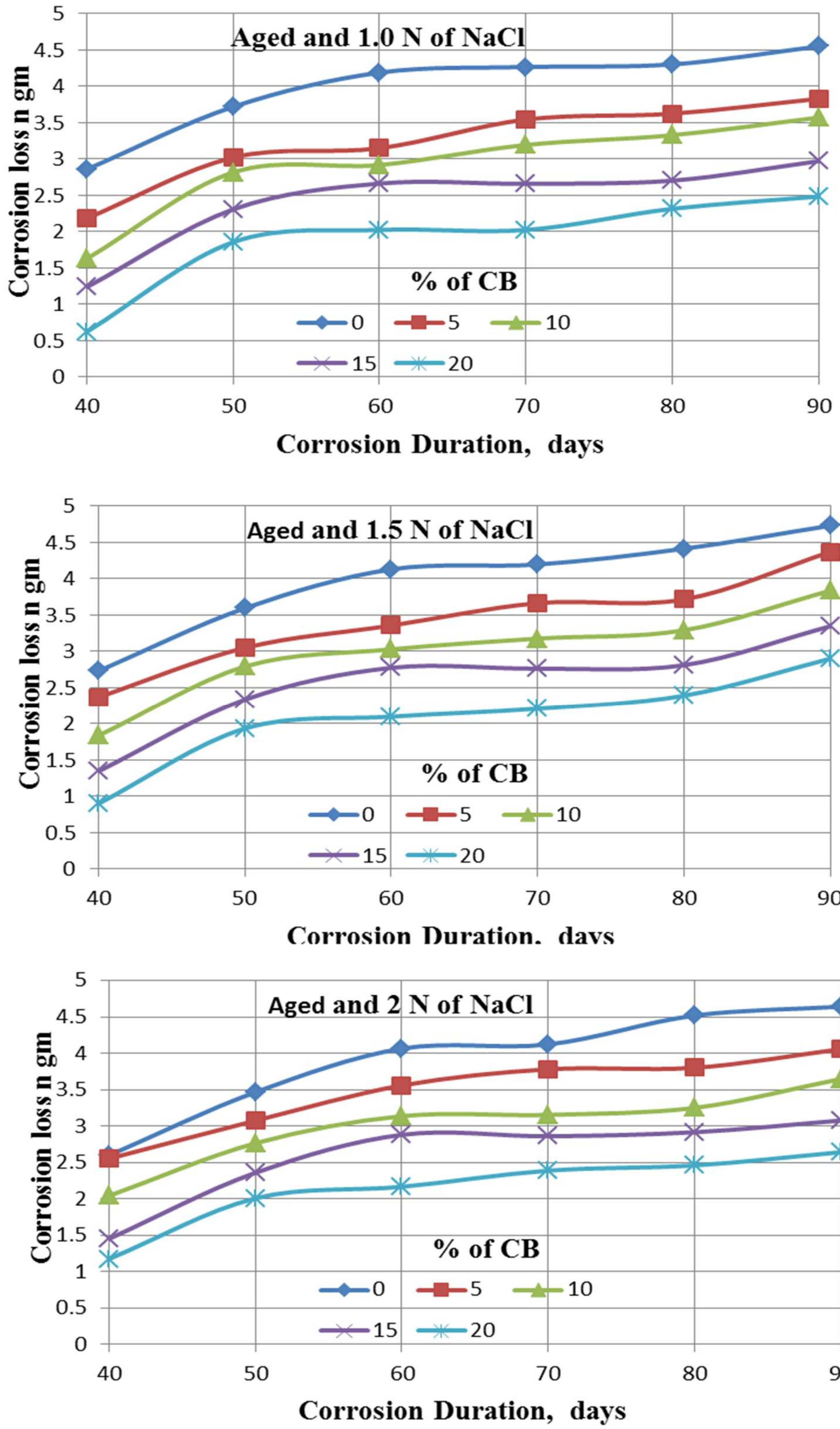

Fig. 5.34 Effect of corrosion duration on aggregated average corrosion wt. Loss of aluminum matrix Al and aluminum composites incorporated with graphite for different normality of aged specimens.

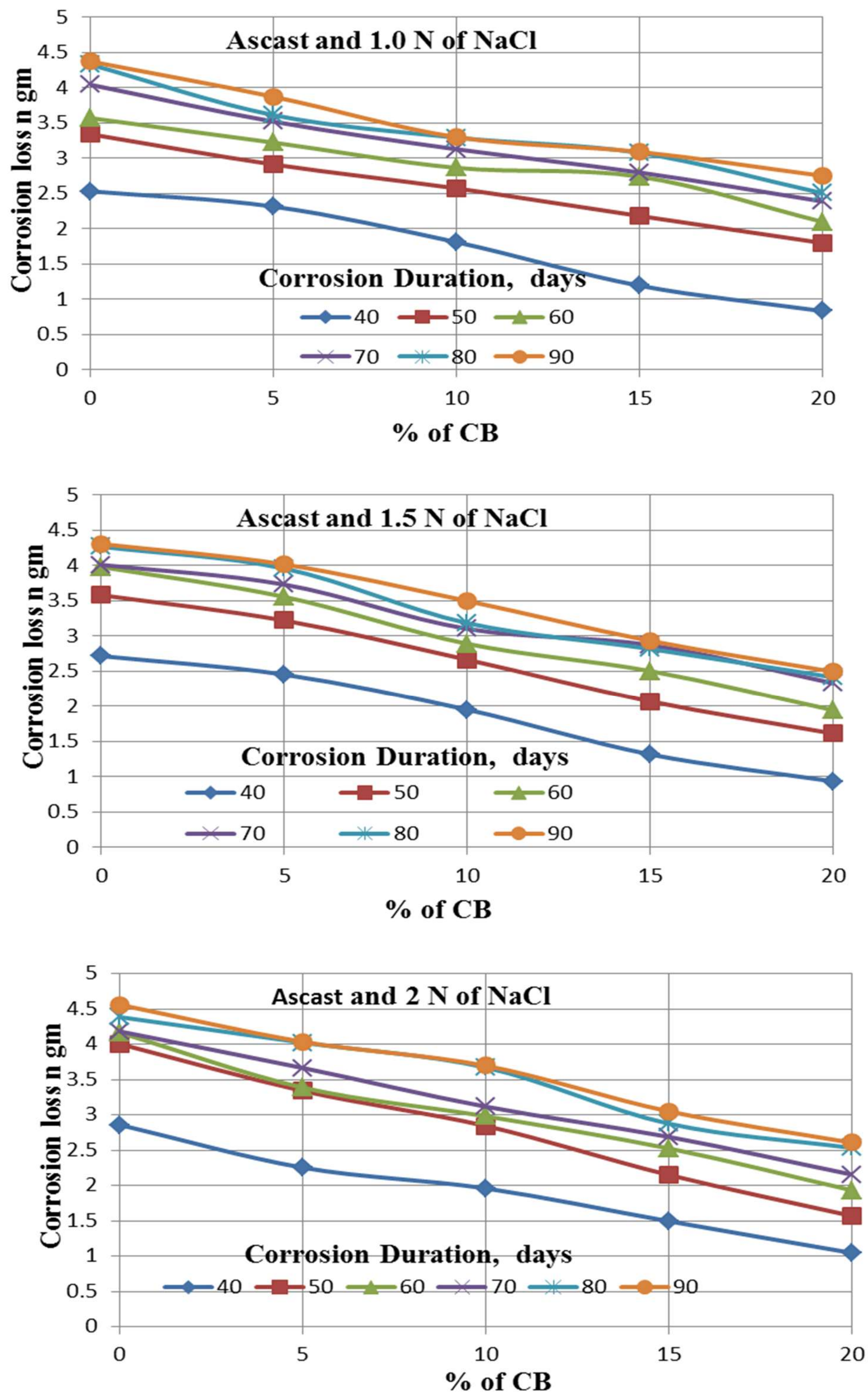

Fig. 5.35 Effect of % wt of Graphite on aggregated average corrosion wt. Loss of aluminum matrix Al and aluminum composites incorporated with graphite for different normality of as cast specimens.

5.9.2 SIGNIFICANCE OF % OF GRAPHITE ON CORROSION LOSS

Fig. 5.36 shows that the corrosion loss for as cast and aged condition Al/GR composites respectively as the function of % GR at different normality and corrosion duration. Since the graphite generally is an inert and remains stable, which is affected hardly by NaCl medium when exposed to corrosion. Though, the corrosion loss shows decrement when % of graphite increased due to which mask the area of specimens to exposure to corrosion media. The corrosion medium has rich, aggressive Cl ions results pitting on the interfaces of metal matrix and reinforcement. This interface region is formed due to a high density dislocation emerged during the mismatch occurred from the thermal differential, which developed more stress concentration around the particles which lead to allotropic transformation.

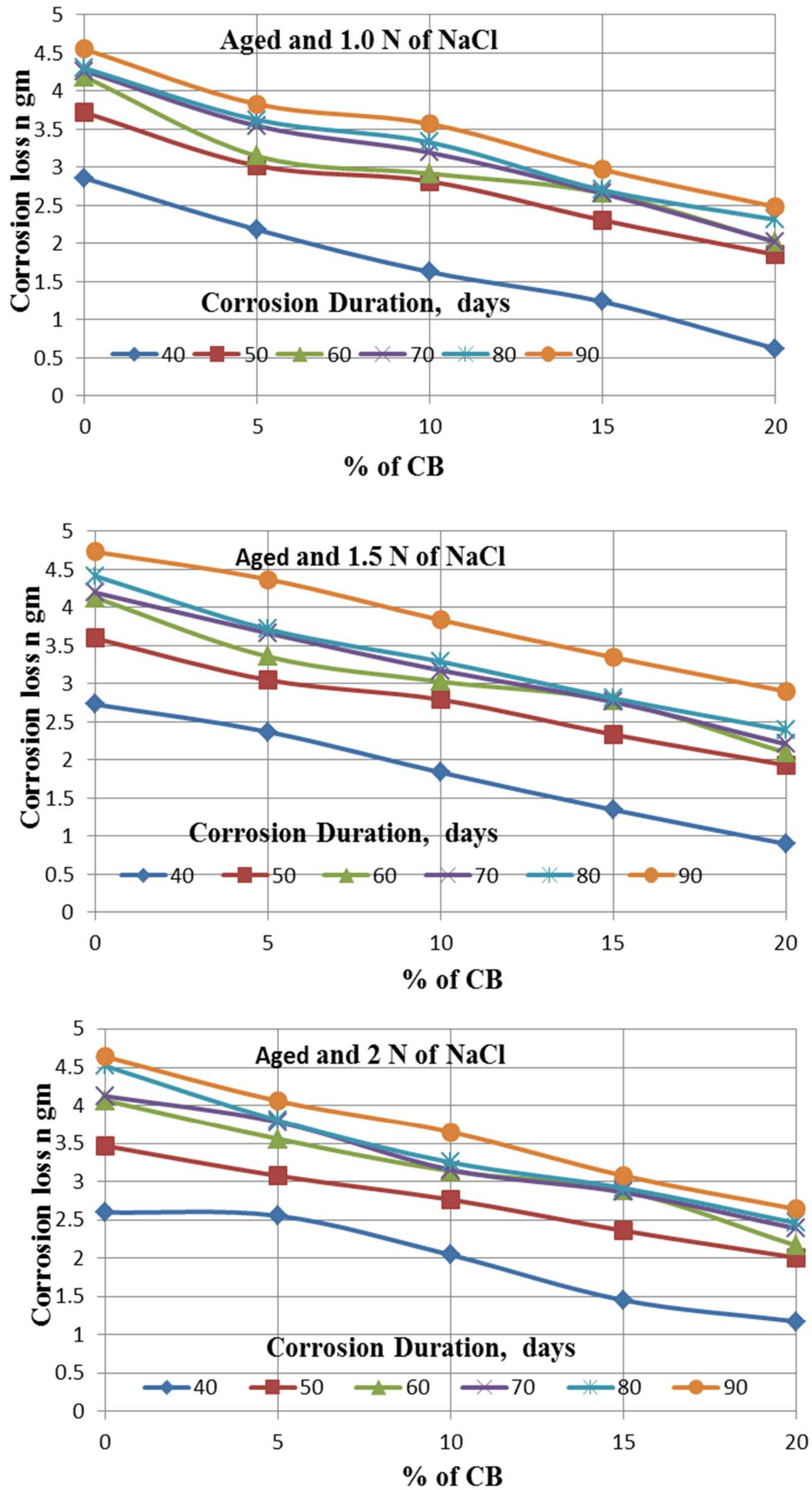

Fig. 5.36 Effect of % wt of Graphite on aggregated average corrosion wt. Loss of aluminum matrix and aluminum composites incorporated with graphite for different normality of as cast specimens.

Both allotropic transformation and strain energy associated with dislocation density promote the more in pit initiation process. Few graphite particles came out from the aluminum matrix alloy due to severe corrosion occurred at the interface of graphite and aluminum composites. Some authors [243-246] have found that composite materials have more pitting attack than that of matrix alloy due to occurrence of more severe corrosion taking place at the interface. In other hand, a resultant enhancement in the porosity is noticed, when there is an increment in the % of graphite & due to the decrease in the inter particle spacing [247]. More the exposing area of the specimen, an increment in the corrosion rate is observed and enhances the inter porosity of the specimens.

In this current research work, the corrosion loss per area predominantly contributes for the development of pits on its surface. In an aluminum alloy, there is more severity at the initial stage due to fresh used acid, which develops pits on the surface. Formation of more pits leads to more area exposure and further severe corrosion and severe material loss can be seen. More pits can be observed on the composite surfaces clearly. But more surface damage can be seen in the matrix alloy due to formation of flakes that is not seen in the composites. In GR reinforced Al composites, the pit formation depending on the graphite distribution in an aluminum the matrix. The higher GR leads to more options for film disruption and higher pits initiation.

5.9.3 INFLUENCE OF NORMALITY ON THE CORROSION RATE

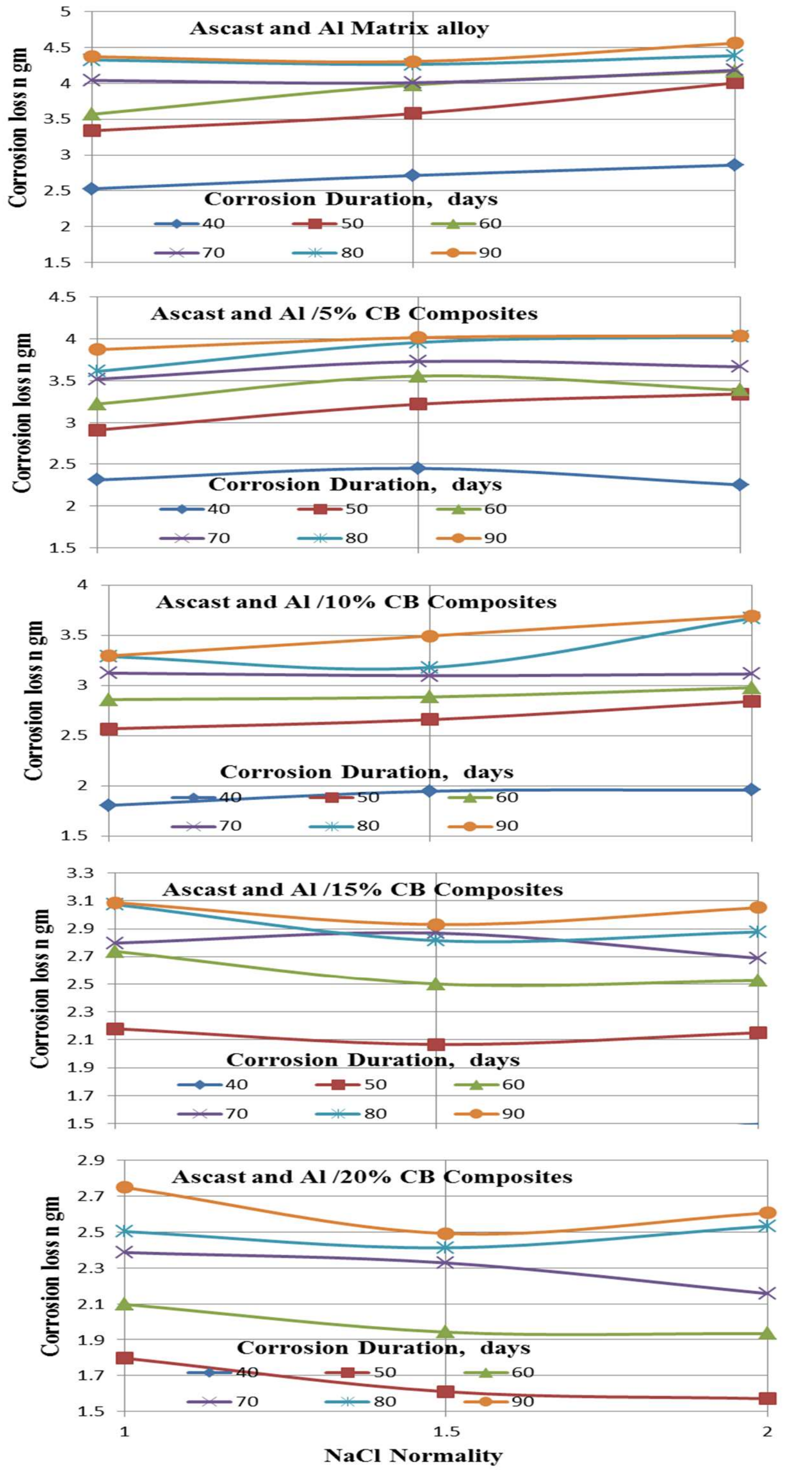

Fig. 5.37 Effect of normality of NaCl of GR on aggregated average corrosion wt. Loss of aluminum and aluminum composites reinforced with graphite 126 for as cast condition

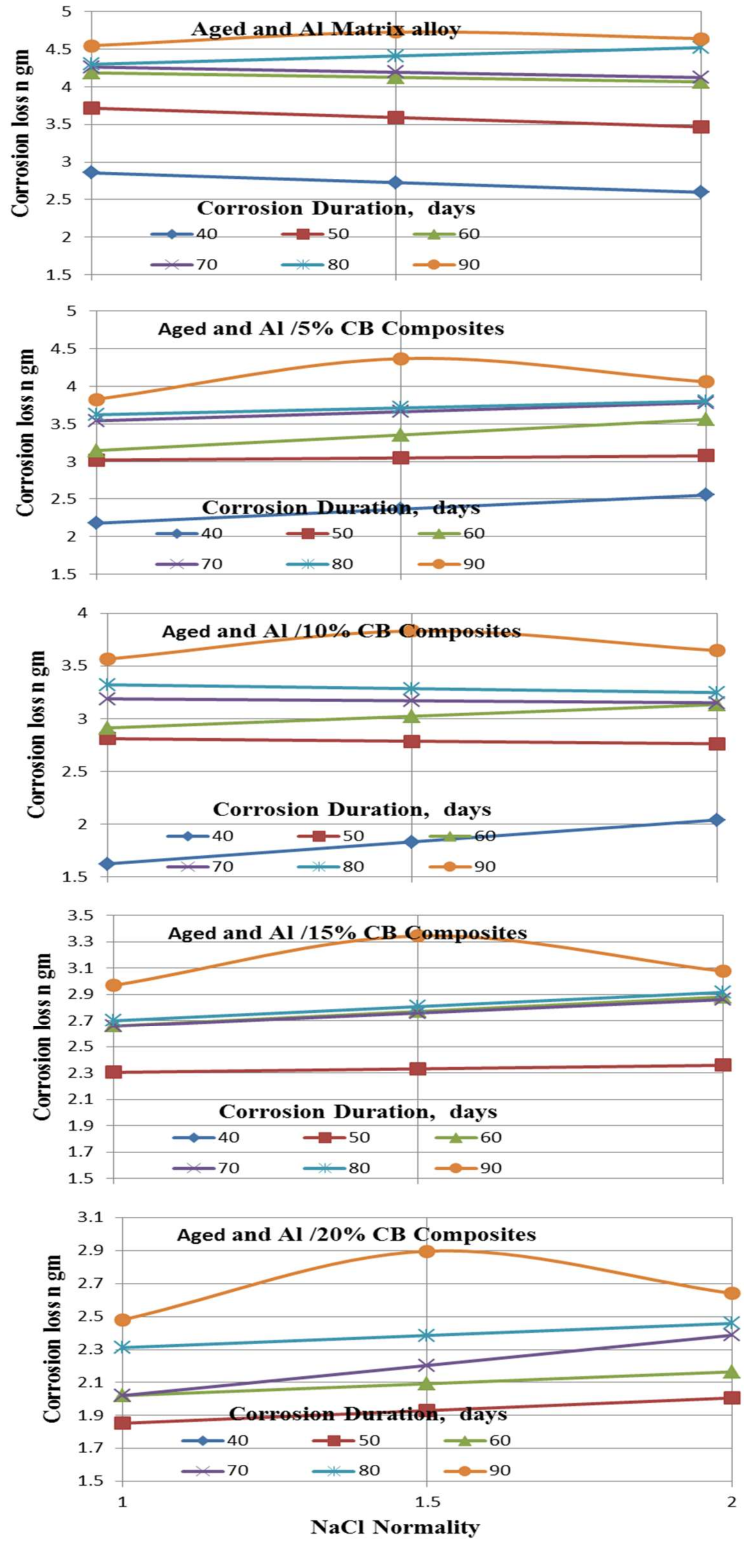

Fig. 5.38 Effect of normality of NaCl of GR on aggregated average corrosion wt. Loss of aluminum and aluminum composites reinforced with graphite for $_1a_2s_7$aged condition

Fig. 5.37 and 5.38 displays the weight loss during corrosion as a function of NaCl normality of as cast and aged condition respectively for Al and Al/GR composites and different exposure duration. It is well established that the corrosion rate increases with increase in normality (its solution's concentration) due to more free Cl ions in the corrosion medium. Only higher duration i.e., 80 and 90 days exposure shows different nature because of faster passivation of the specimen irrespective of matrix and composites. The higher percentage of GR exhibited lesser corrosion weight loss than that of reference materials.

5.9.4 EFFECT OF AGEING CONDITION ON CORROSION WEIGHT LOSS

The corrosion weight loss result is shown in Fig. 5.39, 5.40 and 5.42 for 1N, 1.5N and 2 N of NaCl corrosion medium respectively to explore the significance of ageing on corrosion rate. Corrosion loss no significant improvement was observed after ageing for composite but some improvement was observed in matrix alloy. The insignificant improvement in corrosion rate is because of the following reasons.

- The development of a porous aluminum oxide on the surface of the aged specimen due to oxidation during ageing, which partially protects the specimens.
- The stress relaxation could be attributed to ageing, which may cause slight improvement in corrosion resistance.
- The homogeneity in material composition leads to slight improvement corrosion resistance.
- The ageing reduces the mismatch strain leading to increase in resistance of corrosion.

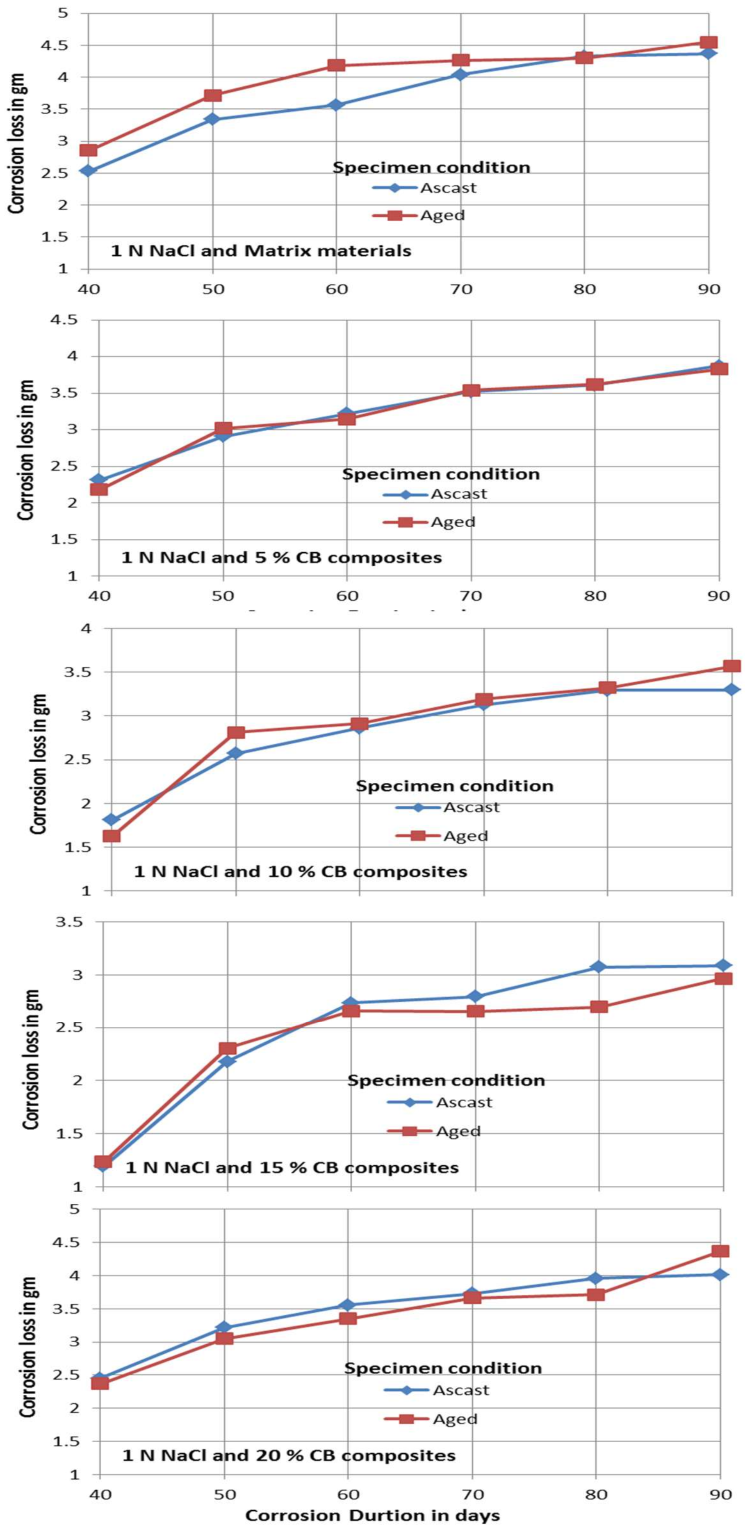

Fig. 5.39 Effect of ageing on aggregated average corrosion wt. Loss of aluminum Matrix and aluminum composite incorporated with graphite for 1 Normality solution

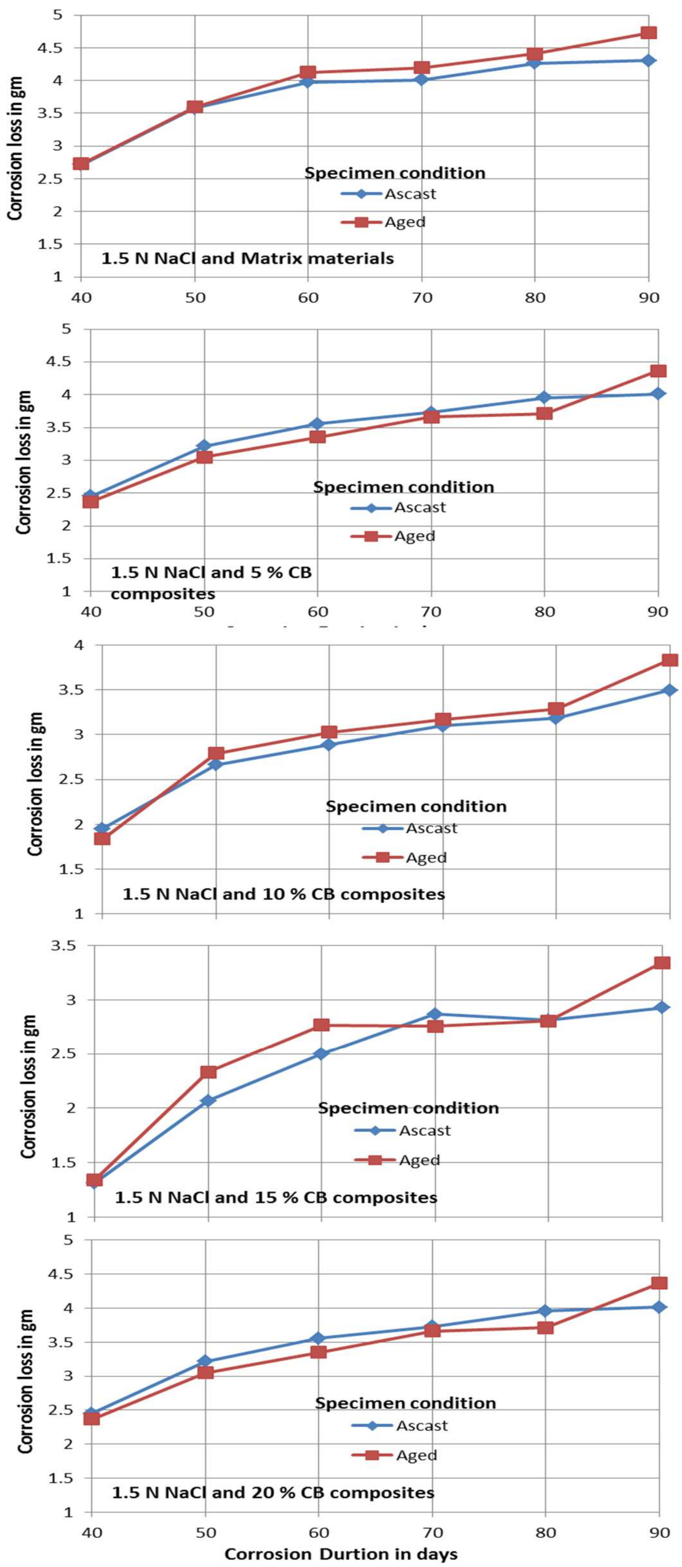

Fig. 5.40 Effect of ageing on aggregated average corrosion wt. Loss of aluminum matrix and aluminum composite incorporated with graphite for 1.5 Normality solution

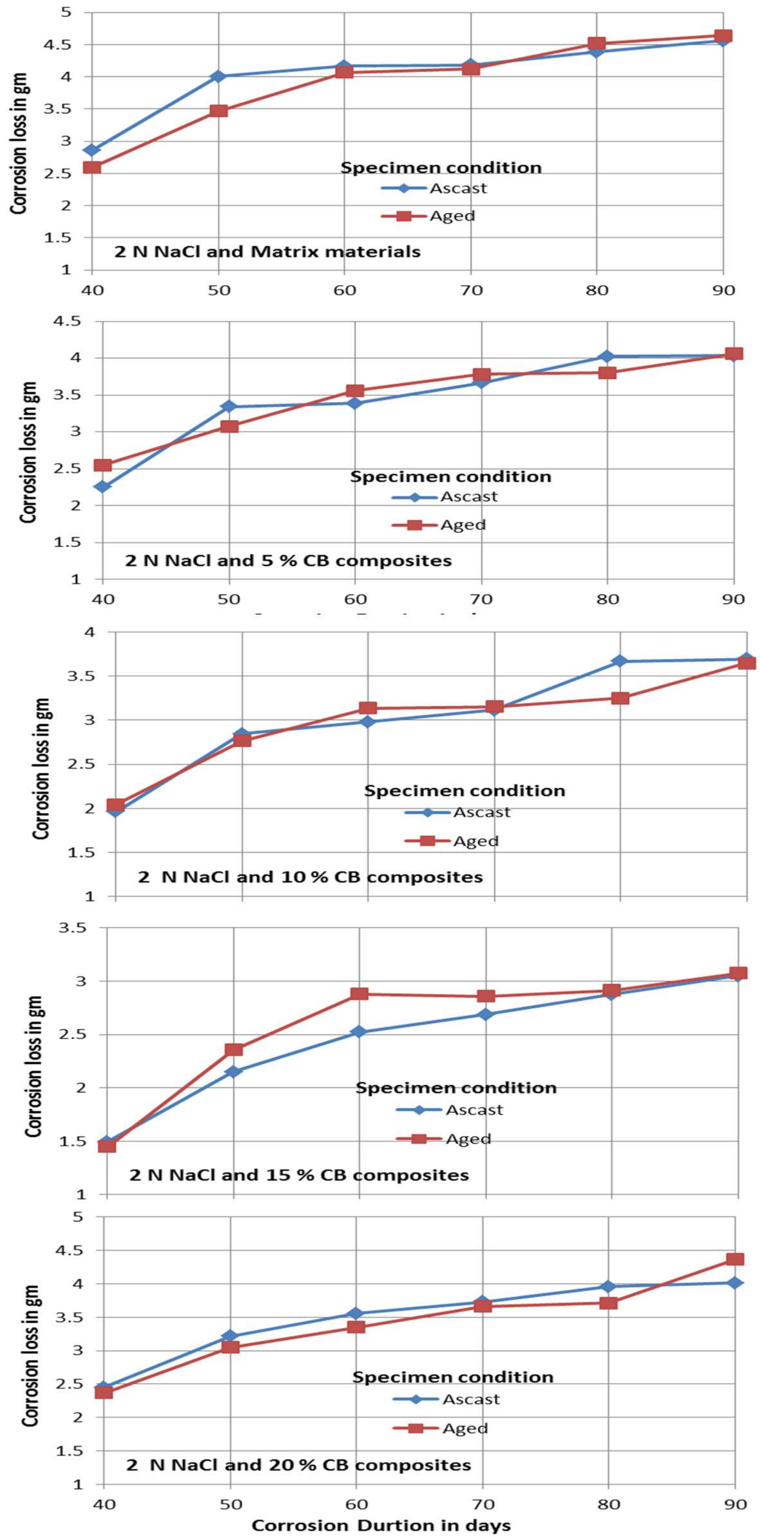

Fig. 5.41 Effect of ageing on aggregated average corrosion wt. Loss of aluminum matrix and aluminum composite incorporated with graphite for 2 Normality solution

5.9 .5 CORROSION MORPHOLOGY

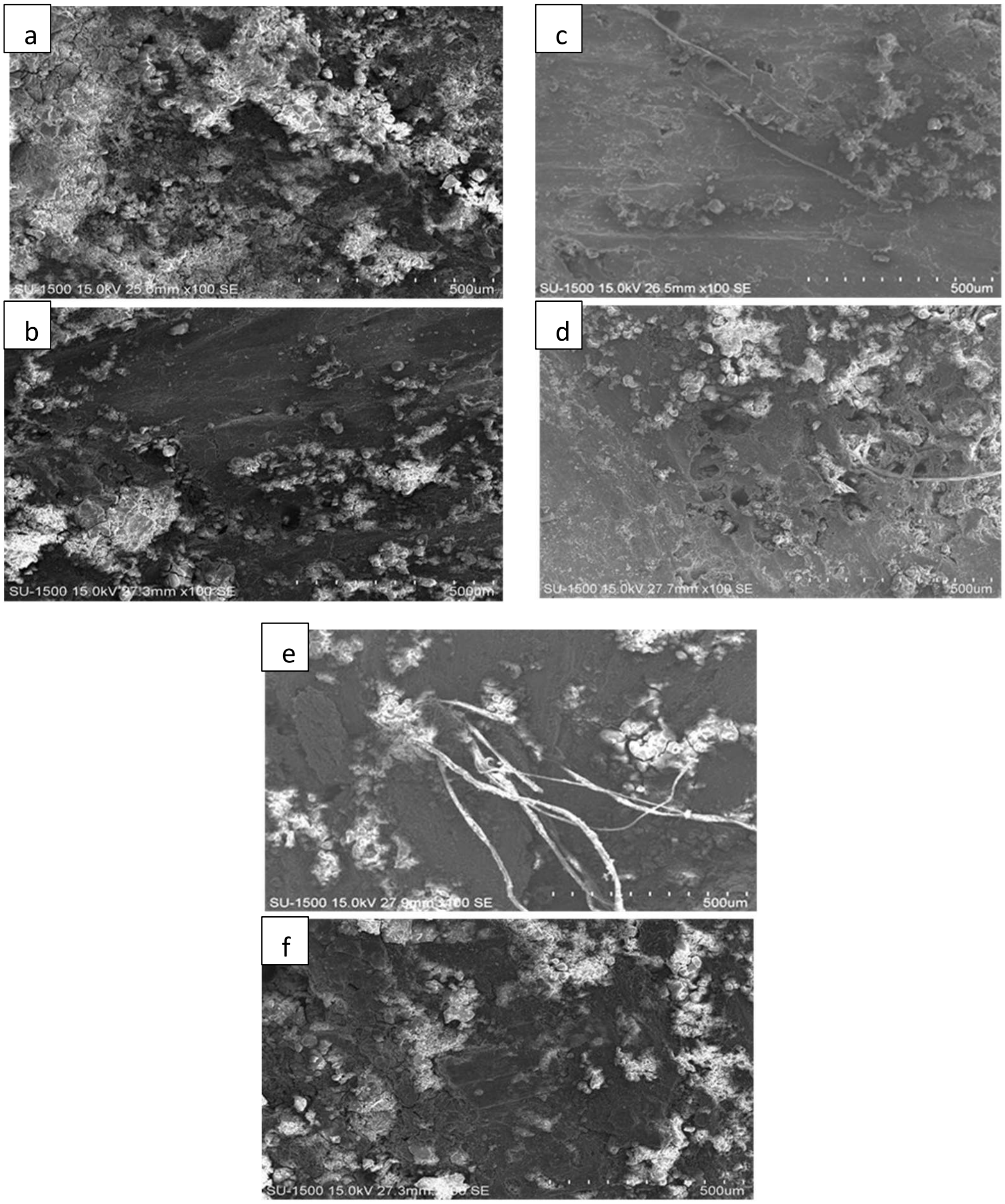

Fig. 5.42 Corroded surfaces of Al alloy/ GR composites for a) as cast, b) aged (Al matrix alloy), c) as cast 5% GR, d) aged 5% GR, e) as cast 20% GR and f) aged 20% GR composites

Fig. 5.42 displays the morphology of specimens of aluminum matrix and aluminum composite incorporated with graphite which were espoused in the corrosion medium for 90 days. The pitting is one of the major contributors for corrosion and hence almost all corrosion morphology absorbed the same. The specimen demonstrated shallow pits in case of aluminum matrix specimen and round pit in the case of composite specimens. The Al/GR composites, highly intensify localized attack as seen at the interface between particle-matrix alloys.

The adjacent pits in the matrix did not show any generalized attack, but in the composites pits occur preferentially in the GR particle or clusters, which leads to few wide pits on the surfaces. But in the case of matrix alloy the number of shallow fits was observed. In Al matrix alloy two types of corrosion mechanism are seen, such as shallow pitting and thin flakes.

In the present research, aluminum alloy contains primarily two phases like basic aluminum and a eutectic silicon. It also consists of precipitates such as Mg2Si, AlFeSi [241], $CuAl_2$ [242], [FeMn] SiAl compound, etc., [243] during the preparation of an alloy. This alloy precipitation, enriched the conductivity near the inter-metallic phase, which delivers a comfortable path way to exchange an electron which is required in hydrogen reduction. But, it cannot convert hydrogen ions to hydrogen gas since silicon is less-active. Usually, silicon acquires positive values for its potential reduction of electrodes. Aluminum normally acquires a negative sign for its planned electrode potential [248], which demonstrated supplementary reaction compared to hydrogen in reducing hydrogen ions into hydrogen gas. Therefore, silicon allows aluminum to act like anode by experiencing oxidation reaction or de electronation.

It is of opinion that, an incorporation of alloying elements viz Si and cu changes the potential during corrosion in the proper direction and decreases the corrosion resistivity of aluminum [249 - 250]. [251] have enlightened during their studies, which, by enhancing % of copper, the corrosion resistivity of an aluminum alloy is decreased.

Apart from all the elements mentioned, an aluminum alloy which is powerful for matrix alloy due to its anodic nature and hence results in higher rate of corrosion rate because of the development of local cells.

CHAPTER 6

CONCLUSIONS

In conclusion, graphene-reinforced aluminum metal matrix composites (AMMCs) exhibit significant improvements in tensile strength, hardness, compression strength, fatigue, wear, and corrosion compared to traditional aluminium alloys. The addition of graphene, a carbon material in the form of two dimension having exceptional mechanical properties, enriches the whole presentation of the composite material.

- A significant enhancement in tensile strength of the composite can be achieved by incorporating graphene into the aluminum matrix. Graphene’s high intrinsic strength and its capability to transfer the load efficiently amongst aluminum particles result in improved resistance against deformation and fracture under tensile forces.
- Graphene as a reinforcement is main responsible in enhancing the hardness of the AMMCs. The existence of graphene sheets restricts dislocation movement, resulting in enhanced hardness and resistance to plastic deformation. Graphene also acts as a barrier against grain growth, which further enhances composite’s hardness.
- The graphene reinforcement in AMMCs also leads to improved compression strength. Graphene sheets prevent the collapse of aluminium particles under compressive loads by providing additional strength and stability. This reinforcement mechanism results in enhanced resistance to compression and increased load-bearing capacity.
- Graphene reinforcement improves the fatigue strength of AMMCs. The presence of graphene sheets helps to disperse and inhibit crack propagation, which reduces the susceptibility to fatigue failure. Graphene's high strength and ability to efficiently transfer stress between aluminum particles contribute to increased fatigue resistance.

- An addition of graphene with the aluminum matrix hinders in initiation &growth of cracks during cyclic loading. Graphene acts as a barrier and prevents crack propagation by bridging and dispersing the stress concentrations, thereby enhancing the fatigue property and life of the composites.
- Graphene reinforcement enhances the damage tolerance of AMMCs under cyclic loading. The graphene sheets serve as a toughening agent, absorbing and distributing energy during fatigue loading. This improves the overall resistance to crack initiation and propagation, leading to extended fatigue.
- Several studies and experimental investigations have demonstrated that the wear rate can be reduced remarkably by incorporating graphene into aluminium matrices and enhances the overall tribological properties. The presence of graphene provides a strong reinforcement network within the composite, increasing its hardness, strength, and load-bearing capacity.
- Moreover, graphene's excellent lubricating properties and low friction coefficient contribute to reducing wear and frictional losses in AMMCs. The graphene acts as a solid lubricant which develops a protective layer to protect the surfaces due to direct contact creating friction amongst the sliding surfaces. This resulted in reduced wear rates, minimized surface damage, and improved durability of the composite materials.
- Firstly, graphene acts as a barrier layer on composite’s surface and effectively minimizes the contact amongst the aluminum matrix and corrosive media. This barrier layer inhibits the dispersal of corrosive medias like ions, oxygen and water towards the aluminum matrix, thus reducing the corrosion rate.
- Secondly, graphene possesses excellent electrical conductivity, which can facilitate the development of a protective layer of oxide over the surface of an aluminum matrix which further acts as a passive film, providing a physical and chemical barrier against corrosion.

- Furthermore, graphene's high mechanical strength and stability enriches the overall mechanical properties of the AMMCs. At the time of reinforcement of aluminum matrix, graphene can enhance its resistance to mechanical stress, prevents the origination and spread of corrosion- related cracks and defects.
- Additionally, a unique structure of graphene allows for improved bonding between inter faces amongst the graphene and aluminum matrix. This strong interfacial interaction ensures better load transfer, which enhances the overall stability and integrity of the composite material, making it more resistant to corrosion-induced failure.
- However, it is important to note that while graphene reinforcement offers significant corrosion resistance improvements, it may not completely eliminate corrosion. Factors such as the quality of graphene dispersion, processing conditions, and exposure environment can influence the effectiveness of corrosion protection in graphene-reinforced AMMCs.

Overall, an aluminum metal matrix composite incorporated with graphene remarkably enhances its compression strength, tensile strength, fatigue, hardness, wear and corrosion. These enhancements make graphene-reinforced AMMCs highly promising materials for various applications that require superior mechanical properties, such as aerospace, automotive, and structural components.

CHAPTER 7

FUTURE SCOPE

(i) The incorporation of graphite particles within the specified proportional quantity enhances the wear resistance of hybrid composites at the expenditure of strength of its matrix material, but, it is further suggested to overcome by mixing hard ceramics like silicon carbide, aluminum oxide, boron carbide into aluminum matrix material.

(ii) It can be further suggested to use hybrid metal matrix composites reinforced with graphite can reduce wear loss and frictional coefficient of composites at higher speed.

(iii) The literature review suggested to use further the stir casting method as the most commercial and economical fabricating technique followed by powder metallurgy for self-lubricated aluminum hybrid composites.

(iv) Hence it is further recommended that the combination of silicon carbide and graphite hybrid reinforcement in fabricating aluminum based self-lubricated hybrid metal matrix composites in obtaining better quality of composites with further enhanced fatigue property.

(v) The comprehensive literature in this review discovered that most of the research is done in the area of self-lubricating hybrid composites by incorporating graphite as a solid lubricant into aluminum matrix alloys; however in future, researchers may focus on the use of deferent other metallic and ceramic particulates like titanium, zirconium, magnesium, nickel, silver, copper, zinc, bronze, alumina, silicon nitride. It is also suggested to explore in the area of bio reinforcements.

(vi) The extensive literature discussed in this research work has discovered that majority of researchers attentive on very few mechanical properties like hardness and tensile strength of self-lubricating hybrid composites; whereas other properties like toughness, impact strength, fatigue strength, compressive strength and creep have investigated less.

REFERENCES

1. Zheng Kailun, Politis Denis J., Wang Liliang., & Lin Jianguo. (2018). A Review on forming techniques for manufacturing lightweight complex—shaped aluminum panel components. *International Journal of Lightweight Materials and Manufacture*, 1(2), 55-80.https://doi.org/10.1016/j.ijlmm.2018.03.006

2. Thackeray M.M., Wolverton C., & Isaacs E.D. (2012) Electrical energy storage for transportation—approaching the limits of and going beyond, lithium-ion batteries. *Energy Environ. Sci*., 5, 7854-7863. https://doi.org/10.1039/C2EE2189ZE

3. Wanhill R.J.H. (2014). Aerospace applications of aluminum–lithium alloys. *Elsevier*, 503-535. https://doi.org/10.1016/B978-0-12- 401698-9.00015-X

4. Xiao W. B., Wang, Y. Wu Y., & Yang X. (2017). Constitutive modeling of flow behavior and microstructure evolution of AA7075 in hot tensile deformation. *Mater. Sci. Eng. A*, 712, 704-713.DOI: 10.1016/i.msea.2017.12.028

5. Rao K. J., & Wei. (2001). Performance of a new dry lubricant in the forming of aluminum alloy sheets. *Wear,* 249(1-2), 85-92. https://doi.org/10.1016/S0043-1648 (01)00526-9

6. Djavanroodi F., Abbasnejad D.S., & E.H. Nezami. (2011). Deep drawing of aluminum alloys using a novel hydroforming tooling. *Mater. Manuf. Process*., 126(5), 796- 801. https://doi.org/10.1080/10426911003720722

7. Emadi P., Andilab B., Borodianskiy K., & Ravindran C. (2022). Strengthening of Mg-Al-Zn-Mn alloy using SiC/Al nanocomposite extrusion. *J.Alloys Compd.,* 922, 20-29. https://doi.org/10.1016/j.jallcom.2022 .122243

8. Malaki M., Xu, W., Kasar A.K., Menezes P.L., Dieringa, H., Varma R.S., & Gupta M. (2019). Advanced Metal Matrix Nanocomposites. *Metals*, 9(3), 330-342. https://doi.org/10.3390/met9030330

9. Tajzad I., & Ghasali E. (2020). Production methods of CNT-reinforced Al matrix composites. *A review. J. Compos Compd*. 2(1– 9),314-325.DOI:10.29252/jcc.1.2.1

10. Hanizam H., Salleh M.S., Omar M.Z., & Sulong, A.B. (2019) Optimization of mechanical stir casting parameters for fabrication of carbon nanotubes–aluminum alloy composite through Taguchi method. *J. Mater. Res. Technol,* 8, 2223–2231.DOI:10.1016/j.jmrt.2019.02.008

11. Sekar K., Malleus K., & Joseph MA. (2014). Effect of T6 heat treatment in the microstructure and mechanical properties of A356 reinforced with Nano Al2O3 particles by combination effect of stir and squeeze casting. *Procedia Mater Sci*, 5: 444– 453,https://doi.org/10.1016/j.mspro.2014.07.287

12. Özdemir I., Cöcen U., & Önel K. (2000). The effect of forging on the properties of particulate-SiC- reinforced aluminum-alloy composites. *Compos Sci Technol*, 60, 411–419. DOI: 10.1016/S0266-3538(99)00140-2

13. Purohit R., Qureshi M.M.U., & Rana R.S. (2017). The effect of hot forging and heat treatment on wear properties of Al6061-Al2O3 Nano composites. *Composites Science and Technology*, 4((2), Part A, 4042–4048. DOI:10.1016/j.matpr.2017.02.306

14. Yuan, C.; Tan, Z.; Fan, G.; Chen, M.; Zheng, Q.; Li, Z. (2019) Fabrication and mechanical properties of CNT/Al composites via shift-speed ball milling and hot-rolling. J. Mater. Res. 2019, 34, 2609–2619.DOI: https://doi.org/10.1557/jmr.2019.219

15. Aigbodion V.S., & Hassan S.B. (2007) Effects of silicon carbide reinforcement on microstructure and properties of cast Al–Si–Fe/SiC particulate composites .*Materials Science and Engineering A*, 447(1–2), 355-360.https://doi.org/10.1016/j.msea.2006.11.030

16. Reddy Pencha M., Shakoor R.A., Parande Gururaj., Manakari Vyasaraj. Ubaid F., Mohamed A.M.A., & Gupta Manoj (2017).Enhanced performance of Nano-sized SiC reinforced Al metal matrix nanocomposites synthesized through microwave sintering and hot extrusion techniques. *Progress in Natural Science: Materials International,*27(5), 606-614,https://doi.org/10.1016/j.pnsc.2017.08.015

17. Balasubramanian I & Maheswaran R (2015). Effect of inclusion of SiC particulates on the mechanical resistance behavior of stir-cast AA6063/SiC composites. *Material & Design*, 65, 511–520.http://dx.doi.org/10.1016/j.matdes.2014.09.067

18. Hassani A., Bagherpour. E & Qods F. (2013). Influence of pores on workability of porous Al/SiC composites fabricated through powder metallurgy + mechanical alloying. *Journal of Alloys and Compounds*,591,132–142.,DOI:10.1016/j.jallcom

19. Junwu Liu., Zhixiang Z., Jianmin W., Yucheng W., & Jun Lü (2008). Pressure less infiltration of liquid aluminum alloy into SiC preforms to form near-net-shape SiC/Al composites. *Journal of Alloys and Compounds*,465,239–243,https://doi.org/10.1016/j.jallcom.2007.10.055

20. Ramesh C. S., Pramod S and Keshavamurthy R (2001).A study on microstructure and mechanical properties of Al 6061–TiB2 in-situ composites. *Materials Science and Engineering*, 528, 4125– 4132. https://doi.org/10.1016/j.msea.2011.02.024

21. Ramesh C. S & Keshavamurthy R (2012).Influence of forging on mechanical properties of Ni–P .coated Si3N4 reinforced Al6061 composites. *Materials Science and Engineering*,12,59–66.https://doi.org/10.1016/j.msea.2012.04.081

22. Shi W.C., Yuan L., & Shan D.B. (2014). Effect of forging on the microstructure and tensile properties of 2024Al/Al18B4O33w composite. *Material Science & Engineering A,* 615, 313-319.https://doi.org/10.1016/j.msea.2014.07.092

23. Pradeep Kumar G, Keshavamurthy R, Ramesh C & Bharathesh T. P (2015).Mechanical properties of Hot forged Al6061-TiB2 In-situ Metal Matrix Composites. *Materials Today Proceeding*, 2, 3107- 3115. https://doi.org/10.1016/j.matpr.2015.07.270

24. Cavaliere P & vangelista E (2005). Isothermal forging of metal matrix composite: Recrystallization behavior by means of deformation efficiency. *Composite science and technology*, -66, 357-362.https://doi.org/10.1016/j.compscitech.2005.04.047

25. Durrant G & Scott V.D (1993). The effect of forging on the properties and microstructure of saffil fiber reinforced aluminum. *Composite Science & Technology,* 49, 153-164,https://doi.org/10.1016/0266- 3538(93)90055-L

26. Ceschini L, Minak G and Morri A (2009).Forging of the AA2618/20 vol. % Al2O3p composite: Effects on microstructure and tensile properties. *Composite science and Technology*, 69, 1783-1789.https://doi.org/10.1016/j.msea.2014.07.092

27. Ceschini L, Minak G, Morri A & Tarterini F. (2009).Forging of the AA6061/ 23 vol% AlO3p Composite: Effects on microstructure and tensile properties. *Materials Science and Engineering.*A513, 176-184.https://doi.org/10.1016/j.compscitech.2008.08.027

28. Zhoua L, Huanga Z, Wangb C & Z. Y. Maa (2016).Constitutive flow behavior and finite element simulation of hot rolling of SiCp/2009Al Composite. *Mechanics of Materials*, 93, 32-42

29. El-Sabbagh A, Soliman M, and Palkowski H (2012). Hot rolling behavior of stir-cast Al 6061 and Al 6082 alloys – SiC fine particulates reinforced composites. *Journal of Materials Processing Technology*, 212, 497–508

30. Gronostajski J, Marciniak H, & Matuszak A (1996).Production of composites of the base of AlCu4 alloy chips. *Journal of Materials Processing technology*, 60, 719-722

31. Ezatpour H, Torabi-Parizi M & Sajjadi S (2013). Microstructure and mechanical properties of extruded Al/Al2O3 composites fabricated by stir-casting process. *Trans. Nonferrous Met. Soc. China*, 23, 1262−1268

32. Cao J, Krishnan N, Wang Z, H. Lu,& Swanson A (2004).Micro forming: Experimental investigation of the extrusion process for micro pins and its numerical simulation using RKEM. *Journal of Manufacturing Science and Engineering*, 126(4). 642–652

33. Verma Deep., Chandrasekhar P, & Singh S (2013).Investigations into Deformation Characteristics during Open-Die Forging of SiCp Reinforced Aluminum Metal Matrix Composites. *Hindawi Publishing Corporation Journal of Powder Technology ,* Article ID 183713, 14-23

34. Hemanth S Thulasi, Arum Kumar Y & Srinath M.S (2015).Design and Manufacturing Simulation of Preform for Thread Rolling Operation. *International Journal of Modern Engineering Research*, 5, 62-68

35. Y. Shen, J. Garnier, L. Allais, J. Crepin, O. Ancelet & J. M. Hiver (2011).Experimental and numerical characterization of anisotropic damage evolution of forged Al6061-T6 alloy. *Procedia Engineering*, 10, 3429-3434

36. O, Madjid A, and Nacer E (2011). Numerical and experimental study of ductile fracture of an aluminum alloy during forging process. *Computer Methods in Mechanics*, 10.2-5

37. Behrens A & Just H (2002).Verification of the damage model of effective stresses in cold and warm forging operations by experimental testing and FE simulations. *Journal of Materials Processing Technology,* 125–126, 295–301

38. Corbin M. Grohol, Yung C. Shin a, Alex Frank (2021) Laser cladding of aluminum alloy 6061 via off-axis powder. *Injection Surface and Coatings Technology*, 415, 127099

39. Jing, Z., Cao, Q., Jun, H. (2021). Corrosion, wear and biocompatibility of hydroxyapatite bio-functionally graded coating on titanium alloy surface prepared by laser cladding, *Ceram. Int.* 47, 24641–24651

40. Hussein, R.O., Nie, X., Northwood (2010). Influence of process parameters on electrolytic plasma discharging behavior and aluminum oxide coating microstructure. *Surf. Coat. Technol*. 2, 155, 165

41. M. Asif, K. Chandra and P.S. Misra (2011) Development of Aluminum Based Hybrid Metal Matrix Composites for Heavy Duty Applications. *Journal of Minerals & Materials Characterization & Engineering*, 10, (14) 1337-1344

42. Patel D. R., Patel N. S. (2016). Development of Al-SiC MMCs for making valves. *Ijariie publication*, 2(3), 2395-4396

43. Hyo Lee, Jae S. Yeo, Duk J. Yoon & Kyung H. Na (2001).The fabrication process and mechanical properties of SiCp/Al-Si metal matrix composites for automobile air-conditioner compressor pistons. *Journal of Materials Processing Technology*, 113, 202-208

44. Zhoua L, Huanga Z, Wangb C & Z. Y. Maa (2016).Constitutive flow behavior and finite element simulation of hot rolling of SiCp/2009Al Composite. *Mechanics of Materials*, 93, 32-42

45. El-Sabbagh A, Soliman M, & Palkowski H (2012). Hot rolling behavior of stir-cast Al 6061 and Al 6082 alloys – SiC fine particulates reinforced composites. *Journal of Materials Processing Technology*, 212, 497–508

46. Yu-Tuan Chou & Shao-Yi Hsia (2015). Fabrication Improvement of Cold Forging Hexagonal Nuts by Computational Analysis and Experiment Verification. *Hindawi Publishing Corporation*, 20, Article ID 835038, 1-11

47. W. He, Y.F. Zhang, K.S. Lee, L. Lu, S.S. Xie, & Q.J. Jin (1996).Microstructure and mechanical properties of an Al/SiCp composite cold die forged gear. *Material & Design*, 17, 97-102

48. An, L.; Ma, Y.; Liu, Y.; Sun, L.; Wang, S.; Wang, Z, & Yunying (2018). Effects of additives, voltage and their interactions on PEO coatings formed on magnesium alloys. *Surf. Coat. Technol*. 354, 226–235

49. Ainhoa Riquelme & Pilar Rodrigo (1993). An Introduction on the Laser Cladding Coatings on Magnesium Alloys. *Metals*, 11(12), 11-18

50. Riquelme, A.; Rodrigo, P.; Escalera-Rodríguez, M.D.; Rams, J. (2016) Analysis and optimization of process parameters in Al–SiCp laser cladding. Opt. Lasers Eng. 2016, 78, pp 165–173

51. Su, Y.; Yue, T (2020). Microstructures of the bonding area in laser cladded Zr-based amorphous alloy coating on magnesium. *Mater. Today Commun*. 25, 108-115

52. Jun, Y.; Sun, G.; Wang, H.-Y.; & Jia, S (2006). Laser (Nd: YAG) cladding of AZ91D magnesium alloys with Al+Si+Al2O3. *J. Alloys Compd.* 407, 201–207

53. Sijo MT, & Jayadevan KR (2016). Analysis of stir cast aluminum silicon carbide metal matrix composite: a comprehensive review. *Procedia Technol*; 24: pp 379–385

54. Lurie S, Volkov-Bogorodskiy D, & Solyaev Y, (2016). Multiscale modelling of aluminum-based metal–matrix composites with oxide Nano inclusions. *Comput Mater Sci*, 116, 62–73

55. Lee Y-S, Yeon B-H, & Hyun S-K, (2012). A new fabrication method to improve metal matrix composite dispersibility. *Mater Lett*, 89,279– 282

56. Mazar Atabaki M, Idris J (2012). Low-temperature partial transient liquid phase diffusion bonding of Al/Mg2Si metal matrix composite to AZ91D using Al-based interlayer. *Mater Des*, 34,832–841.

57. Alarifi IM (2019). Investigation the conductivity of carbon fiber composites focusing on measurement techniques under dynamic and static loads. *J Mater Res Technol*, 8(5), 4863–4893

58. Min-Feng Y, Laurie O, Dyer M.J, Moloni K, Kelly T.F & Ruoff R.S (2000). Strength and breaking mechanism of multi walled carbon Nano tubes under tensile load. *Science* (2000) 287,637–640

59. Dhand V, Rhee K.Y, Kim H.J, & Jung D.H (2013). A comprehensive review of graphene nanocomposites: research status and trends. *J Nanometer*, 158, 1–14

60. Liu J, Fernandez B, Rodriguez P, Naher S, & Brabazon (2016). Powder processing methodology for production of graphene oxide reinforced aluminum matrix composites. *Adv. Mater Process Technol* 2(4), 437– 450

61. Nieto A, Bisht A, Lahiri D, Zhang C, & Agarwal A (2017) Graphene reinforced metal and ceramic matrix composites: a review *.Int Mater Rev* (2017) 62,291–302

62. Yu YX (2014) Binding energy and work function of organic electrode materials phenanthraquinone, pyromellitic anhydride and their derivatives adsorbed on graphene. ACS *Appl Mater Inter-faces* 6, 16267–16275

63. Hu Z, Tong G, Lin D, Chen C, Guo H, Xu J,& Zhou L (2016) Graphene- reinforced metal matrix nanocomposites—a review. *Mater Sci Technol* 32, 1–24

64. Gao C, Zhan B, Chen L, & Li X A (2017) micro mechanical model of graphene-reinforced metal matrix nanocomposites with consideration of graphene orientations. *Compos Sci Technol*, 152,120–128

65. Suthar J, Patel KM (2018). Processing issues, machining and applications of aluminum metal matrix composites. *Mater Manuf Process*, 33,499– 527

66. Saravanan Senthil M.S, Sivaprasad K, Susila P, & Babu K (2011) Anisotropy models in precise crystallite size determination of mechanically alloyed powders. *Phys B Condens Matter*, 406,165–168

67. Chu K, Jia C (2014) Enhanced strength in bulk grapheme–cop-per composites. *Physica Status Solidi,* 211,184–190

68. Zhang J, Chen Z, Zhao J, & Jiang Z (2018) Microstructure and mechanical properties of aluminum–graphene composite powders produced by mechanical milling. *Mech Adv Mater Mod Process*, 4, 1–9

69. Stankovich S, Dikin D.A, Dommett G.H, Kohlhaas KM, Zimney E.J, Stach EA, Piner R.D, Nguyen S.T,& Ruoff R.S (2006) Graphene-based composite materials. *Nature* 442:282–286

70. Anthony H.G, & Xavior M (2017) Encapsulation and microwave hybrid processing of Al 6061-graphene-sic composites. *Mater Manuf Process*, 33, 19–25

71. Naseer A, Ahmad F, Aslam M, Guan BH, Harun W.S.W,Muhamad N, Rafi Raza M, & German RM (2019) A review of processing techniques for graphene-reinforced metal matrix composites. *Mater Manuf Process, 34,957*–985

72. Bains P.S, Sidhu S.S, & Payal H.S (2015) Fabrication and machining of metal matrix composites: a review. *Mater Manuf Process,* 31,553–573

73. Sahoo B, Joseph J, Sharma A, & Paul J (2016) Surface modification of aluminum by graphene impregnation. Mater Des, 116, 51–64

74. Raveen R, Yoganandh J, Sathish Kumar S, & Neelakandeswari N (2019) Preparation and characterization of pulsed electrodeposited cobalt–graphene nanocomposite coatings. *J Mater Des App* l233, 2469–2477

75. Sharma P, Sharma S, & Khanduja D (2015) On the use of ball milling for the production of ceramic powders. *Mater Manuf Process*, 30, 1370– 1376

76. Toozandehjani M, Matori K.A, Ostovan F, & Aziz S.A (2017), Mamat M.S.E.Effect of milling time on the microstructure, physical and mechanical Properties of Al-Al_2O_3 nanocomposite synthesized by ball milling and powder metallurgy. *Materials,* 10, 12-32

77. German RM (2016) Sintering simplified: surface area, density and grain size relations. *Mater Sci Forum*, 835, 50–75

78. Bastwros M, Kim G.Y, Zhu C, Zhang K, Wang S, Tang X, & Wang X (2014), Effect of ball milling on graphene reinforced Al6061composite fabricated by semi-solid sintering. *Compos Part B Eng*.60:111–118

79. Prabhu B, Suryanarayana C, Ann L, & Vaidyanathan R (2006). Synthesis and characterization of high-volume fraction Al–Al2O3nanocomposite powders by high-energy milling. *Mater Sci Eng. A*, 425,200-211

80. Torchynska T.V., & Filali B.E, (2017). Emission, Defects, & structure of ZnO nanocrystal films obtained by electrochemical method Chapter 4. In: Thirumalai J (Ed) Thin film processes and facts on surface phenomena and technological facets. *Intech, London*, 6(21), 55–87

81. Aperador W, Caicedo J, Esteve J, & Zambrano G (2012). A practical application of X-ray spectroscopy in Ti-Al-N and Cr-Al-N thin films chapter 2. In: Sharma SK (Ed) X-Carbon Letters spectroscopy. *Intech, London*, 4(11), 21–38

82. Zheng R, Hao X, Yuan Y, Wang Z, Ameyama K, & Ma C (2013). Effect of high volume fraction of B4C particles on the microstructure and mechanical properties of aluminum alloy based composites. *J Alloy Comp.* (3)576:291–298

83. Rashad M, Pan F, Tang A, & Asif M (2014). Effect of graphene Nano platelets addition on mechanical properties of pure aluminum using a semi-powder method. *Prog Nat Sci Mater Int.* 24:101–108

84. Meyers M.A, Mishra A, & Benson D.J (2006) Mechanical properties of nanocrystalline materials. *Prog Mater Sci* (2006) 51:427–556

85. Sekhar R, & Singh T.P (2015) Mechanisms in turning of metal matrix composites: a review. *J Mater Res Technol* 4:197–207

86. Zhang C, Yao D, Yin J, Zuo K, Xia Y, Liang H, & Zeng Y (2019) Effects of β-Si3N4 whiskers addition on mechanical properties and tribological behaviours of Al matrix composites. *Wear* 4(30), 145–156

87. Liu ZY, Wang Q.Z, Xiao B.L, Ma Z.Y (2010). Clustering model on the tensile strength of PM processed SiCp/Al composites. *Compos Appl Sci Manuf*, 41:1686–1692

88. Bastwros M.H, & Esawi A.M.K (2013). A Friction and wear behavior of Al–CNT composites. *Wear*. 307:164–173

89. Adegbenjo A.O, Obadele B.A, & Olubambi P.A (2018) Densification, hardness and tribological characteristics of MW CNT reinforced Ti6Al4V compacts consolidated by spark plasma sintering. *J Alloy Comp* 749:818–833

90. Diler E.A, Ipek R (2013) Main and interaction effects of matrix particle size, reinforcement particle size and volume fraction on wear characteristics of Al-SiCp composites using central composite design. *Compos Part B*, 50:371–380

91. Gao X, Yue H, Guo E, Zhang S, Wang B, Guan E, Song S, Zhang H (2018) Preparation and tribological properties of homogeneously dispersed graphene-reinforced aluminum matrix composites. *Mater Sci Technol*, 34: 1316–1322

92. Khan MM, Dixit G (2017) Abrasive wear characteristics of silicon carbide particle reinforced zinc-based composite. Silicon India, 10:1315– 1327

93. Chi H, Jiang L, Chen G, Qiao J, Lin X, Wu G (2016) The tribological behavior evolution of TiB2/Al composites from running-in stage to steady stage. *Wear* (2016) 368–369:304–313

94. Seenuvasaperumala A.E.P, & Jayavel R (2017). Influence of graphene hexaboride reinforced magnesium composite for the mechanical and tribological behavior. *Tribol Int* 111:18–25

95. Khun N.W (2015) Scratch-induced wear behavior of aluminum alloy under dry and wet conditions. *J Mechatron* , 3:1–6.

96. Das D.K, Mishra P.C, Singh S, & Thakur R.K (2014) Properties of ceramic- reinforced aluminum matrix composites—a review. *Int J Mech Mat Eng,* 9:1–16.

97. Carvalho O, Miranda G, Soares D, & Silva F.S (2016) Carbon nanotube dispersion in aluminum matrix composites—quantification and influence on strength. *Mech Adv Mater Struct*, 23:66–73.

98. Il-Young Kim, Jung-Hee Lee, Gyu-Sun Lee, Seung-Hyun Baik, Young Jig Kim, & Young-Ze Lee (2009). Friction and wear characteristics of the carbon nanotube–aluminum composites with different manufacturing conditions, *Wear*, 267(1–4), 593-598

99. Yufeng Wu, Gap-Yong Kim, Alan M. Russell (2012). Effects of mechanical alloying on an Al6061–CNT composite fabricated by semi-solid powder processing, *Materials Science and Engineering*: A 538, 164-172

100. H.J. Choi a, G.B. Kwon, G.Y. Lee, & Lee D.H. (2008). Reinforcement with carbon nanotubes in aluminum matrix composites. *Scripta Materialia*, 59(3), 360-363

101. Bastwros Mina, Kim GapYong, Can Zhu , Zhang Kun , Wang Shiren , Xia oduan Tang , & Wang Xinwei (2014). Effect of ball milling on graphene reinforced Al6061 composite fabricated by semi-solid sintering. *Composites Part B Engineering,* 60, 111-118

102. X. Tian, X.F. Lu, B.Y. Xia, X.W. David), & Lou (2020), Advanced electro catalysts for the oxygen reduction reaction in energy conversion technologies, *Joule*, 4, 45–68

103. C.F. Shih, T. Zhang, J. Li, & C. Bai, Powering the future with liquid sunshine, *Joule*. 2 (2018) 1925–1949

104. Y. Li, & J. Lu (2017) Metal-air batteries: will they be the future electrochemical energy storage device of choice. *ACS Energy Letter,* 2, 130–137.

105. H.-F. Wang, C. Tang, & Q. Zhang (2018), A review of precious-metal-free bifunctional oxygen electro catalysts: rational design and applications in Znir batteries, *Adv. Funct. Mater*. 28, 1803329, 130–137

106. E. Davari, & D.G. Ivey (2018), Bifunctional electro catalysts for Zn–air batteries, sustain, *Energy Fuels.* 2, 39–67

107. S. Song, W. Li, Y.-P. Deng, Y. Ruan, Y. Zhang, X. Qin, & Z. Chen (2020), TiC supported amorphous MnOx as highly efficient bifunctional electro catalyst for corrosion resistant oxygen electrode of Zn-air batteries", *Nano Energy*. 67, 104208, 201-208

108. Y. Zhang, Y.-P. Deng, J. Wang, Y. Jiang, G. Cui, L. Shui, A. Yu, X. Wang.& Chen (2021). Recent progress on flexible Zn-air batteries, *Energy Storage Mater*. 35, 538–549

109. Z. Chen, X. Liao, C. Sun, K. Zhao, D. Ye, J. Li, G. Wu, J. Fang, H. Zhao, & J. Zhang (2021), Enhanced performance of atomically dispersed dual-site Fe- Mn electro catalysts through cascade reaction mechanism, *Appl. Catal. B Environ*. 288, 120-127

110. L. Li, Z. Chang, & X.B. Zhang (2017).Recent progress on the development of metal-air batteries. *Adv. Sustain. Syst.* 1, 170-178

111. D. Jiao, Z. Ma, J. Li, Y. Han, J. Mao, T. Ling,& S. Qiao (2020).Test factors affecting the performance of zinc–air battery. J. *Energy Chem.* 44, 1–7

112. J. Ma, J. Li, R. Wang, Y. Yang, P. Yin, J. Mao, T. Ling,& S. Qiao (2021).Hierarchical porous S-doped Fe–N–C electro catalyst for high-power-density zinc–air battery. *Mater. Today Energy*. 19, 100-108

113. D. Yu, Y. Ma, F. Hu, C. Lin, L. Li, H. Chen, X. Han,& S. Peng (2021).Dual-sites coordination engineering of single atom catalysts for flexible metal-air batteries. *Adv. Energy Mater*. 11, 210-219

114. Z. Zhang, Y.-P. Deng, Z. Xing, D. Luo, S. Sy, Z.P. Cano, G. Liu, Y. Jiang, & Z. Chen (2019).Ship in a Bottle design of highly efficient bifunctional Electro catalysts for long-lasting rechargeable Zn–Air batteries. *ACS Nano*. 13, 7052–7072

115. Y. Gong, Y. Xu, Y. Que, X. Xu, Y. Tang, D. Ye, H. Zhao, & J. Zhang, (2022).Prussian blue analogues derived electro catalyst with multi catalytic centers for boosting oxygen reduction reaction in the wide pH range. *J. Colloid Interface Sci*. 612, 639–649

116. J.T. Mefford, X. Rong, A.M. Abakumov, W.G. Hardin, S. Dai, A.M. Kolpak, K.P. Johnston, & K.J. Stevenson (2016).Water electrolysis on La1xSrxCoO3 perovskite electro catalysts. *Nat. Commun*. 7 110-119.

117. H. Wang, M. Zhou, P. Choudhury, & H. Luo (2019).Perovskite oxides as bifunctional oxygen electro catalysts for oxygen evolution/reduction reactions – a mini NB review. *Appl. Mater. Today*. 16 56–71

118. A. Safakas, G. Bampos, & S. Bebelis (2019).Oxygen reduction reaction on La0.8Sr0.2CoxFe1-xO3-d perovskite/carbon black electro catalysts in alkaline medium. *Appl. Catal. B Environ*. 244, 225–232

119. Srivyas, P. D. & M. S. Charoo (2018). Role of reinforcements on the mechanical and tribological behavior of aluminum metal matrix composites – a review. *Materials Today: Proceedings*, 5, 20041–20053

120. Zhao, Z. P. Bai, W. Du, B. Liu, D. Pan, & R. Das (2020). An overview of graphene and its derivatives reinforced metal matrix composites: preparation, properties and applications. *Carbon*, 15, 969– 979

121. Hashim, H., M. S. Salleh, M. Z. Omar, A. B. Sulong, & A. A. Rahman. (2021).Influence of short heat treatment on the microstructures and mechanical properties of Thixo formed aluminum alloy composite". *Journal Tribology*, 28, 96–104

122. Arif, M. A., M. Z. Omar, and Z. Sajuri (2018). Formation of spheroidal microstructure in semi-solid state of Al-4.8Si-2.8Cu-0.5Mg aluminium alloy. *Jurnal Kejuruteraan*, 30, 275–280

123. Ramnath Vijaya B., C. Elanchezhian, M. Jaivignesh, S. Rajesh, C. Parswajinan, A. Siddique Ahmed Ghias (2014). Evaluation of mechanical properties of aluminium alloy-alumina-boron carbide metal matrix composites. *Materials and Design*, 58, 332–338

124. Panizam, H., M. S. Salleh, M. Z. Omar, A. B. Sulong, & M. A. M. Arif (2020). Effects of hybrid processing on microstructural and mechanical properties of thixo formed aluminum matrix composite. *Journal of Alloys and Compounds*, 836 45-51

125. Krishna, S., & M. Karthik (2014).Evaluation of hardness strength of aluminium alloy (AA6061) reinforced with silicon carbide. *International Journal on Recent Technologies in Mechanical and Electrical Engineering (IJRMEE)*, 1(4), 14–18

126. Sharma A, Sharma V M, Mewar S, Pal S K & Paul J (2018), Friction stir processing of Al6061-SiC-graphite hybrid surface composites, *Mater. Manuf. Process*, 33,795–804

127. Manjunath Ramesh, Kumar Deepak,& Kumar Ajay (2021).A Review on the Significance of Hybrid Particulate Reinforcements on the Mechanical and Tribological Properties of Stir-Casted Aluminum Metal Matrix Composites *Journal of Bio and Tribo-Corrosion* 7:122-132, https://doi.org/10.1007/s40735-021-00558-9

128. Doddamani S, & Kaleemulla M (2019). Comparisons of experimental fracture toughness testing methods of Al6061–Graphite particulate composites. *J Fail Anal Prev*.19 (3):730–737

129. Ezema I.C, Aigbodion V.S, & Okonkwo E.G, (2020).Fatigue properties of value-added composite from Al-Si-Mg/palm Kernel shell ash nanoparticles. *Int J Adv Manuf Technol,* 107(7–8):3247–3257

130. Devaganesh S, Kumar P.K.D, & Venkatesh N, (2020). Study on the mechanical and tribological performance of hybrid SiC-Al7075 metal matrix composites. *J Mater Res Technol*, 9(3):3759–3766

131. Kumar C.R, Malarvannan R.R.R,& Jai Ganesh V (2020).Role of SiC on mechanical, tribological and thermal expansion characteristics of B4C/Talc Reinforced Al-6061 hybrid composite. *Silicon*, 12(6):1491– 1500

132. Ali A.F.M, Omar M.Z, & Hashim H (2021). Recent development in graphene-reinforced aluminium matrix composite: a review. *Rev Adv Mater Sci*.60 (1):801–817

133. Hann X, Liao Z, & Axinte D (2022).Towards the understanding the effect of surface integrity on the fatigue performance of silicon carbide particle reinforced aluminium matrix composites. *J Manuf Processes*.73:518–530

134. Lukasak D.A, Koss D.A (1993).Microstructural influences on fatigue crack initiation in a model particulate-reinforced aluminium alloy MMCS. *Composites*. 24(3):262–269

135. Pramanik A, Dixit A.R, & Chattopadhya S, (2017). Fatigue life of machined components. *Adv Manuf*, 5(1):59–76. DOI: 10.1007/s40436-016-0168-z

136. Luk MJ, Mirza FA, & Chen DL, (2015). Low cycle fatigue of SiCp reinforced AA2009 composites. *Mater Design*, 66(5):274–283

137. Jufeng W, Jinshui C, & Chengjun G (2019). Effect of heat treatment on low cycle fatigue properties of Cu–Cr–Zr alloy.*Mater Charact,* 158:109-119

138. Razavi S.M.J, Avanzino A, & Corniche G, (2021). Effect of heat treatment on fatigue behavior of as-built notched Co-CrMo parts produced by selective laser melting. *Int J Fatigue*, 142:105-112

139. Benachour M, Benachour N, & Benguediab M (2013). Fatigue crack initiation of Al-alloys effect of heat treatment condition. *Int J Mech Aerosp Ind Mechatron Eng.*, 7:2270–2272

140. Reddy S.T, Manohar H.S, Anand S.N (2019).Effect of black carbon nano- fillers on tribological properties of Al6061 aluminium metal matrix composite. *Mater Today Proc*.9; 20(2):202–207

141. Jana P, Oza M.J.K, & Schell K.G, (2022). Study of the elastic properties and thermal shock behavior of Al– SiC-graphite hybrid composites fabricated by spark plasma sintering. *Ceram Int*. 48(4):5386–5396

142. Ordonez M.F.C., Farias M.C.M., & Descartes S, (2021). Tribofilm formation during dry sliding of graphite and MoS2 based composites obtained by spark plasma sintering. *Tribol Int*. 160:107035

143. Alaneme K.K, & Aluko A (2012). Fracture toughness (K1C) and tensile properties of as-cast and age-hardened aluminum (6063) silicon carbide particulate composites. *Scientia Iranica*. 19(4):992–996.

144. Achutha M.V, Sridhara B.K. & Budan A (2008). Fatigue life estimation of hybrid aluminium matrix composites. *Int J Des Manuf Technol*. 2(1):14–21

145. Saleem M, Ashok Raj J, & Kumar G.S.S. Design and analysis of aluminum matrix composite spur gear. *Adv Mater Process Technol*.8 (1), 408-416

146. Oskouei R.H, & Ibrahim R.N (2011). The effect of a heat treatment on improving the fatigue properties of aluminium alloy 7075-T6 coated with TiN by PVD. *Procedia Eng*. 10:1940–1946

147. P. Xiong, Z.J. Jia, M. Li, W.H. Zhou, J.L. Yan, Y.H. Wu, Y. Cheng, & Y.F. Zheng (2018).Biomimetic Ca, Sr/P-doped silk fibroin films on Mg— 1Ca alloy with dramatic corrosion resistance and osteogenic activities. *ACS Biomater. Sci. Eng*., 4(9), 3163-3172

148. M. Ali, M.A. Hussein, & N. Al-Aqeeli (2019).Magnesium-based composites and alloys for medical applications: A review of mechanical and corrosion properties. *J. Alloys Compd*, 792, 1162-1173.

149. A.V. Koltygin, V.E. Bazhenov, R.S. Khasenova, A.A. Komissarov, A.I. Bazlov, & V.A. Bautin (2019).Effects of small additions of Zn on the Microstructure, mechanical properties and corrosion resistance of WE43B Mg alloys. *Int. J. Miner. Metall. Mater*, 26(7), 858-868

150. H.R. Bakhsheshi-Rad, E. Hamzah, A.F. Ismail, M. Aziz, M. Daroonparvar, S. Parham, Z. Hadisi, & M.A.M. Yajid (2018).Titania carbon nanotubes nanocomposite coating on Mg alloy: Microstructural characterization and mechanical properties. *Mater. Sci. Technol*, 34(4), 378-389

151. Y.Z. Ma, C.L. Yang, Y.J. Liu, F.S. Yuan, S.S. Liang, H.X. Li, & J.S.Zhang (2019).Microstructure, mechanical, and corrosion properties of extruded low-alloyed Mg—xZn—0.2Ca alloys. *J. Miner. Metall. Mater,* 26(10), 1274-1285

152. H.R. Bakhsheshi-Rad, M.R. Abdul-Kadir, M.H. Idris, & S. Farahany, (2012).Relationship between the corrosion behavior and the thermal characteristics and microstructure of Mg—0.5Ca—xZn alloys. *Corros. Sci.*, 64,184-195.

153. O. Guler, Y. Say, & B. Dikici (2020).The effect of graphene Nano sheet (GNS) weight percentage on mechanical and corrosion properties of AZ61 and AZ91 based magnesium matrix composites. *J. Compos. Mater*, 54(28), 4473-4484

154. M.E. Turan, Y. Sun, F. Aydin, H. Zengin, Y. Turen, & H. Ahlatci (2018). Effects of carbonaceous reinforcements on microstructure and corrosion properties of magnesium matrix composites. *Mater. Chem. Phys.* 218, 182-193.

155. Y. Say, O. Guler, & B. Dikici (2020) Carbon nanotube (CNT) reinforced magnesium matrix composites: The effect of CNT ratio on their mechanical properties and corrosion resistance. *Mater. Sci. Eng. A,* 798, 139-149.

156. A. Lekatu, A.E. Karantzalis, A. Evangelou, V. Gousia, G. Kaptay, Z. Gács,P. Baumli, & A. Simon (2015).Aluminum Reinforced by WC and TiC Nanoparticles (ex-situ) and Aluminide Particles (in-situ): Microstructure, Wear and Corrosion Behavior. *Mater. Des*, 6(5), 1121–1135

157. S.J. Yan, S.L. Dai, X.Y. Zhang, C. Yang, Q.H. Hong, J.Z. Chen, & Z.M. Lin (2014).Investigation Aluminum Alloy Reinforced by Graphene Nano flakes. *Mat. Sci. Eng. A Struct.* , 6(12), 440–444

158. Ö. Güler, Y. Say, & B. Dikici (2020).The Effect of Graphene Nano-Sheet (GNS) Weight Percentage on Mechanical and Corrosion Properties of AZ61 and AZ91 Based Magnesium Matrix Composites. *J. Compos. Mater.* 54, 4473–4485

159. S. Jabbarzare, H.R. Bakhsheshi-Rad, & A.A. Nourbakhsh (2022).Effect of Graphene Oxide on the Corrosion, Mechanical and Biological Properties of Mg-Based Nanocomposite. *Int. J. Miner. Metall. Mater.* 29, 305–319

160. B.P. Singh, S. Nayak, K.K. Nanda, B.K. Jena, S. Bhattacharjee, & L. Besra (2013).The Production of a Corrosion Resistant Graphene Reinforced Composite Coating on Copper by Electrophoretic Deposition. *Carbon*, 61, 47–56

161. S. Narayanan, G.G. Sozhamannan, K. Hemalatha, & V.S.K. Venkatachalapathy (2021).Study on Pitting Corrosion Behavior of Graphene Oxide Reinforced Metal Matrix Composites. *Mater. Today: Proc.,* 39, 160–164

162. D. Peng, J. Wu, X. Yan, X. Du, Y. Yan, & X. Li (2016).The Formation and Corrosion Behavior of a Zirconium-Based Conversion Coating on the Aluminum Alloy AA6061. *J. Coat. Technol. Res*, 13, 837–850

163. S.I. Magaino, M. Soga, K. Sobue, A. Kawaguchi, N. Ishida, & H. Imai (1999).Zinc Corrosion in Simulated Acid Rain, Electrochemical. *Acta,* 44, 4307–4312

164. M.S. Sharifiyan, A. Shanaghi, H. Moradi, & P.K. Chu (2017).Effects of High Concentration of Benzotriazole on Corrosion Behavior of Nanostructured Titania-Alumina Composite Coating Deposited on Al 2024 by Sol-Gel Method . *Surf. Coat. Technol*, 321, 36–44

165. S. Narayanan, G.G. Sozhamannan, K. Hemalatha, K. Velmurugan, & V.S.K. Venkatachalapathy (2021), "Corrosion and Hardness Behavior of Al/GO Nanocomposites Processed by the Ultrasonic Gravitational Stir Casting Method. *Int. J. Corros*., 4(1), 1–8

166. L.A. Falcon, E.B. Bedolla, J. Lemus, C. Leon, I. Rosales, & J.G. Gonzalez-Rodriguez (2011). Corrosion Behavior of Mg-Al/TiC Composites in NaCl Solution. *Int. J. Corros*, 3(4), 1–7.

167. Huang, X., Wang, L., Song, Y.; Ge, F., Zhang, Y., Meng, X., Ge, H., & Zhao, Y (2021).Effect of Al2O3 nanoparticles on the corrosion behavior of aluminum alloy in simulated vehicle coolant. *J. Alloys Compd*. 874, 159-167

168. Latief, F.H.; Sherif, E.M.; & Junaedi, A.A.A.H (2011). Fabrication of exfoliated graphite Nano platelets-reinforced aluminum composites and evaluating their mechanical properties and corrosion behavior. *J. Anal. Appl. Pyrolysis*, 92, 485–492

169. Choi, J.S.; La, M.; Kim, D.; Choe, K.H.; Hyun, S.K.; & Kim, M.J (2021).Effect of electric current on the microstructural refinement of pure aluminum. *J. Mater. Res. Technol*., 12, 818–830

170. Yehia, H.M.; Nouh, F.; El-Kady, O.A.; Abd-Elaziem, W.; & Elsayed, E.M. (2022).Studying the Microstructure, Electrical, and Electrochemical Behavior of the Cu-10WC/x GNs for Electrochemical Machining Electrode and energy Application. *Mach. Mach. Mater*. 12, 818–830

171. S. Suresha, & B.K. Sridhara (2011).Wear characteristics of hybrid aluminium matrix composites reinforced with graphite and silicon carbide particulates. *Composites Science and Technology*, 70, 1652–1659

172. Jayashree P .K. M. C .Shankar Gowri, & A.Kinina (2013). Review on Effect of Silicon Carbide (SiC) on Stir Cast Aluminum Metal Matrix Composites. *International Journal of Current Engineering and Technology*, ISSN 2277 – 4106, 6(7), 1-12

173. V. Hari Haran, Mohan Kumar V., & Ganeshwaran P., (2014). A Review on Tribological and Mechanical Behaviors of Aluminum Metal Matrix Composites. *International Journal on Mechanical Engineering and Robotics*. 2, 2321 -2329

174. S. Cem Kumus (2012).Thermal Expansion and Thermal Conductivity Behaviors of Al-Si/SiC/graphite Hybrid Metal Matrix Composites (MMCs).*Journal of Material Science.* ISSN 1392–1320, 18, 31-40

175. D.Weiss (2012). Ablation of Hybrid Metal Matrix Composites. *Journal of American Foundry Society. Eck Industries, Manitowoc, WI*, 18, 1652–1659

176. S .Jeyabalakrishnan (2015). Temperature Distribution Analysis of Friction Stir Welding of Al-Sic-Gr Hybrid Composites. *International Journal of Innovative Research in Science, Engineering and Technology.* 3297: (4), 818–830

177. Kenneth Kanayo, (2013). Fabrication characteristics and mechanical behavior of rice husk ash – Alumina reinforced Al Mg Si alloy matrix hybrid composites. *J. Mater. Res. Technol*, 6, 818–830

178. Janiwarad Vinayak, Shadakshari R., Annaiah M.H., Mahesha K (2013). The Effect of Heat treatment on Microstructure, Mechanical properties and Damping behavior of hybrid composite of A356.0. *International Journal of Innovative Research in Science, Engineering and Technology*.2, 418–430179 Adnan N., & Saleh Ali H (2013). Effect of Heat Treatment on Strain Life of Aluminum Alloy AA 606. *Journal of Materials Science Research*. 2 (2).179-187, DOI:10.5539/jmsr.v2n2p51

180. R.H. Oskouei & Ibrahim R.N (2011). The effect of a heat treatment on improving the fatigue properties of aluminum alloy 7075-T6 coated with TiN by PVD. *Procedia Engineering,* 10(11), 1940-1946.DOI:1016/j.proeng.2011.04.321

181. M. Benachour, N Benachour & Benguediab M (2013). Fatigue Crack Initiation of Al-Alloys Effect of Heat Treatment Condition. *International Journal of Mechanical, Aerospace, Industrial and Mechatronics Engineering*.7, 310–320.

182. K.K. Alaneme. & Aluko A.O (2012). Fracture toughness (K1C) and tensile properties of as-cast and age-hardened aluminum (6063)–silicon carbide particulate composites. *Scientia Iranica*, 2, 622–630

183. Alaneme & Aluko (2008) some studies on fatigue crack growth rate of aluminum alloy 6061. *Journal of materials processing technology*, 2, 313–320

184. Small man & Ngan Achutha M.V (2008) Fatigue life estimation of hybrid Aluminium matrix composites. *International Journal on Design and Manufacturing Technologies*, 2,310-318

185. Abarghouie S.M.R.M., & Reihani S.M.S., (2010), Ageing behavior of a 2024 Al alloy SiCp composite, *Materials and Design,* 31, 2368-2374

186. Akhter R., Ivanchev L., & Burger H.P., (2007), Effect of pre/post T6 heat treatment on the mechanical properties of laser welded SSM cast A356 aluminum alloy, *Material Science and Engineering, A,* 447, 192– 196

187. Anthony K., (2006), Composite materials after seventy years, *Journal of Material Science*,.41, 905-912

188. Kalkani A., & Yilmaz S., (2008), Synthesis and characterization of aluminum alloy 7075 reinforced with silicon carbide particulates, *Materials and Design,* 29, 775-780

189. Choi D.N., Kim Y.H., Byung-Wook A.H.N., Kim Y.,& Jung S.B., (2013),Microstructure and mechanical property of A356 based composite by friction stir processing, *Transactions of Nonferrous Metals Society, China*, 23,335-340

190. Hanumanth G.S., & Irons G.A., (1993), Particle incorporation by melt stirring for the production of metal matrix composites*, Journal of Materials Science,* 28, 2459-2465

191. Leng J., Wu G., Zhou Q., & Dou Z., (2008), Mechanical properties of SiC/Gr/Al composites fabricated by squeeze casting technology, *Scripta Materialia*, 59, 619-622

192. Miracle D.B. & Donaldson S.L., (2001), Mechanical properties of SiC/Gr/Al composites fabricated by squeeze casting technology, *Composites, Vol.21, 10th edition*, *ASM Handbook, ASM International*, 838-867

193. Kumar Prasanna M., Sadashivappa K., Prabhukumar G.P., Basavarajappa S., (2006), Dry sliding wear behavior of garnet particles reinforced zinc- aluminum alloy metal matrix composites, *Materials Science (Medziagotyra)*,12(3),209-213

194. Seah K.H.W., Sharma S.C., & Girish B.M., (1997), Mechanical properties of cast and heat treated ZA- 27/graphite particulate composites. *Composite Part A: Applied Science and Manufacturing*, 28(3), 251-256

195. Prasad S.V. & Asthana R., (2004), Aluminium metal matrix composites for automotive applications: Tribological considerations. *Tribology Letter*, 17, (3), 445-452

196. Yu X.-D., Wang Y.-W., & Wang F.-C., (2007), Effect of particle size on mechanical properties of SiCp/5210 Al metal matrix composites, *Transactions of Nonferrous Metals Society, China*, 17, 276-279

197. Bindumadhavan P.N, Wah H.K, & Prabhakar O, (2001), Dual particle size (DPS) composites: Effect on wear and mechanical properties of particulate metal matrix composites, *Wear*, .248, 112-120

198. Ames W.,& Alpas A.T., (1995), Wear mechanism in hybrid composites of graphite-20 Pct. SiC in A356 aluminum alloy (Al-7 Pct. Si-0.3 Pct. Mg), *Metallurgical and Materials Transactions*,26A, 85-97

199. Wang Z, & Zhang R.J, (1991), Mechanical behavior of cast particulate SiC/Al (A356) metal matrix composites. *Metallurgical Transactions A,* 22 A, 1585-1593

200. Rohatgi P.K., (1993), Metal matrix composites, *Defence Science Journal*, 43(4), 323-349

201. Hassani A, Bagherpour E & Qods F (2014).Influence of pores on workability of porous Al/SiC composites fabricated through powder metallurgy + mechanical alloying. *Journal of Alloys and Compounds,* 591,132–142

202. Junwu Liu, Zhixiang Z, Jianmin W, Yucheng W, & Jun Lü (2008), Pressure less infiltration of liquid aluminum alloy into SiC preforms to form near-net-shape SiC/Al composites. *Journal of Alloys and Compounds,* 465, 239–243

203. Ramesh C, Pramod S & Keshavamurthy R (2011).A study on microstructure and mechanical properties of Al 6061–TiB2 in-situ composites. *Materials Science and Engineering,* A 528, 4125–4132

204. Ramesha C & Keshavamurthy R (2012). Influence of forging on mechanical properties of Ni–P coated Si3N4 reinforced Al6061 composites. *Materials Science and Engineering*, 551, 59– 66

205. W.C. Shi, L. Yuan, & D.B. Shan (2014).Effect of forging on the microstructure and tensile properties of 2024Al/Al18B4O33w composite, *Material Science & Engineering A*, 615, 313-319

206. Kumar Pradeep G, Keshavamurthy R, Ramesh C & T. P. Bharathesh (2015) .Mechanical properties of Hot forged Al6061-TiB2 In-situ Metal Matrix Composites. *Materials Today: Proceeding*. 2, 3107-3115

207. P. Cavaliere & E. vangelista (2004). Isothermal forging of metal matrix composite: Recrystallization behavior by means of deformation efficiency, *composite science and technology*, 66, 357-362

208. F. Rotundo a, L. Ceschini b, A. Morri b, T.-S. Jun c, & A.M. Korsunsky c (2010), Mechanical and microstructural characterization of 2124Al/25 vol. % SiCp joints obtained by linear friction welding (LFW) Composites. *Part A Applied Science and Manufacturing*, 41(9)1028-1037

209. Mumin Sahin, Can Guler. Cenk Misirli (2018). Properties of Al/SiC metal matrix composites, *Materials Testing* 60(6): 647-652

210. M. Taha, A. El-Sabbagh, M. Soliman, & H. Palkowski (2013), Rolling of cast Al-SiCp particulate metal matrix composites and strip mechanical properties, *Materials Science,* 3, 347-352

211. Ainhoa Riquelme, Pilar Rodrigo, María Dolores Escalera-Rodriguez & oaquín Rams (2021). Evaluation of the Wear Resistance and Corrosion Behavior of Laser Cladding Al/SiC Metal Matrix Composite Coatings on ZE41 Magnesium Alloy, *Coatings*, 11(6), 6-17

212. M Modghan, M Mazinani, G.R Ebrahimi, & H.R Ezatpour (2024). Mechanical properties and fracture surface of Al-Al2O3 nano/micro-composites produced by accumulative roll bonding. *Canadian Metallurgical Quarterly*, 5(7), 1-14

213. Y Cao, V Fatemi, S Fang, K Watanabe, T Taniguchi, & E Kaxiras (2018). Unconventional superconductivity in magic-angle graphene super lattices. *Nature*, 556 (7699), 43-50

214. M Rezayat, J.J.R Rovira, & A.M García (2023). Phase transformation and residual stresses after laser surface modification of metastable austenitic stainless steel. *AIP Conference Proceedings* 2848 (1) 23-32

215. M Rezayat, M Karamimoghadam, M.S Yazdi, M Moradi, & M Bodaghi (2023). Statistical analysis of experimental factors for synthesis of copper oxide and tin oxide for antibacterial applications. *The International Journal of Advanced Manufacturing Technology*, 11(3), 1-14

216. F Liang, C Shen, & F Wu (2017). An iterative BP-CNN architecture for channel decoding. *IEEE Journal of Selected Topics in Signal Processing*, 12 (1), 144-159

217. S Behera, R Kumar Gautam, S Mohan, & A Chattopadhyay (2015). Mechanical and tribological properties of chemically modified jute/epoxy composites. *Plastics*, *Rubber and Composites*, 5(12), 1-13

218. Nils M Denda, Peter Behrens, & Andreas M Schneider (2023). Mapping scheme as key element in coarse-graining of methacrylate-based polymers, *Materials Today Communications*, 4,106-118

219. CK Maity, N Goswami, K Verma, S Sahoo, & G.C Nayak (2020). A facile synthesis of boron nitride supported zinc cobalt sulfide nano hybrid as high- performance pseudo capacitive electrode material for asymmetric supercapacitors. *Journal of Energy Storage*, 32, 101-109

220. Shrabani De, Sourav Acharya, Chandan Kumar Maity, & Ganesh Chandra Nayak (2023). Boron Nitride/Ti3C2Tx MXene Nano sheet/WS2 Nanostructure Ternary Composites for All-Solid-State Flexible Asymmetric Supercapacitors. *ACS Applied Nano Materials*, 23,231-242

221. Yufeng Yin, Qianjun Liu, Yiting Zhao, Tingting Chen, Jing Wang, Liang Gui,& Changyu Lu (2023). Recent Progress and Future Directions of Biomass-Derived Hierarchical Porous Carbon: Designing, Preparation, and Supercapacitor Applications. *Energy & Fuels*, 37 (5), 3523-3554

222. Salim Hassan Siddiki, Verma Kartikey, Chakraborty Bhaswati, Sushrut Das, Kumar Thakur Vijay, & Ganesh Chandra Nayak (2023). Defect Dipole-Induced HfO2-Coated Ti3C2Tx MXene/Nickel Ferrite Nanocomposites for Enhanced Microwave Absorption. *ACS Applied Nano Materials,* 6 (3), 1839-1848

223. Shrabani De, Sourav Acharya, Chandan Kumar Maity, & Ganesh Chandra Nayak (2023). Polyindole-Stabilized Nano cellulose-Wrapped Ti3C2Tx (MXene) Nanocomposite for Asymmetric Supercapacitor Devices". *ACS Applied Energy Materials*, 6 (2), 969-980. https://doi.org/10.1021/acsaem.2c03423

224. P.B. Pawar a, R.M. Wabale, & A.A. Utpat (2018).A Comprehensive Study of Aluminum Based Metal Matrix Composites: Challenges and Opportunities. *Procedia Engineering,* 5(11), Part 3, 23937-23944

225. S. Suresh, N. Shenbag, & Moorthi Vinayaga (2012).Aluminium-Titanium Diboride (Al-TiB_2) Metal Matrix Composites: Challenges and Opportunities. *Procedia Engineering,* 38, 89-97

226. V.K. Lindroos, & M.J. Talvitie (1995).Recent advances in metal matrix composites. *Journal of Materials Processing Technology*, 53(1–2), 273-284

227. Hyo S Lee, Jae S Yeo, Soon H Hong, Duk J Yoon & Kyung H Na (2001).The fabrication process and mechanical properties of SiCp/Al–Si metal matrix composites for automobile air-conditioner compressor pistons. *J. of Mater. Proc. Tech*. 113(1-3) 202-8

228. Z Wang, Z Liang, B Wang, C Zhang, & L Kramer (2004).Processing & property investigation of single-walled carbon nanotube (SWNT) buckypaper/epoxy resin matrix nanocomposites. *Composites Part A: applied science and manufacturing* 35 (10), 1225-1232

229. Xu, H.; Yuan, H.; Yu, J.; & Lin, S (2019). Study on the competitive adsorption and correlational mechanism for heavy metal ions using the carboxylated magnetic iron oxide nanoparticles (MNPs-COOH) as efficient adsorbents. *Appl. Surf. Sci*. 473, 960–966

230. Fatimah, I.; Amaliah, S.N.; Andrian, M.F.; Handayani, T.P.; Nurillahi, R.; Prakoso, N.I.; Wicaksono, W.P.; & Chuenchom, L (2019).Iron oxide nanoparticles supported on biogenic silica derived from bamboo leaf ash for rhodamine B photo degradation. *Sustain. Chem. Pharm*, 13, 100-112

231. Manjunath Ramesh, Kumar Deepak, & Kumar Ajay (2022). Experimental study on the effect of age hardening and graphite particulate on the microstructure of aluminum metal matrix composites. ICMME, *Materials today proceedings*. 1(21), 233-242, https//doi.org/10.1016/j.matpr.2023.02.38

232. Manjunath Ramesh, Kumar Deepak, & Kumar Ajay (2022).Investigation of the effect of age hardening on the mechanical properties of aluminum metal Matrix composites reinforced with graphite particulate. *ICMME 2022, Materials today proceedings*, 1(21), 233-242, https//doi.org/10.1016/j.matpr.2023.02.163

233. M Krishna, S.C Sharma, & H.N.N Murthy (2000).Influence of heat treatment on the properties of Al6061/albite composites. *Transactions of the Indian Institute of Metals*, 56 (4), 399-408

234. S.C Sharma, D.R Somashekar, & B.M Satish (2001). A note on the corrosion characterization of ZA-27/zircon particulate composites in acidic medium. *Journal of Materials Processing Technology* 118 (1-3), 62-64

235. Manjunath Ramesh, Kumar Deepak & Kumar Ajay (2022).Influence of ageing on fatigue properties of graphite reinforced aluminum composites. *Advances in Materials and Processing Technologies,* DOI: 10.1080/2374068X.2022.2145041

235. S.C Sharma. (2001) The sliding wear behavior of Al6061–garnet particulate composites. *Wear,* 249 (12), 1036-1045

236. G Ranganath, S.C Sharma, & M Krishna. (2024) Dry sliding wear of garnet reinforced zinc/aluminum metal matrix composites. *Wear*, 251 (1-12), 1408-1413

237. S.C Sharma. (2001) A study on stress corrosion behavior of Al6061/albite composite in higher temperature acidic medium using autoclave *Corrosion science.* 43 (10), 1877-1889

238. S.C Sharma. (2001) Elastic properties of short glass fiber-reinforced ZA-27 alloy metal matrix composites. *Journal of materials engineering and performance*, 10, 468-474

239. T Henry, E Smith, & C Bakis (2024). Determination of effective ply-level properties of filament wound composite tubes loaded in compression. *Journal of Testing and Evaluation*, 43 (1), 96-107

240. W.C. Moshier & G.D. Davis (1990). Interaction of molybdate anions with the passive film on aluminum. *Corrosion*, 46(1), 43- 50

241. M.J Beliatis, K.K Gandhi, L.J Rozanski, R Rhodes, & L. McCafferty (2014). Hybrid graphene-metal oxide solution processed electron transport layers for large area high-performance organic photovoltaics. *Advanced Materials* 26 (13), 2078-2083

242. M.V Krishna, & A.M Xavior (2014). An investigation on the mechanical properties of hybrid metal matrix composites. *Procedia Engineering*, 97, 918-924, https//doi.org/10.1016/j.proeng .2014.12.367

243. Colman S. L, Scott V. D, & Enaney M.C (2011).Corrosion Behavior of Aluminum Based Metals Matrix Composites", *Jr of Mat Sc.Davenport,* 297, 11-24, DOl: 10.10078/BF00111758

244. A. J, Isacs H. S, Kendig M. W (1991).Investigations on the Role of Cerium Compound on the Corrosion Inhibition of Aluminum. *Corrs Sc*, 32 (516), 653-661

245. M Ansfield F., & S.L. Jeanjagnet (1984).The Evaluation of Corrosion Protection Measures for Metal Matrix Composites. *Corros Sc*, 26, 727-734

246. Rohatgi, P.K (2003).Aqueous corrosion of Metal Matrix Composites. *Comprehensive Composite Materials*, (2003), 3(18), 481-500

247. Yue, T.M; Wu, Y.X; & Man H.C (2009) On the Role of CuAl2 Precipitates in Pitting Corrosion of Aluminium (2009), SiC Metal Matrix Composites. *Jr of Materials Sc Letters,* 9, 1003-1006

248. Zaki Ahmad & Abdul Aleem B. J (2009).The Effect of Inhibitors on the Susceptibility of AL 6013, SiC Interface to Localized Corrosion. *Jr of Mat Eng*, *Perf*, (2009), 18(2), 129-136

249. Berkely, D.W, Sallam H.E, Nayeb Hasemi, H, (1998) .The effect of PH on the mechanism of Corrosion and Stress Corrosion and Degradation of Mechanical Properties of AA6061 and Nextel 440 Fiber-Reinforced AA 6061Composites.*Corros Sc*, 40(3), 141-152

LIST OF PUBLICATIONS

(Ramesh M Orcid ID: Orcid.org/0000-0003-0252-1929)

1. Manjunath Ramesh, Kumar Deepak & Kumar Ajay. A review on the significance of hybrid particulate reinforcements on the mechanical and tribological properties of stir casted aluminum metal matrix composites (2021). Journal of tribo and bio corrosion, https://doi.org/10.1007/s40735-021-00558-9:122.

2. Manjunath Ramesh, Kumar Deepak & Kumar Ajay. Influence of ageing on fatigue properties of Graphite reinforced aluminum composites (2022), advances in materials and processing technologies, https://doi.org/10.1080/2374068x.2022.2145041.

3. Manjunath Ramesh, Kumar Deepak & Kumar Ajay. Investigation of the effect of age hardening on the mechanical properties of aluminum metal matrix composites reinforced with graphite particulate", ICMME 2022, materials today proceedings, https//doi.org/10.1016/j.matpr.2023.02.163.

4. Manjunath Ramesh, Kumar Deepak & Kumar Ajay. Experimental study on the effect of age hardening and graphite particulate on the microstructure of aluminum metal matrix composites" ICMME 2022, Materials today proceedings. https//doi.org/10.1016/j.matpr.2023.02.38.

Ramesh M

EXPERIMENTAL INVESTIGATION ON MECHANICAL PROPERTIES OF ALUMINUM METAL MATRIX COMPOSITE AN...

Quick Submit

Quick Submit

University of Petroleum & Energy Studies

Document Details

Submission ID

trn:oid:::1:3196213906

Submission Date

Mar 27, 2025, 5:47 PM GMT+5:30

Download Date

Mar 27, 2025, 5:58 PM GMT+5:30

File Name

Ramesh_UPES_THESIS_for_plag_run.pdf

File Size

7.3 MB

168 Pages

35,599 Words

184,303 Characters

4% Overall Similarity

The combined total of all matches, including overlapping sources, for each database.

Filtered from the Report

- Bibliography
- Quoted Text
- Small Matches (less than 14 words)

Match Groups

44 Not Cited or Quoted 4%
Matches with neither in-text citation nor quotation marks

2 Missing Quotations 0%
Matches that are still very similar to source material

0 Missing Citation 0%
Matches that have quotation marks, but no in-text citation

0 Cited and Quoted 0%
Matches with in-text citation present, but no quotation marks

Top Sources

1% Internet sources
3% Publications
1% Submitted works (Student Papers)

Integrity Flags

1 Integrity Flag for Review

Replaced Characters
39 suspect characters on 17 pages
Letters are swapped with similar characters from another alphabet.

Our system's algorithms look deeply at a document for any inconsistencies that would set it apart from a normal submission. If we notice something strange, we flag it for you to review.

A Flag is not necessarily an indicator of a problem. However, we'd recommend you focus your attention there for further review.